10-20-2017

The Biochemical Assessment Of Two Secreted Acid Phosphatases From Leishmania Tarentolae, Their Response To Electric Fields, Glycosidase Incubation, And/or Vanadium

Benjamin M. Dorsey
Illinois State University, bmdors2@gmail.com

THE BIOCHEMICAL ASSESSMENT OF TWO SECRETED ACID PHOSPHATASES FROM *LEISHMANIA TARENTOLAE*, THEIR RESPONSE TO ELECTRIC FIELDS, GLYCOSIDASE INCUBATION, AND/OR VANADIUM

Benjamin M. Dorsey

121 Pages

Leishmaniasis, as defined by the Center for Disease Control and Prevention, is a neglected tropical disease with 1.6 million new cases reported each year. However, there is yet to be safe, effective, and affordable treatments provided to those affected by this disease (Leishmaniasis, 2016). Still underappreciated as potential pharmaceutical targets, especially for cutaneous leishmaniasis infections, are the two isozymes of secreted acid phosphatase (SAP), secreted acid phosphatase 1 (SAP1) and secreted acid phosphatase 2 (SAP2). These enzymes are involved in the survival of the parasite in the sand fly vector, and the prevention of host macrophages from forming parasitophorous vacuole and hydrogen peroxide (Fernandez Soares, Saraiva, Meyer-Fernandez, Souto-Padron, 2013;M. Baghaei and M. BAGHAEI, 2003). Thus, the kinetic behavior of these SAPs is of interest. Vanadium (V^{5+}), specifically the monomeric oxyanion orthovanadate (VO_4^{3-}), is reported to be a competitive inhibitor of phosphatases (VanEtten, Waymack, Rehkop, 1974; Abbott, Jones, Weinman, Backhoff, McLafferty, Knowles,1979; Knowles, 1980; Gressor, Tracey, Stankiewwicz, 1987; Gordon, 1991; Li, Ding, Baruah, Crans, Wang, 2008). Orthovanadate serves as a known competitive inhibitor for the enzyme inhibition experiments done in the research presented here. The application of electric or electromagnetic fields as a medicinal therapeutic is not new (Holden, 2017). The utility of

applying electric fields for the treatment of leishmaniasis is under studied (Hejazi, Eslami, Dalimi, 1972), and the application of electric fields to *Leishmania* secreted acid phosphatases has not yet been reported. The results of such studies using *L. tarentolae* as a model system, with and without the addition of orthovanadate, are reported here. Furthermore, the effect specific electric fields have on the kinetic parameters of *L. tarentolae* SAPs are also reported.

KEYWORDS: Leishmania, Leishmaniasis, Secreted Acid Phosphatase, Electric Field, Glycosidase, Orthovanadate, Potential Treatment

THE BIOCHEMICAL ASSESSMENT OF TWO SECRETED ACID PHOSPHATASES FROM *LEISHMANIA TARENTOLAE*, THEIR RESPONSE TO ELECTRIC FIELDS, GLYCOSIDASE INCUBATION, AND/OR VANADIUM

BENJAMIN M. DORSEY

A Thesis Submitted in Partial
Fulfillment of the Requirements
for the Degree of

MASTER OF SCIENCE

Department of Chemistry

ILLINOIS STATE UNIVERSITY

2017

THE BIOCHEMICAL ASSESSMENT OF TWO SECRETED ACID PHOSPHATASES FROM *LEISHMANIA TARENTOLAE*, THEIR RESPONSE TO ELECTRIC FIELDS, GLYCOSIDASE INCUBATION, AND/OR VANADIUM

BENJAMIN M. DORSEY

COMMITTEE MEMBERS:

Marjorie A. Jones, Chair

Jon A. Friesen

Craig C. McLauchlan

ACKNOWLEDGMENTS

I would first like to thank my research advisor, Dr. Jones, for her immense support and guidance during my time at Illinois State University. I would like to thank Dr. Friesen and Dr. McLauchlan for their input on this work.

I would like to acknowledge the faculty, staff, my fellow students, and my lab peers at Illinois State University for providing a supportive, accepting, and challenging environment in which I was able to grow and learn.

I would like to thank the Kurz Fellowship and The Millennium Pain Center for summer support. Their support allowed me to focus my summer efforts on completing research required for this thesis work.

Finally, I thank my family and friends that offered support to me while I completed my degree. Without you all, completing this work would not have been possible.

B. M. D.

CONTENTS

TABLES

FIGURES

CHAPTER I

INTRODUCTION

Leishmania, Leishmaniasis, and Current Treatment Options

Leishmaniasis is defined by the Center for Disease Control and Prevention as a neglected tropical disease carried by the sand fly vector. It affects populations in Asia, India, the Middle East, Africa (particularly in the tropical region and North Africa, with some cases elsewhere), Central and South America and southern Europe (Leishmaniasis, 2016). No cases of leishmaniasis have been reported in Australia or the Pacific islands. This disease is caused by any of 20 species of the parasitic protozoan *Leishmania* (Leishmaniasis, 2016). Leishmaniasis presents clinically in three forms: visceral, cutaneous, and mucocutaneous (Leishmaniasis, 2016). Over 1.6 million new cases of leishmaniasis are reported yearly (Leishmaniasis, 2016), and current treatment options include: pentavalent antimony salts, amphotericin B, liposomal amphotericin B, ketoconazole, itraconazole, and fluconazole (Leishmaniasis Professionals, 2016). Treatments can cost from $ 20-$252 USD per day, and treatments can last from 20 days to 4 months or longer depending on how long it takes for the lesion to heal (World Health Organization Leishmaniasis Treatment Cost, 2017). *Leishmania* diseases are becoming more wide spread, and there are few good drug therapies, thus new directions of treatments should be explored. As a consequence of sequencing *Leishmania major* and *Leishmania infantum* genomes, a large number of potential new drugs targets have been identified (Chawla, Madhubala, 2010). These potential drug targets include: the sterol biosynthetic pathway, the glycolytic pathway, the purine salvage pathway, nucleotide transporters, purine salvage enzymes, the glycosylphosphatidylinositol (GPI) pathway, protein kinases, mitogen-activated protein kinases (MAP kinases), proteinases, folate biosynthesis, the glyoxalase system, the trypanothione

pathway, topoisomerases, and the hypusine pathway (Chawla, Madhubala, 2010). However, non-drug treatments affecting these or other potential targets may also be of value in treating leishmaniasis.

Phosphatases

Phosphatases are hydrolytic enzymes (EC 3.1) that are responsible for the hydrolysis of phosphoesters from substrate producing a phosphate and an alcohol (ExPASy, 2016). There are three general types of phosphatases; acid phosphatases, neutral phosphatases, and alkaline phosphatases (Vincent, Crowder, Averill, 1992; Gani, Wilkie, 1997). These enzymes are categorized based upon their pH optimum. Most relevant to this thesis work are acid phosphatases. Acid phosphatases are located, in humans, in the cellular components of bone, spleen, kidney, liver, intestine, and are also found in the blood (Henneberry, Engel, Grayhack, 1979). The pathogenesis of *Leishmania* changes during the life cycle from the amastigote form to the promastigote form of the parasite. (Mojtahedi, Clos, Kamali-Sarvestani, 2008). *In vitro* parasites in the stationary phase of their growth curve are more infective to macrophages than are parasites in the logarithmic phase (Mojtahedi *et al*., 2008). It has also been reported that the kinetic parameters of secreted acid phosphatases isolated from the *in vitro* stationary phase of *Leishmania major* change, such that the enzymes have a larger V_{max} and a smaller K_m compared to the logarithmic phase enzyme (Navabi, Soleimanifard, 2015). *Leishmania* secreted acid phosphatases are established to play several roles during the life cycle of the parasite, including: aiding in the survival of the parasite in the sand fly alternative host (Fernandes, Soares, Saraiva, Meyer-Fernandez, Souto-Padron, 2013), and formation of the parasitophorous vacuole, thus preventing macrophages from forming hydrogen peroxide (M. Baghaei, M. BAGHAEI, 2003).

Thus, *Leishmania* secreted acid phosphatases are of interest as potential pharmaceutical targets for the treatment of leishmaniasis.

L. tarentolae Secreted Acid Phosphatase Enzymes

Secreted acid phosphatase enzymes are defined as proteins with phosphatase activity that are released from cells into the medium. In general, they are large molecular weight glycoproteins that in some *Leishmania* species are reported to be up to 70 % (w/w) carbohydrate (Ilg, Stierhof, Etges, Adrian, Harbecke, 1991). These proteins have both N- and O- linked sugars. The O-linked carbohydrate polymers are reported to be up to 32 repeat units in length (Lippert, Dwyer, Li, Olafson, 1999). There are at least two genes reported for *Leishmania* (Shakariana, Ellisa, Mallinsonac, Olafsonb, Dwyera, 1997). Furthermore, it is reported that these enzymes promote parasite survival in the sand fly, and promote the formation and evolution of the parasitophorous vacuole, in host macrophages, by dephosphorylating macrophage membrane proteins, thus preventing macrophage hydrogen peroxide production (M. Baghaei, M. BAGHAEI, 2003). Furthermore, the flagellar pocket of *Leishmania* is specialized, and is the location for the discharge of the two different secreted acid phosphatases, the most regularly secreted protein for *Leishmania major*, the human parasite (Isnard, Shio, Oliver, 2012; Fernandes *et al*., 2013). *L. tarentolae*, which infect reptiles but not humans, have also been shown to secrete acid phosphatases (Mendez, Dorsey, McLauchlan, Beio, Turner, Nguyen, Su, Beynon, Friesen, Jones, 2014).

L. tarentolae serves as a good model system for the investigation of the two *Leishmania* secreted acid phosphatases for several reasons. First, *L. tarentolae* are easy to grow, and their growth in culture is easily assessed. *L. tarentolae* do not infect humans, thus are less risky to work with. *L. tarentolae* have utility in the macrophage model system used to assess infectivity. Finally, *L. tarentolae* are sensitive to current treatment options, thus therapeutics that are effective in this

model system may also work on the *L. major* species (Taylor, Munoz, Cedeno, Velez, Jones, Robledo, 2010). Furthermore, to test the role of N-linked carbohydrate found on *L. tarentolae* secreted acid phosphatases, cell supernatants containing these enzymes can be incubated with PNGase F, a glycosidase. PNGase F is a glycoaminidase, thus cleaving the N-C bond between asparagine and N-acetylglucosamines (PNGase F, 2017). These incubations will allow the investigation of the role of N-linked carbohydrate in secreted acid phosphatase enzyme activity.

Electric Fields Applied as a Therapeutic, in General

Electromagnetic fields are composed of an electric component, and a perpendicular magnetic component. When applying an electric field to a biological sample, two types of processes may occur: Faradaic or non-Faradaic processes. Faradaic processes are electron transfer reactions, where as non-Faradaic process involve reorientation of solvent molecules and charges at the electrode surface (Merrill, Bikson, Jefferys, 2005). Electrons move from potentials that are more negative to potentials that are more positive. When applying cathodic current (negative voltage) to a biological sample, thus making the sample's potential more positive than the electrode, electrons move from the electrode to the sample. Cathodic current (Cat.) is thus reductive to the sample. Furthermore, while making the medium of the biological sample more negative, the cell potential becomes more positive. The cell potential is relative and is based on the charge outside of the cell versus the charge on the inside of the cell. As the exterior of the cell becomes more negative, the interior of the cell becomes relatively more positive, thus potentially causing depolarization for voltage-gated processes (Biophysics of Membrane Potential, 2017). When applying anodic current (positive voltage), the biological sample becomes more negative, thus electrons are transferred from the sample to the electrode (Merrill *et al*., 2005). Anodic current (And.) is thus oxidative to the biological sample. Furthermore,

while making the medium of the biological sample more positive, the cell potential becomes more negative. As the exterior of the cell become more positive, the interior of the cell becomes relatively more negative, thus potentially causing hyperpolarization for voltage-gated processes (Biophysics of Membrane Potential, 2017). The Food and Drug Administration has approved the application of electromagnetic fields, with differential properties, for the following indications: electric bone growth stimulators, for the treatment of non-union fractures, failed joint fusion following arthrodesis, failed spinal fusion, congenital pseudoarthritis, palliative treatment of post-operative edema and pain, and major depressive disorder (Holden, 2017). Many of the mentioned potential drug targets for the treatment of leishmaniasis have some component that is voltage regulated. Some examples include the following. The movement of acetyl-CoA from within the mitochondria to the cytoplasm that requires transport of pyruvate across the inner and outer mitochondrial membranes. The outer mitochondrial membrane pyruvate transporter is a voltage regulated membrane protein (King, 2017). MAP kinases have been reported to be regulated by a calcium/calmodulin-dependent protein kinase cascade that is itself regulated by secondary messenger Ca^{2+} (Enslen, Tokumitsu, Stork, Davis, Soderling, 1996). If calcium concentrations in cells are affected by the movement of calcium inward through voltage gated calcium transporters, these processes will be impacted. The importance of these processes in normal cellular metabolism warrant the investigation of their response to the application of an electric field for therapeutic treatment of leishmaniasis.

As a therapeutic, electricity has been applied to *L. major* in culture, and has been applied to two different types of mouse models, Naval Medical Research Institute (NMRI) strain or Bagg Albino (BALB/c) strain, for the treatment of pre-existing *L. major* lesions (Hejazi, Eslami, Dalimi, 1972). These authors tested the following conditions: 3, 6, 9, or 12 Volts with current

ranging from 0.19-10.65 mA (Direct current). Their *in vivo* experiments showed that when the electrodes were placed 2 cm apart, direct voltages of 3, 6, 9, and 12 volts at various currents killed all *L. major* promastigotes. Furthermore, when the electrodes were 2 cm apart, the application of 3 volts for 10 minutes caused the pH to drop from 7 to 4. This drop in pH has several physical and chemical implications. First, the drop in pH occurred due to the oxidation of water (see equation 1).

$2\ H_2O\ (l) \rightarrow 4\ H^+\ (aq) + 4\ e^- + O_2\ (g)$ Equation 1.

Because electrons were removed from water to produce protons (hence the drop to more acidic pH), we infer that the driving force for this reaction was the applied voltage. To cause the oxidation of water, this applied potential must have been anodic, or positive voltage, in character. Thus, these authors investigated the effects of anodic waveforms on *L. major*.

Hejazi *et al*. (1972) treated *L. major* infected mice with electricity that was applied twice a week for three weeks after the inoculation of 4-6 week old mice (NMRI or BALB/c) with *L. major* (10^6 stationary phase parasites). The diameter of skin lesions was measured as a metric to determine the effectiveness of the electrical therapies. The NMRI mice with infection, but with no treatment, reached a maximum lesion diameter of ~4 mm and spontaneously healed completely by week 10. The NMRI mice with infection and electrical therapeutic (3 V, 0.05 mA for 10 min) reached a maximum lesion diameter of 2.5 mm, and were healed completely at 6 weeks. Thus, in the NMRI mice, electricity was therapeutic, and lead to remission of lesions with no reoccurrence up to 23 weeks (the duration of the study). It should be noted that the control mice were also in complete remission at 23 weeks, but their remission took longer to initiate (10 weeks). The BALB/c mice with infection, but with no treatment, reached a maximum lesion diameter of ~16 mm and were all dead by week 20. The BALB/c mice with infection and electrical therapies (3 V,

0.05 mA for 10 min) reached a maximum lesion diameter of ~17 mm, and were still alive at 23 weeks. The electricity treated mice had lesions the same size as the control from weeks 1-3. At week 3 electricity treatment occurred, and the control lesions continued to grow while the treated lesions reached a minimum of ~0 mm at week 8. On week 9 the treated lesions began to grow linearly, and reached a maximum diameter of ~ 17 mm at week 23, at which point the study ended (Hejazi *et al*., 1972). These data indicate that electricity applied as a therapeutic does have an effect on lesion size, but depending on the species of mouse, the lasting effect is different, and thus different therapeutic durations may be required. The authors did not speculate on the therapeutic mechanism.

Electric Fields for the Purpose of Affecting *L. tarentolae* Motility, Clumping, Cell Viability, and Secreted Acid Phosphatase Activity

With this in mind, we propose evaluating the effects of applying electric fields to *L. tarentolae*. We wanted to test the ability of *L. tarentolae* to secrete acid phosphatases, the catalytic activity of secreted acid phosphatases, as well as cell motility (as evaluated by microscopy), and cell viability (MTT assay). We are especially interested in the potential effect of the application of an electric field to induce or inhibit the release of secreted acid phosphatase from *Leishmania* since it had reported that *Leishmania* secreted acid phosphatase (SAP) has an important role in the infectivity by *Leishmania* (Vannier-Santos, Martiny, de Souza, 2002). Thus, these data have implications for clinical treatments of cutaneous *Leishmania* infections.

Vanadium Background, Vanadium Human Exposure, Vanadium Chemistry and Speciation

Vanadium, element number 23, is found in the soil, water and air, and can enter the human body through the lungs or digestive tract (Agency for Toxic Substances and Disease

Registry, 2016; Rehder, 2013). Atmospheric vanadium is found in dust, marine aerosol, and volcanic emissions. Air is typically not a large source of vanadium exposure for humans. Cigarette smokers are exposed to approximately 4 μg of vanadium per cigarette smoked (Agency for Toxic Substances and Disease Registry, 2016). Water and soil are likely the greatest sources of vanadium, other than food supplements, that humans are exposed to. Water and soil can typically contain 0.04-220 μg/L vanadium (Agency for Toxic Substances and Disease Registry, 2016). The typical total amount of vanadium in humans is 1 mg (Rehder, 2013). Vanadium is a very versatile element and has 5 common oxidation states available, with the vanadium (V) oxidation state being the overwhelmingly dominant species in aqueous solution. Vanadium forms covalent adducts with oxygen, which produce numerous different species of vanadium in its (V) oxidation state as a function of pH (Figure 1, Baes, Mesmer, 1976).

Speciation of vanadium, specifically decavanadate speciation in acidic media, has been investigated (Figure 1, Baes, Mesmer, 1976). It is clear that under acidic conditions, protonation status changes either by deprotonation or cation exchange with the medium, and vanadium speciation is a function of vanadium concentration, solution pH, and ionic strength of the solution (F. Rossotti, H. Rossitti, 1956; Corigliano, Pasquale, 1975). Because of this, vanadium speciation, degree of protonation, and degree of proton displacement by cations in solution are likely different for solutions of different composition. Therefore, when using decavanadate or orthovanadate as inhibitors of phosphatases, it is not always clear what species are present, or what species are responsible for inhibition of the enzyme being assayed.

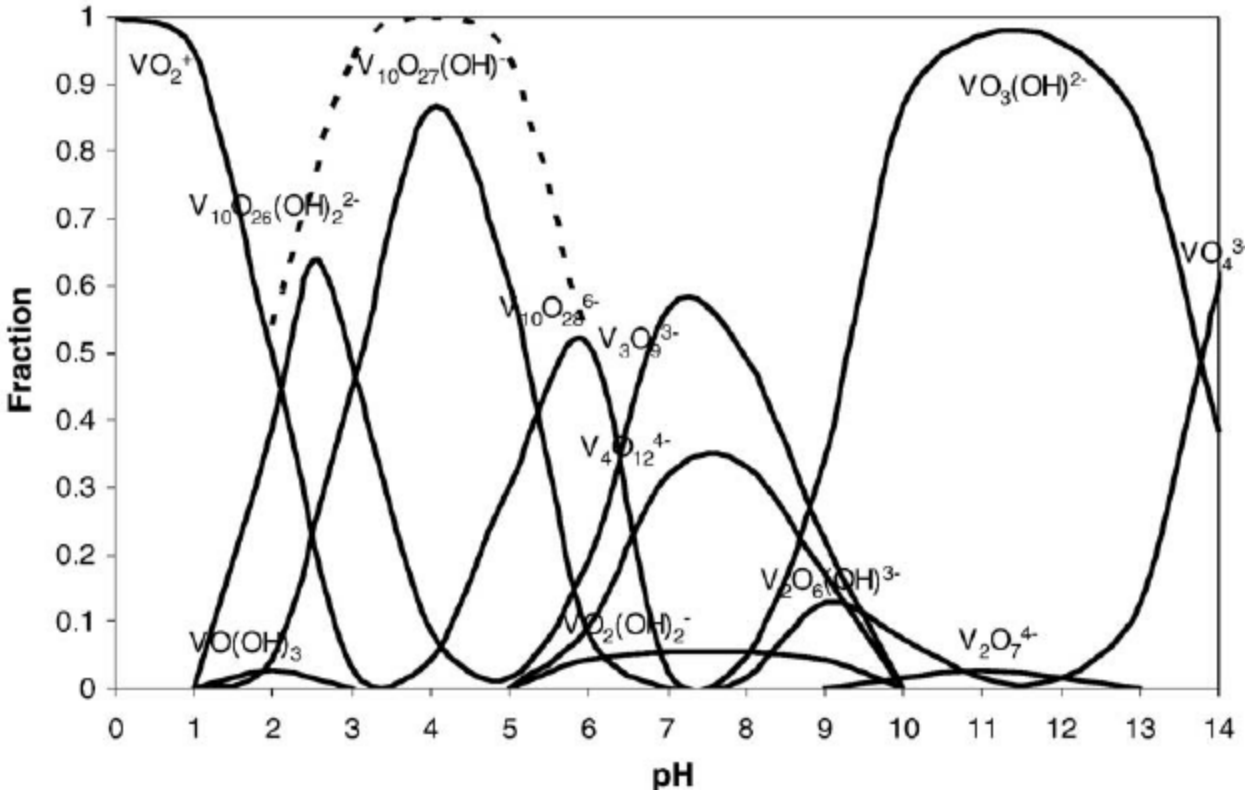

Figure 1. Vanadium (V) speciation as a mole fraction of total vanadium present at a given pH, over the typical pH scale (0-14) (Baes, Mesmer, 1976). This speciation diagram is for a 0.1 m vanadium solution

Vanadium is a Potential Medicinal Agent as a Phosphatase Inhibitor

It is well known that oxovanadium species act as phosphatase inhibitors (VanEtten *et al*., 1974; Abbott, Jones, Weinman, Bockhoff, McLafferty, Knowles, 1979; Knowles, 1980; Gressor, Tracey, Stankiewwicsz, 1987; Gordon, 1991; Li, Baruah, Crans, Wang, 2008;). How vanadium acts as a phosphatase inhibitor is thought to be through the action of a vanadium (V) monomeric oxyanion, vanadate, mimicking a 5 coordinate high energy intermediate of the transition state phosphate, therefore behaving as a competitive inhibitor (Abbott *et al*., 1979; Knowles, 1980; Rehder, 2013). There are numerous crystal structures of phosphatases, with nitrogen-containing, oxygen containing, or sulfur-containing active site amino acids, deposited in the Protein Data Bank, that have been recently reviewed (McLauchlan, Peters, Willsky, Crans, 2015). These

phosphatases function to hydrolyze esters, phosphoesters, and phosphoanhydrides. These crystal structures had been soaked with vanadium complexes, the majority of experiments using orthovanadate, at pH values ranging from 5.40-8.00. The overwhelming majority of these phosphatases, regardless of the type of active site amino acid residues (O, N, or S containing), have a monomeric form of vanadium (VO_3^{2-} or VO_4^{3-}) present in the phosphatase active site upon solving the crystal structure. It should be noted at the used concentrations of vanadium and in this pH range, that di-, tri-, and tetrameric vanadium species are predicted to be the major forms of vanadium present, and not the monomeric forms (VO_3^{2-} or VO_4^{3-}) that are reported in the enzyme's active site. Thus, there is a discrepancy between what one might hypothesize about the species responsible for inhibition (the major species present is responsible for the inhibition), and what one actually finds (a minor species present is responsible for the inhibition). Regardless, it is thought that these monomeric species are likely responsible for phosphatase inhibition. There is, however, a likely discrepancy between solid state speciation of vanadium that occurs under soaking conditions, and aqueous speciation of vanadium that occurs in enzymatic assays because crystal dynamic conditions are likely to be different than those of the more flexible protein under enzymatic assay conditions in terms of pH, ionic strength, and vanadium concentration. Therefore, the species of vanadium present in enzymatic assays cannot necessarily be assumed to be the same as the species present after crystal soaking experiments. To further stress the importance of speciation, crystallographic soaking studies that used metavanadate (50 mM) starting material, under acidic conditions (pH 5.0) produced protein crystals of *B. stearothermophilus* phosphatase with trivanadate, $V_3O_8^{2-}$, located in the putative active site, when in fact, the authors had expected to find orthovanadate, VO_4^{3-} (PDB ID 1h2f., Rigden, Littlejohn, Henderson, Jedrzejas, 2003).

Using acid phosphatase amino acid sequence alignment from rat (*APR. norvegicus* EC3.1.3.2, PDB 1rpt) as a comparative model to *Leishmania* secreted acid phosphatases, it can be seen that there is in fact overlap between the reported vanadate binding residues in the *APR. norvegicus* and the *L. mexicana* acid phosphatases (SAP1L.mex gene accession number Z46969.1 and SAP2L.mex gene accession number Z46970.1). The gray and black highlights are the amino acids reported to be in the active site. Gray highlights indicate different amino acids between species. Black highlights indicate identical amino acids between species. Using the amino acid numbering from *APR. norvegicus*, the following residues are responsible for coordinating vanadate, Arg11, His12, Arg15, Arg79, and His257, and are highlighted in red in Figure 2.

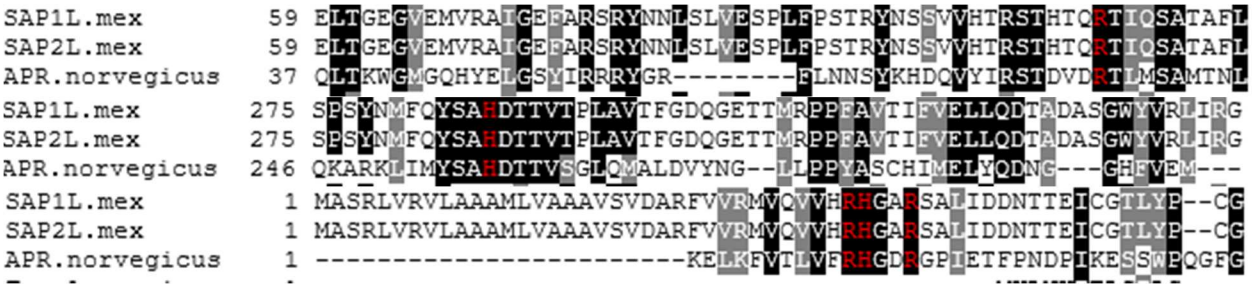

Figure 2. Multiple Sequence Alignment of three acid phosphatases. This sequence alignment was completed using Kalign and the BoxShade Server (Kalign, 2016; BoxShade Server, 2017)

To further investigate the ambiguities of vanadium speciation and phosphatase inhibition, we use a previously published model (Baumhardt, Dorsey, McLauchlan, Jones, 2015) for comparing competitive enzyme inhibitors to compare decavanadate and orthovanadate as inhibitors of *L. tarentolae* secreted acid phosphatases. These studies can give insight into the clinical use of these and other vanadate complexes as anti-*Leishmania* therapies.

Because leishmaniasis is an endemic disease with costly treatment options, and multiple cellular targets, including acid phosphatases, here we investigated the effects that electric fields, with or without the presence of vanadium complexes, or glycosidase preincubation have on *L. tarentolae in vitro* for the purpose of discovering new, cheap therapeutics for the treatment of leishmaniasis.

CHAPTER II

MATERIALS AND METHODOLOGY

Cell Culture of *L. tarentolae* and Assessment of Cell Viability by the MTT Viability Assay

L. tarentolae (ATCC 30143) promastigote cells were sterilely grown in brain heart infusion (BHI; 37.0 g/L) supplemented with hemin (10 μM), penicillin (10,000 units/ mL) and streptomycin (10 mg/ mL) following a published method (Morgenthaler, Peters, Cedeno, Constantino, Edwards, Kamowski, Jones, 2008). *L. tarentolae* cell viability was assessed by the 3-(4,5-dimethylthiazol-2-yl)-2,5-diphenyltetrazolium bromide (MTT) viability assay (Mosmann, 1983). The MTT assay serves as a quantitative measure (A595 nm) of cell mitochondrial activity, and therefore indirectly monitors cell viability. Sample absorbance at A595 nm was determined with an iMark microplate reader (BioRad Laboratories, Hercules, CA). The BHI growth medium alone was considered as a blank value subtracted from the sample absorbance (BHI and cells). Results are reported as corrected absorbance (A595 nm/Hr incubation with MTT reagent, or A595 nm/Hr incubation with medium only) mean ± standard deviation (SD) for n = 4 replicates. In all cases where error bars less than 5 % were not shown. In this work, the parasites were grown at room temperature in 25 cm^2 canted flasks (Corning, Inc.; Product number 430372). Samples for assessment by MTT assay were collected daily using sterile technique.

Microscopy of *L. tarentolae*

Microscopic analysis of *L. tarentolae* for motility, shape, and clumping was undertaken. The parasites were observed microscopically to monitor the effect of each treatment on the parasite. A Jenco International, Inc. (Portland,OR) inverted compound microscope Model CP-2A1 was used. This microscope can be adjusted to focus on cells at the bottom, middle, or upper focal planes of the culture flask which will allows observations of the parasite throughout the

culture medium. Images of cells (at 400x magnification) were taken using the camera on the Google Pixel cellular phone. Microscopy was performed on all *L. tarentolae* cell cultures daily.

Preparation of the L. *tarentolae* Acid or Alkaline Phosphatase Enzyme Source

A sample of *L. tarentolae* from each stage of the growth curve (lag, log, stationary, and senescence) was collected and centrifuged (2000xg, 10 ºC, 10 minutes). The supernatant was collected and stored on ice until it was used for acid or alkaline phosphatase enzyme assays. The pellet was immediately resuspended in a volume of BHI equal to the volume of supernatant collected from that same sample. The pellets were then stored on ice until they were used in acid or alkaline phosphatase enzyme assays.

Secreted Acid or Alkaline Phosphatase Enzyme Assay

Secreted acid or alkaline phosphatase (SAP) activity was evaluated using *para*-nitrophenyl phosphate (*p*NPP) as substrate following the method of Mendez *et al*. (2014). This assay at room temperature was performed in 1.5 mL polypropylene tubes in a total reaction volume of 0.9 mL. Sodium acetate buffer (500 µL, 0.5 M, pH 4.5) was used for acid phosphatase assays. Tris-Base (500 µL, 0.5 M, pH 8.3) was used for alkaline phosphatase assays. The enzyme source was *L. tarentolae* cell supernatant or pellet from each phase of the growth curve (300 µL). The substrate (5 mg *p*NPP/1mL buffer), made in sodium acetate buffer (0.5 M, pH 4.5) for acid phosphatase assays, or Tris-Base (0.5 M, pH 8.3) for alkaline phosphatase assays was added (100 µL) to start the reaction (500 µM final concentration). After room temperature incubation for 23 hours, the reaction was stopped with addition of 100 µL of 10 M sodium hydroxide, and samples were vortexed. Product formation was measured by spectroscopy at A405 nm. BHI was used to replace enzyme source for spectrophotometric blanks. Data are reported as absorbance (A405

nm) per day in culture. Product (*para*-nitrophenolate) was calculated from corrected A405 nm/23 Hr divided by molar absorptivity (18,000 $cm^{-1}* M^{-1}$) and reported as µM/ 23 Hr.

Kinetic Enzyme Assay

The order of addition of material to the kinetic enzyme assay was as follows. Sodium acetate buffer (500 µL, 0.5 M, pH 4.5) was used for acid phosphatase assays. The artificial substrate, *para*-nitrophenylphosphate (*p*NPP), was freshly prepared in buffer, then it was added to the assay to give final substrate concentrations of 2.0, 2.6, 3.0, 3.4, 3.7, 4.1, 4.5, 6.0, 8.8, 12.0, 14.0, 18.0, 150.0, 200.0, 250.0, 300.0, 350.0, 400.0, 450.0, 500.0, 550.0, 1000.0, 2000.0, or 4000.0 µM. Lastly, log phase *L. tarentolae* cell supernatant as enzyme source (300 µL) was added to the 1.5 mL polypropylene tubes to start the reaction. The final assay volume was 0.9 mL (n=3). Assays were incubated at room temperature for 23 hours, previously determined to be under apparent first order conditions (Mendez *et al*., 2014), in the dark. To stop the reaction, sodium hydroxide (100 µL, 10 M) was added and the samples were vortexed. Product was then evaluated by spectroscopy (A405 nm). Spectrophotometric blanks were prepared using the same volumes of assay buffer and substrate as experimental samples, but the enzyme source was replaced with brain heart infusion medium, the same medium as the supernatant fraction, but not exposed to cells.

Designing Waveforms for the Production of Electric Fields

Using a comma-separated values (CSV) excel file, the waveforms to be applied to *L. tarentolae* whole cells or cell supernatant were generated. The number of data points (N) is used to determine the time resolution (S) of the signal. The resolution of the signal is the time between current applications. The larger the number of data points (N), the smaller the resolution (S) is.

For these experiments, N = 40,000. The frequency (F), defined as a cycle per second, was then used to calculate the period (T) of the waveform.

$$T = 1/F \qquad \text{Equation 2}$$

The period and number of data points were used to calculate the resolution of the signal (S).

$$S = T/N \qquad \text{Equation 3}$$

The excel file contained two columns, one column for time, and the other for the voltage that is entered into the waveform generator. Time zero will have a value of 0S. Time 1 will have a value of 1S. Time two will have a value of 2S, and so on to fill the 40,000 data points. The value of the voltage in the other column was either be zero or four. When the value is equal to zero, then zero voltage will be applied. When the value is equal to four, then an input of four was sent to the waveform generator (Singlet Function/Arbitrary Waveform Generator) and voltage was then generated from the electrode. To determine when the values of voltage are zero or four, the period of the waveform (T) was divided by three to generate three equal time points; the pulse width (PW), the interphase delay (IPD) and the space between cycles (CS). These three values add up to equal the period (T).

$$T = 2PW + IPD + CS \qquad \text{Equation 4}$$

When the period is divisible by three, producing an integer value, the value of CS is equal to zero. When the period is not divisible by three, producing a non-integer value, the value of CS is the smallest value that will produce a period divisible by three. The following equations are also true:

$$PW = IPD \qquad \text{Equation 5}$$

$$PW = (T-CS)/3 \qquad \text{Equation 6}$$

$$PW = T/3 \text{ if } CS = 0 \qquad \text{Equation 7}$$

To generate Figure 3, a data file containing forty thousand data points, N = 40,000, was used. For a frequency of 5000 Hz, F= 5000 s^{-1}, thus T = 1/F, T = 1/5000, T = 2 * 10^{-4} seconds. The resolution was calculated as S = T/N, S = (2*10^{-4} seconds)/40,000, S = 5*10^{-9} seconds. The time points in the excel file started at zero and grew in increments of 5*10^{-9} s at each iteration. To determine the time of PW, and thus IPD, the period (T = 200 µs) must be divided into three equal parts. To do this, CS will have a value of 2 µs. Using equation 5, PW will be determined.

PW = (T-CS)/3, PW = (200 µs - 2 µs)/3, PW = 66 µs

PW, as calculated for a symmetric waveform, means the cathodic segment will be 66 µs and the anodic segment will be 66 µs. Using equation 4, IPD will be determined.

IPD = PW, IPD = 66 µs

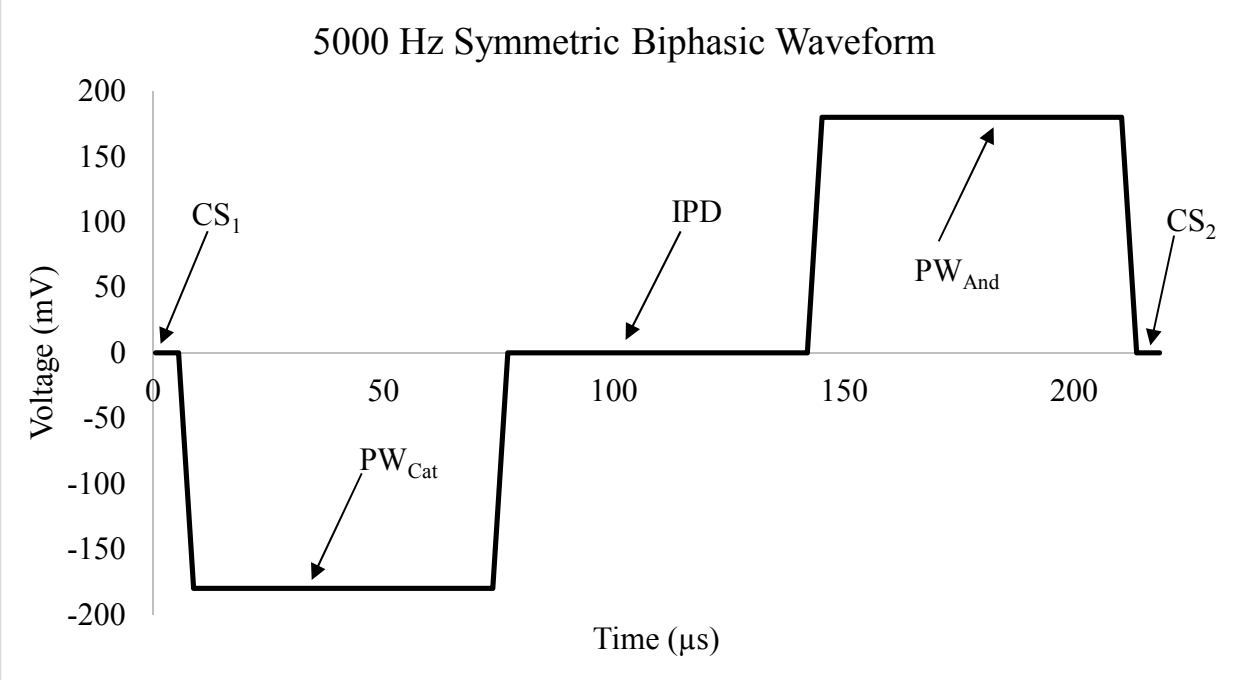

Figure 3. A plot of time (µs) vs. voltage (mV) is shown for a symmetric biphasic waveform

In an excel file, the following spread sheet was written to generate the waveform in Figure 3. From 0-2 µs (The CS), in increments of 0.005 µs (Resolution, S), the voltage input was assigned to 0, thus producing 0 mV (CS_1). This occupies 400 data points. From 2-68 µs, the voltage was assigned to 4, thus producing -180 mV (PW_{Cat}). This occupies 13,200 data points. From 68-134 µs, the voltage of 0 was assigned, thus producing 0 mV (IPD). This occupies 13,200 data points. From 134-200 µs, the voltage of 4 was assigned, thus producing 180 mV (PW_{And}). This occupies 13,200 data points. All 40,000 data points are thus be accounted for. CS_2 immediately follows PW_{And}, and will have identical parameters of CS_1. CS_2 is the space between cycle one and cycle two.

Electrode Tested

The electrode used was a concentric bipolar electrode from FHC Neuro Micro Targeting™ Worldwide. Figure 4 is a model of the general shape of the electric fields that are applied to *L. tarentolae* whole cells or *L. tarentolae* cell supernatant.

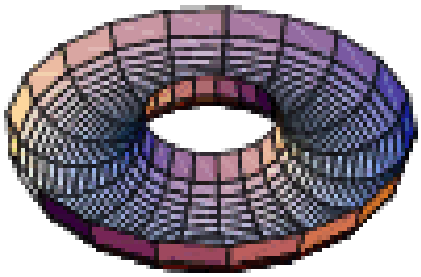

Figure 4. Model of the general shape of the electric field that is applied to either *L. tarentolae* whole cells or cell supernatant is shown

Parameters of Tested Waveforms

The waveforms were loaded on to a singlet arbitrary waveform generator. The following parameters of the waveform that produces the electric filed were modified using an isolator (World Precision Instruments stimulus isolator): frequency (50-10,000 Hz), current (0.1-1.0 mA), polarity of the waveform (symmetric biphasic, cathodic, or anodic), and exposure time (2.5 min-12 hours) to the electric field. A simplified model of the experimental setup is shown in Figure 5.

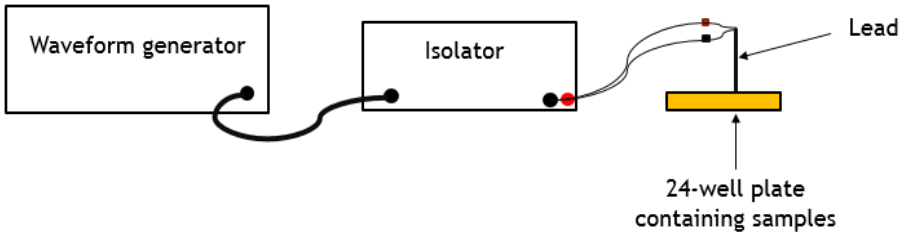

Figure 5. Simplified experimental model of setup to apply electric fields to *L. tarentolae* whole cells or cell supernatant

Testing the Acute Effects of Electric Fields on *L. tarentolae* Growth Curves and Microscopy

L. tarentolae were transferred from 25 cm^2 canted flasks into 24 well plates (Falcon; 0.5 mL per well), taking care to deliver a consistent number of cells to each well. Using a singlet arbitrary waveform generator coupled to a stimulus isolator, an electrode was applied to these cells to expose them to a characterized electric field for a specific amount of time. After exposure to the electric field, *L. tarentolae* were assessed for cell viability by the MTT assay. Immediately following the application of an electric field, these cells were monitored by microscopy. Results were compared to cells not exposed to the electric field.

Testing the Effects of Electric Fields on *L. tarentolae* Acid Phosphatase Activity in Supernatant or Pellet (Cells), Method 1

L. tarentolae were collected from the log phase of their growth curve, centrifuged (2000x*g*, 10 min, 10 ºC), and the supernatant was collected. The cell pellet was resuspended in a volume of BHI growth medium equal to the volume of supernatant collected. The supernatant or pellets were transferred into a 24-well plate (Falcon, 0.5-2.0 mL per well). Using a singlet arbitrary waveform generator coupled to a stimulus isolator, a concentric bipolar electrode was applied to these samples to expose them to an electric field, or not (control). The samples exposed to the same type of electric fields, or not (control), were pooled and rested on ice until they were assessed by the acid phosphatase enzyme assay. The process is outlined in the flow diagram below in Figure 6. Data are plotted as percent different from same time control for n=3. Data were first evaluated by ANOVA, and those that were significantly different were further analyzed. When reporting percent different relative to the same time control, only those data that were statistically different in a paired, two-tailed t-test at the 0.05 level were reported.

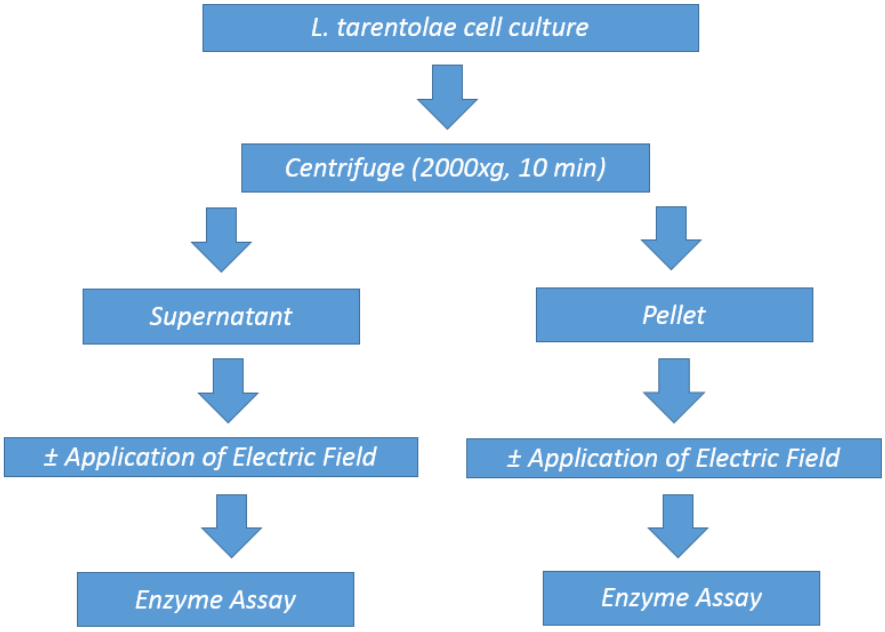

Figure 6. Flow diagram of Method 1. Thus, method 1 allows testing of direct effects of electric field on the previously secreted enzyme

Testing the Effects of Electric Fields on *L. tarentolae* Acid Phosphatase Activity in Supernatant or Pellet (Cells), Method 2

L. tarentolae were collected from the log phase of their growth curve, and were then transferred from culture flasks to 24-well plates (Falcon, 0.5-2.0 mL per well), taking care to deliver a consistent number of cells to each well. Using a single arbitrary waveform generator coupled to a stimulus isolator (World Precision Instruments), a concentric bipolar electrode was applied to these samples to expose the cells an electric field, or not (control). The cells were collected. Cells that were exposed to the same type of electric fields or control cells were pooled. These pools were centrifuged (2000x*g*, 10 min, 10 ºC), and the supernatant was collected. The cell pellets were resuspended in a volume of BHI equal to the volume of the supernatant collected. The samples were rested on ice until they were used in the acid phosphatase enzyme

assays. The process is outlined in Figure 7. Data are plotted as percent different from same time control for n=3. Data were first evaluated by ANOVA, and those that were significantly different were further analyzed. When reporting percent different relative to the same time control, only those data that were statistically different in a paired, two-tailed t-test at the 0.05 level were reported.

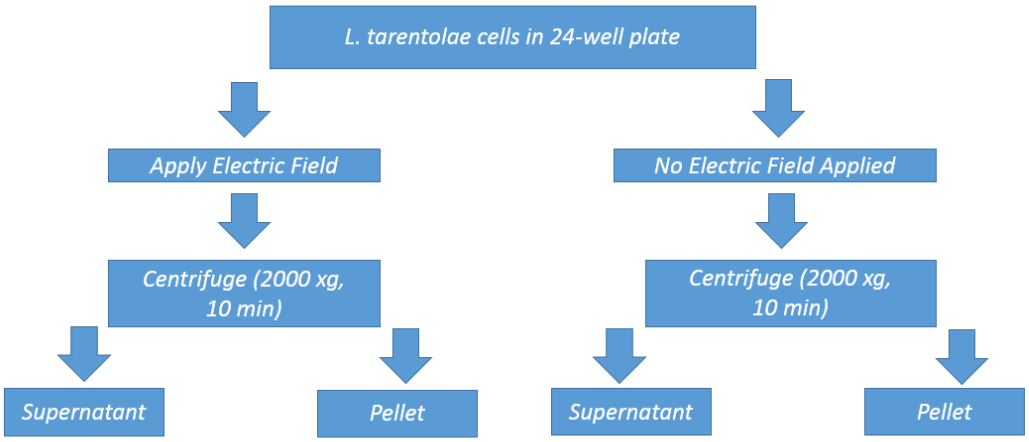

Figure 7. Flow diagram of Method 2. Thus, method 2 allows assessment of the effect of electric field on secretion of acid phosphatase from cells

Secreted Acid Phosphatase Enzyme Inhibition Assay (Following the Method of Baumhardt *et al*., 2015)

To determine which form of vanadium is most useful in *L. tarentolae* secreted acid phosphatase enzyme assays, decavanadate or orthovanadate, the method of Baumhardt *et al*. (2015) was used. Using the previously determined k_M substrate concentration of 391 µM, the log ratio of substrate to total vanadium concentration in the assay was calculated for either orthovanadate or decavanadate (as shown in Table 1). This amount of substrate was used as a

first approximation of k_M from previous work (Mendez *et al*., 2014) with the same enzyme source.

Sample	log[S]/[I]	[Total Vanadium] mM	[Decavanadate] mM	[Orthovanadate] mM
1	-2.0	3.91E+01	3.91E+00	3.91E+01
2	-1.5	1.24E+01	1.24E+00	1.24E+01
3	-1.0	3.91E+00	3.91E-01	3.91E+00
4	-0.5	1.24E+00	1.24E-01	1.24E+00
5	0.0	3.91E-01	3.91E-02	3.91E-01
6	0.5	1.24E-01	1.24E-02	1.24E-01
7	1.0	3.91E-02	3.91E-03	3.91E-02
8	1.5	1.24E-02	1.24E-03	1.24E-02
9	2.0	3.91E-03	3.91E-04	3.91E-03

Table 1. The concentrations of vanadium used as either total vanadium, or orthovanadate, or decavanadate in each sample.

Table 1 indicates the relationship between the log of substrate to inhibitor ratio to the total moles of vanadium, or the total moles of decavanadate, or the total moles of orthovanadate in the assay. It should be noted that for every mole of orthovanadate, there is one mole of vanadium. For every mole of decavanadate, there are ten moles of vanadium. Thus, orthovanadate was used at ten times the molar concentration of decavanadate, but the total moles of vanadium from either compound, in the assay, was the same as listed in Table 1. In all cases the concentration of the artificial substrate, *para*-nitrophenylphosphate (*p*NPP), is 391 μM.

The order of addition of material to the assay was as follows. Sodium acetate buffer (0.5 M, pH 4.5), vanadium as either orthovanadate or decavanadate freshly prepared in assay buffer, and enzyme source (300 μL of log phase *L. tarentolae* cell supernatant) were added to the assay and allowed to preincubate at room temperature for 10 minutes. The artificial substrate, *para*-nitrophenylphosphate (*p*NPP) was added to the assay to give final concentrations of 391 μM

*p*NPP. The final assay volume was 0.9 mL. Assays were incubated at room temperature for 23 hours. To stop the reaction sodium hydroxide (100 µL ,10 M) was added and the samples were vortexed. Product was evaluated by spectroscopy at A405 nm. Spectrophotometric blanks were prepared using the same volumes of assay buffer, vanadium as either orthovanadate or decavanadate, and substrate as experimental samples. The enzyme source was replaced with brain heart infusion, the same medium the enzyme was in for kinetic and inhibition assays. Data are reported as mean ± standard deviation for n=4 replicates.

Secreted Acid Phosphatase Enzyme Inhibition Assays with Pretreatment with Eelectric Fields Followed by Incubation with and without Orthovanadate (25 µM)

To test the effect of pretreating *L. tarentolae* log phase cell supernatant with electric fields followed by incubation with orthovanadate (25 µM), supernatant was collected (50 mL) from the stationary phase of the growth curve, exposed to electric fields, and then used as the enzyme source for end point acid phosphatase assays. This concentration of orthovanadate was selected based on the experiments done using the model reported by Baumhardt *et al*., 2015. This concentration of orthovanadate inhibits *L. tarentolae* secreted acid phosphatase activity, but does not completely shut down the enzyme. Thus, if a synergistic effect occurs between orthovanadate and electric field application, and is large enough, it can be measured. The order of addition of material to the assay was as follows. Sodium acetate buffer (0.5 M, pH 4.5), orthovanadate freshly prepared in assay buffer, and enzyme source (300 µL) were added to 1.5 mL polypropylene tubes for the assay and allowed to preincubate at room temperature for 10 minutes. The artificial substrate, *para*-nitrophenylphosphate (*p*NPP) was added to the assay to give a final concentration of 391 µM *p*NPP. The final assay volume was 0.9 mL. Assays were incubated at room temperature for 23 hours. To stop the reaction sodium hydroxide (100 µL,

10 M) was added and the samples were vortexed, and product was evaluated by spectroscopy A405 nm.

Secreted Acid Phosphatase Kinetics Assay with and without the Preincubation with a Glycosidase, Followed by Pretreatment with and without Electric Fields

The *L. tarentolae* log phase cell supernatant was collected via centrifugation (2000x*g*, 10 min, 10 ºC), incubated with the glycosidase PNGase F (10 µL of PNGase F with activity of 10 U/ µL per 25 mL enzyme pool; Promega Madison, WI) enzyme source for 24 hours at room temperature, and then this enzyme pool was used in kinetic assays. The order of addition of material to the assay was as follows. Sodium acetate buffer (500 µL, 0.5 M, pH 4.5) was added to 1.5 mL polypropylene tubes. The artificial substrate, *para*-nitrophenylphosphate (*p*NPP), was freshly prepared in buffer, then it was added to the assay to give final substrate concentrations of: 2.0, 2.6, 3.0, 3.4, 3.7, 4.1, 4.5, 6.0, 8.8, 12.0, 14.0, 18.0, 150.0, 200.0, 250.0, 300.0, 350.0, 400.0, 450.0, 500.0, 550.0, 1000.0, 2000.0, or 4000.0 µM. Lastly, *L. tarentolae* cell supernatant as enzyme source (300 µL) was added to the 1.5 mL polypropylene tubes. The final assay volume was 0.9 mL (n=3). Assays were incubated at room temperature for 23 hours (previously determined to be under apparent first order conditions (Mendez *et al*., 2014), in the dark. To stop the reaction, sodium hydroxide (100 µL, 10 M) was added and the samples were vortexed. Product was evaluated by spectroscopy (A405 nm). Spectrophotometric blanks were prepared using the same volumes of assay buffer and substrate as experimental samples, but the enzyme source was replaced with brain heart infusion medium, the same medium as the supernatant fraction, but not exposed to cells.

CHAPTER III

RESULTS AND DISCUSSION

Cell Culture of *L. tarentolae* and Assessment of Cell Viability by the MTT Viability Assay

During their growth curve, *L. tarentolae* respond in a predictable manner to the MTT reagent. This predictable and repeatable response is useful as a metric because it gives a context for normal *L. tarentolae* behavior, and serves a reference point from which enzyme pools, whole cells or cell supernatant, are collected. Furthermore, knowing what phase of the growth curve cells are in is useful because it allows more accurate interpretation of an effective potential treatment. Figure 8 shows a typical growth curve with the four characteristic phases of *in vitro* cell growth exhibited by *L. tarentolae*.

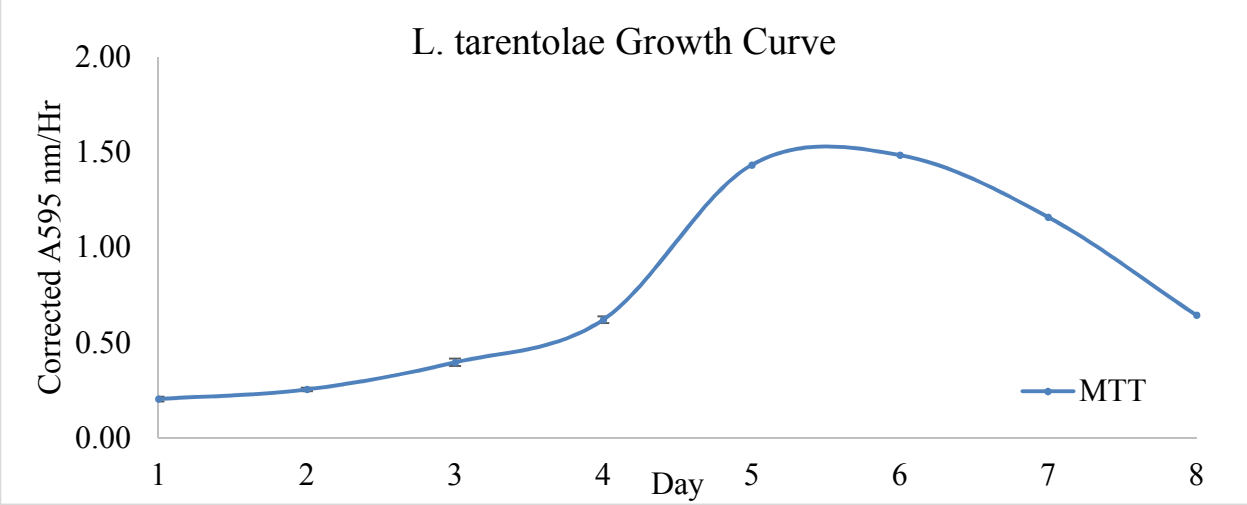

Figure 8. A typical growth curve for *L. tarentolae* with the corrected MTT response plotted on the Y-axis and the day in culture plotted on the X-axis. The lag phase occurs on days 1-3. The log phase occurs on days 4-5. The stationary phase occurs between days 5-6. The senescence phase occurs on days 6-8. Each point is the mean ± standard deviation of n=4 replicates

Microscopy of *L. tarentolae*

During their growth curve, *L. tarentolae* exhibit typical behavior that is observable by light microscopy. During the lag phase (days 1-3), the cells have a distinct, elongated shape, and do not clump. The cells exhibit moderate motility, and the cell population does not appear to be over crowded (Figure 9). During the log phase (days 4-5), the cells have a distinct, elongated shape, and do not clump. The cells exhibit increased motility, and the cell population appears significantly more crowded. Cells exhibit no clumping during this phase (Figure 10). During the stationary phase (between days 5-6), the shapes of most cells are still distinct and elongated. Some cells begin to appear rounded, and the cell population exhibits variable motility. Some cells are moving rapidly, while other cells are not moving at all. The cell population still appears crowded during the stationary phase. Cells exhibit clumping during the stationary phase. Each cell clump contains between 3 and 10 cells (Figure 11). During the senescence phase (days 6-8), the shape of cells becomes increasingly more rounded as the culture ages. The cells that appear more rounded in shape, also appear to not be moving. The cells that are more elongated are still moving, but with decreasingly less rigor. The cell population appears crowded, but the majority of cells are rounded and not moving. Little or no clumping is observed during this phase of the growth curve (Figure 12).

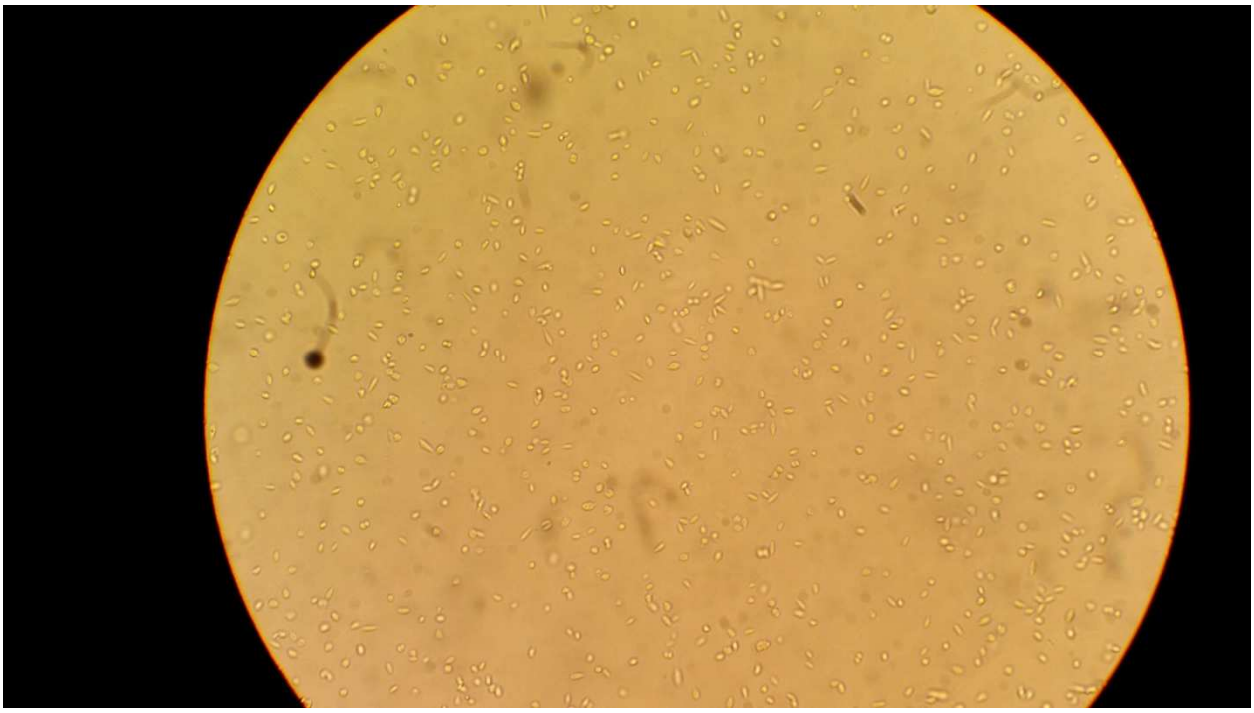

Figure 9. The above image depicts *L. tarentolae* by microscopy (400X) during the lag phase of their growth curve

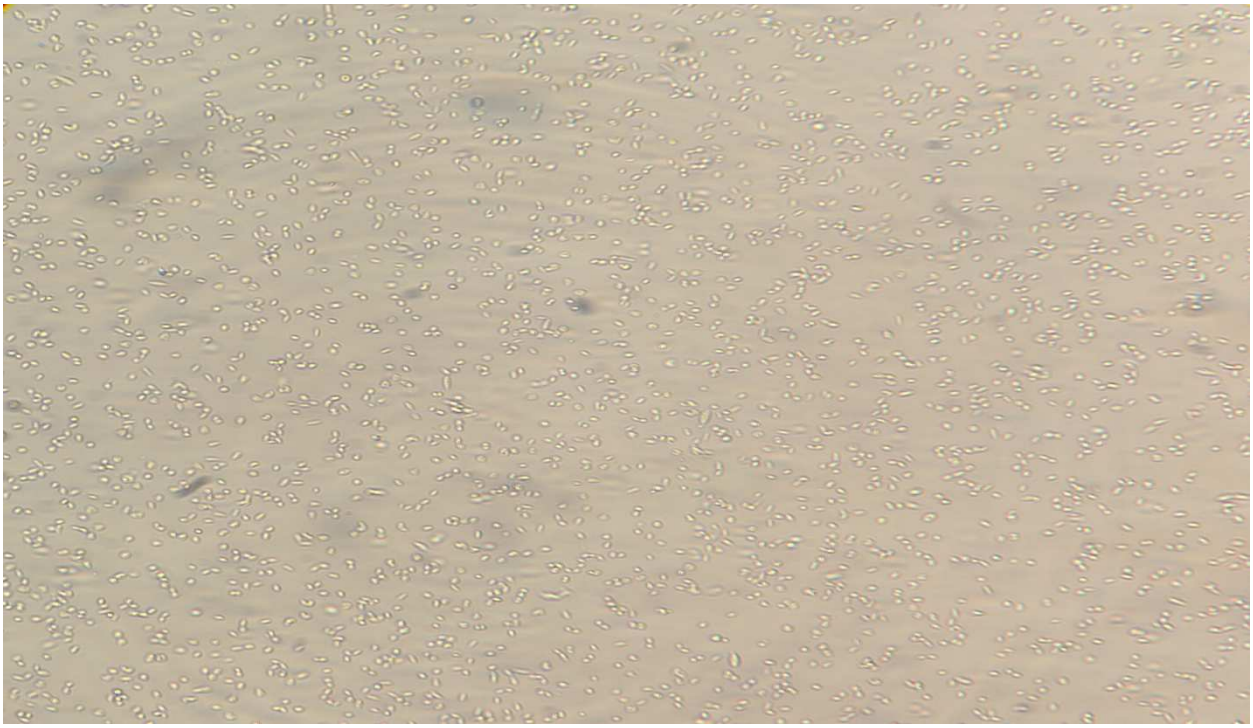

Figure 10. The above image depicts *L. tarentolae* by microscopy (400X) during the log phase of their growth curve

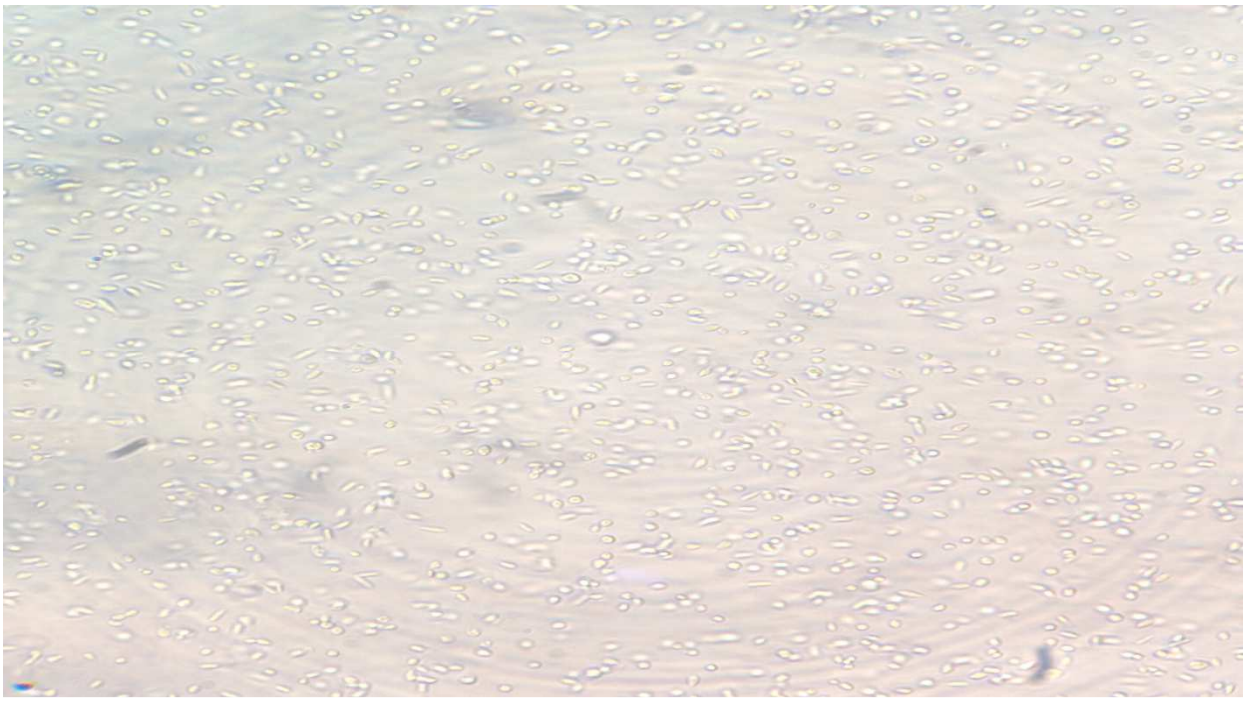

Figure 11. The above image depicts *L. tarentolae* by microscopy (400X) during the stationary phase of their growth curve

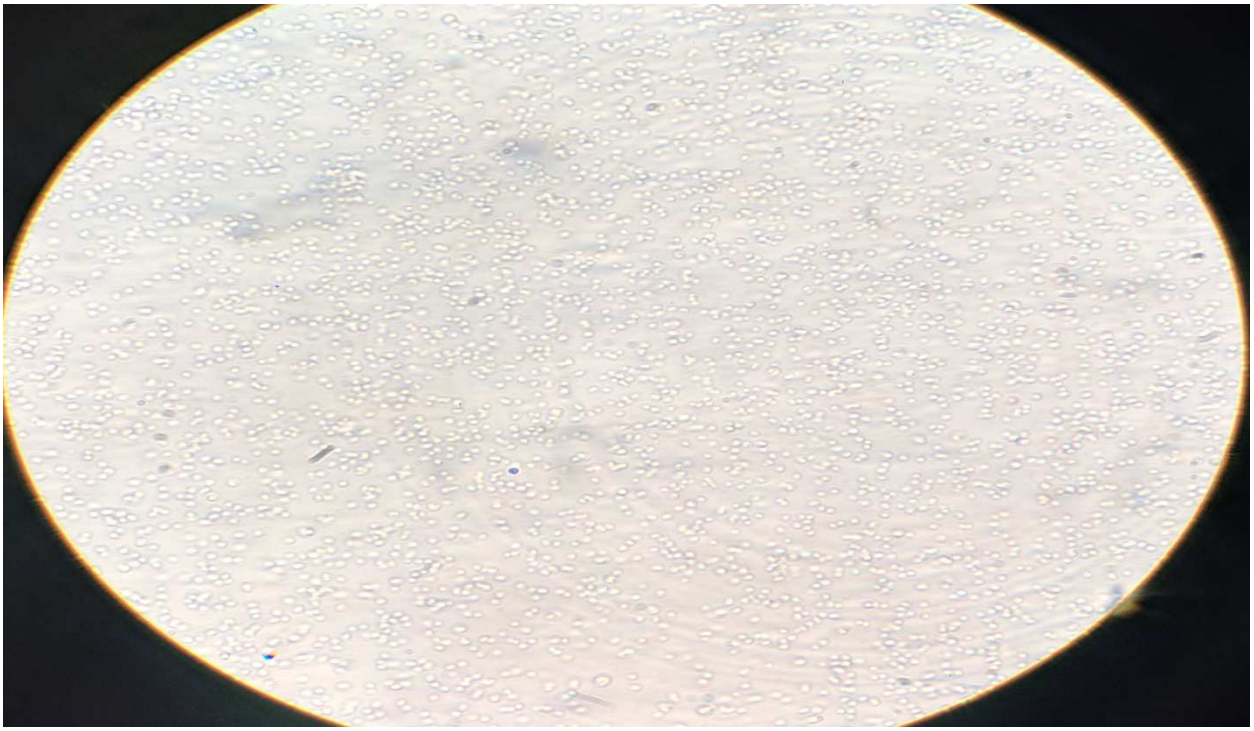

Figure 12. The above image depicts *L. tarentolae* by microscopy (400X) during the senescence phase of their growth curve

Secreted Acid or Alkaline Phosphatase Enzyme Assay

Using the growth curve as a reference point, detectable secreted acid phosphatase activity tracks with the MTT response up to day 6, as shown in Figure 13. When the cells' response to the MTT reagent decreases, the detectable secreted acid phosphatase activity plateaus (days 6-8). Alkaline phosphatase activity in the supernatant was not detectable during any point of the 8 day growth curve, as shown in Figure 13.

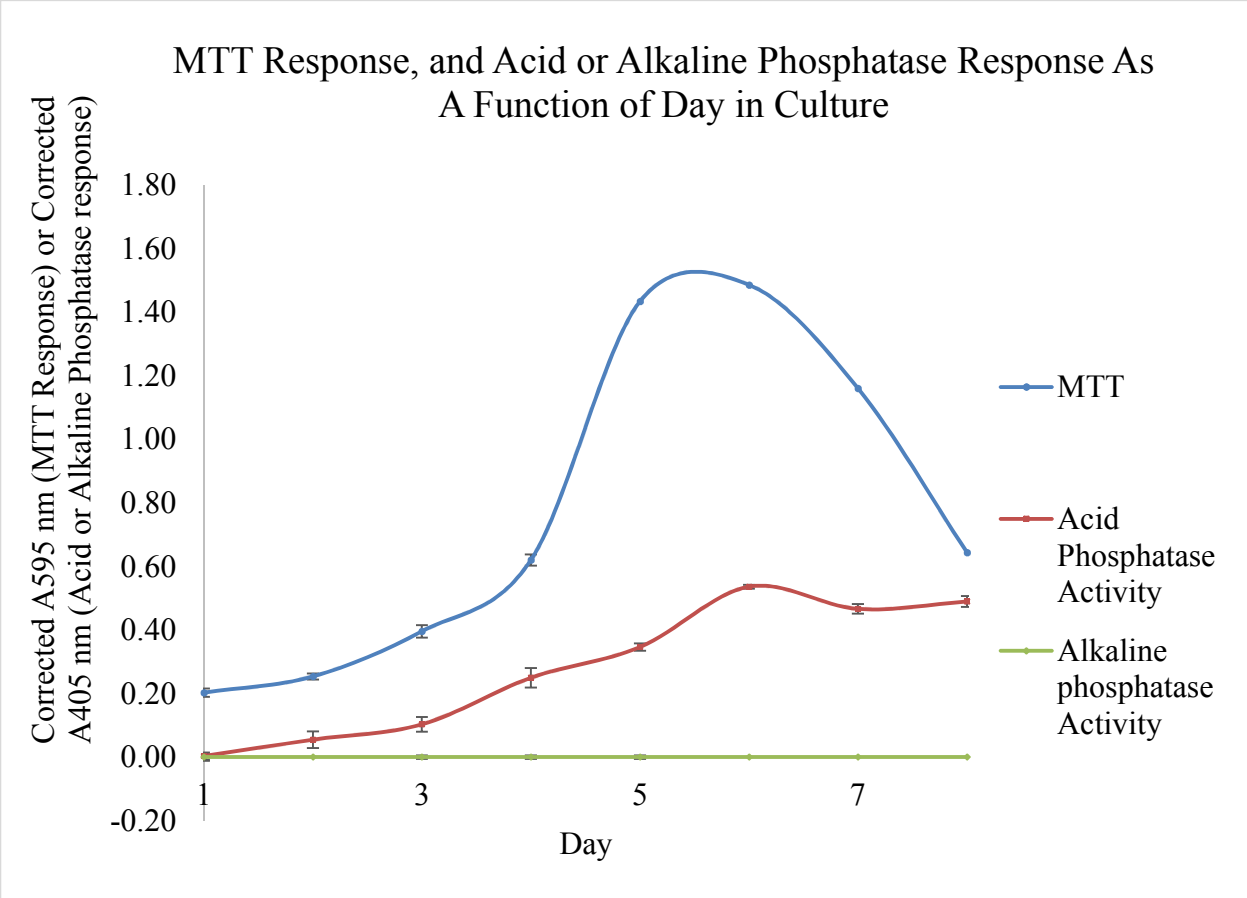

Figure 13. Secreted acid (red curve) or secreted alkaline (lime green curve) phosphatase activity detected as a function of day in culture. The blue curve is the typical *L. tarentolae* growth curve evaluated by MTT response. Each point is the mean ± standard deviation of n=3 replicates

Kinetic Enzyme Assay

The *L. tarentolae* log phase supernatant appeared to exhibit Michaelis-Menten type enzyme behavior as a response to increasing substrate concentrations (Figure 14). The response depicts an apparent first order portion with a large response to increases in substrate concentration. This apparent first order response is followed by a decreased response to increasing substrate concentration, thus indicating that V_{MAX} is being approached by the enzyme pool. A noticeable derivation from the apparent first order trend occurs at 350 µM *p*NPP (indicated by arrow) was, however, suggestive of non-Michaelis-Menten behavior. It should be noted that in this work, V_{MAX} data are not corrected for total amount of enzyme present.

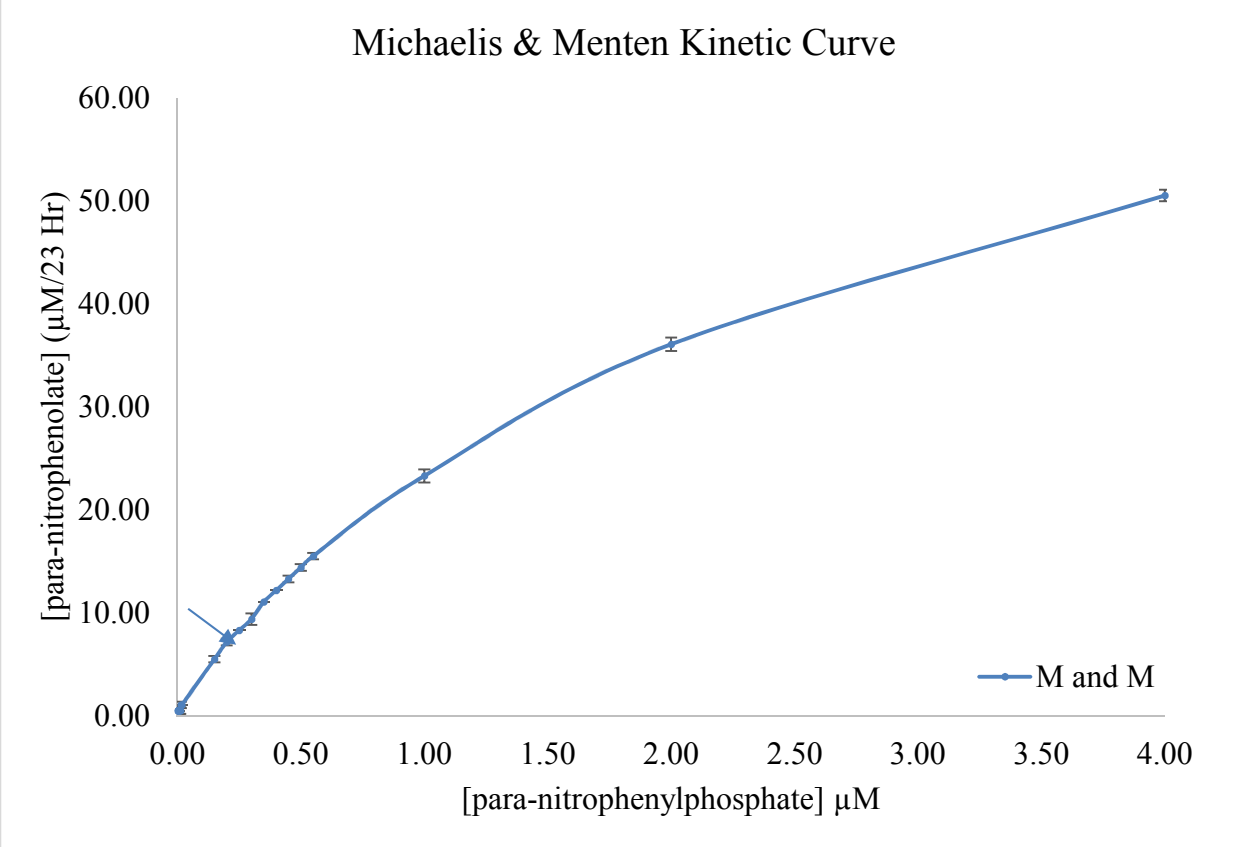

Figure 14. A typical V versus S curve utilizing *L. tarentolae* log phase supernatant as the enzyme source. Each point is the mean ± standard deviation of n=3 replicates

The Lineweaver-Burk linear transformation of the Michaelis-Menten curve, that typically produces a single line for a single enzyme source, produced two different lines for the *L. tarentolae* log phase supernatant (Figures 15, 16, and 17).

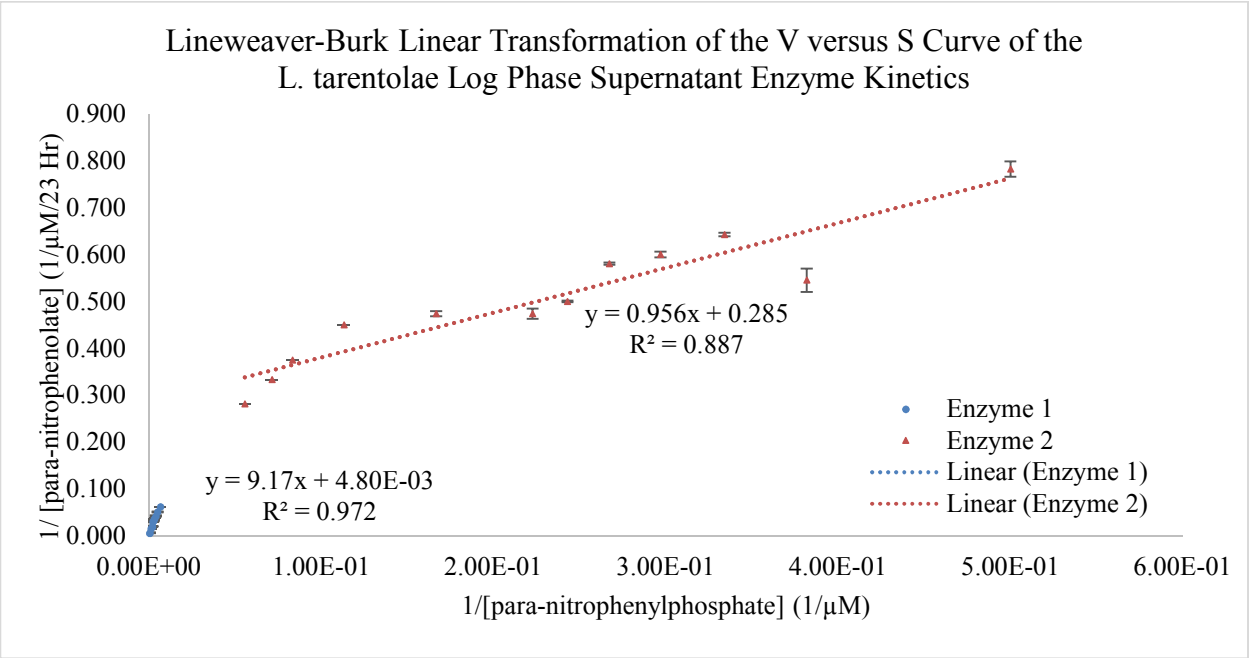

Figure 15. A typical Lineweaver-Burk linear transformation using *L. tarentolae* log phase supernatant as the enzyme source. Enzyme 1 is shown in blue circles. Enzyme 2 is shown in red triangles. Each point is the mean ± standard deviation of n=3 replicates

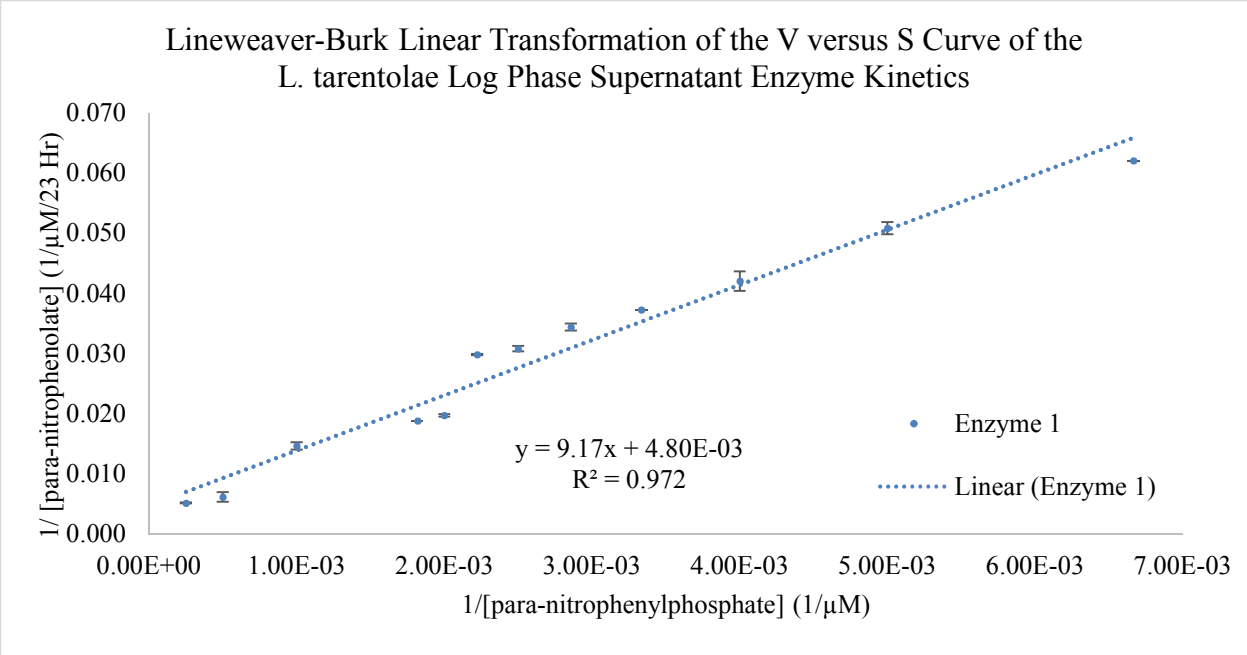

Figure 16. A typical Lineweaver-Burk linear transformation using *L. tarentolae* log phase supernatant as the enzyme source. This graph only depicts the response of Enzyme 1 with n=12 points. Each point is the mean ± standard deviation of n=3 replicates

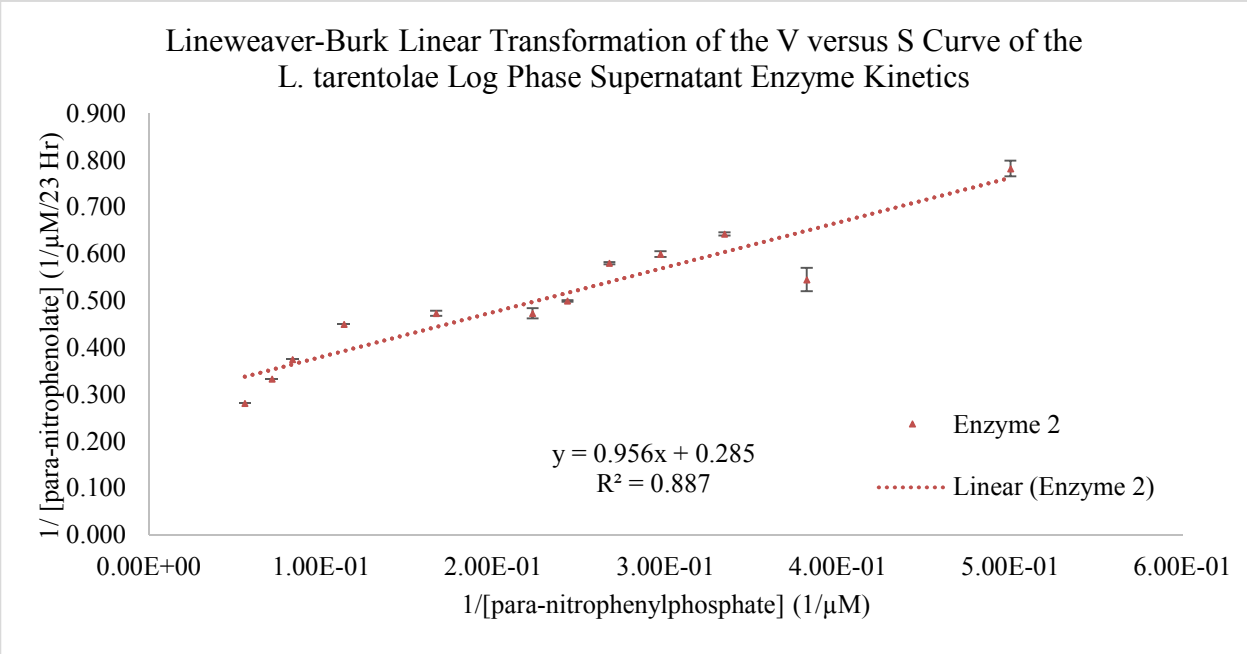

Figure 17. A typical Lineweaver-Burk linear transformation using *L. tarentolae* log phase supernatant as the enzyme source. This graph only depicts the response of Enzyme 2 with n=12 points. Each point is the mean ± standard deviation of n=3 replicates

Enzyme 1 is present and detectable during the course of the entire eight day growth curve (Figure 18). The k_M value for enzyme 1 changes subtly as a function of day in culture. The V_{MAX} value of enzyme 1 changes with culture age (Table 2 and Figure 18). This change, up to day five of the *L. tarentolae* growth curve, is likely due to increasing cell number, and thus increasing amount of total secreted enzyme. The apparent disconnect between the number of viable cells and calculated V_{Max} value of enzyme 1 that occurs on day 6-8 of the *L. tarentolae* growth curve may be explained in two ways. It could be that enzyme 1 is resistant to being denatured and remains active once secreted into the culture medium. It could also be the case that enzyme 1 is stored in *L. tarentolae* whole cells, and is released upon their death, thus leading to a plateau in the calculated V_{MAX} value of enzyme 1, due to an approximately constant amount of enzyme 1 being present in the culture medium. Incubation of day 8 supernatant with the glycosidase, that has recognition for N-linked carbohydrates, noticeably changed experimental k_M and V_{MAX} values of enzyme 1 relative to the non-glycosidase treated supernatant. The k_M decreased by 24.4 %, and the V_{MAX} increased by 13.5 % (Table 2).

Day in culture	K_M (µM)	V_{MAX} (µM/23 Hr)
1	1.36E03±1.3E02	54.9±1.1E-01
2	1.27E03±1.0E02	57.1±1.0E-01
3	1.11E03±9.1E01	63.3±9.0E-01
4	1.27E03±9.0E01	69.4±6.1E-01
5	1.91E03±1.3E02	208±1.0E01
6	1.56E03±6.0E01	159±7.0
7	1.10E03±3.0E01	192±9.0
8	1.28E03±5.0E01	200±8.0
8 + Glycosidase	968±1.3E02	227±50

Table 2. The calculated k_M and V_{MAX} values for enzyme 1 from *L. tarentolae* as a function of day in culture

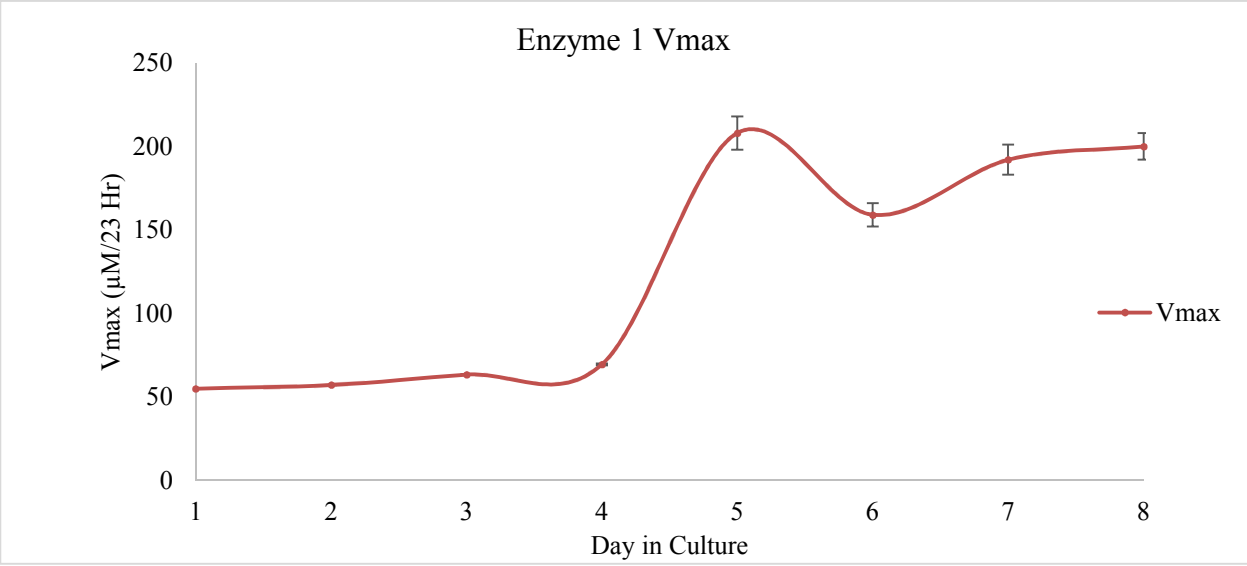

Figure 18. A plot of calculated V_{MAX} value (Y-axis) for enzyme 1 as a function of day in culture (X-axis). This value is not a simple function of culture age. Each point is the mean ± standard deviation of n=3 replicates

Enzyme 2 is not detectable during the first two days of the *L. tarentolae* growth curve, but becomes detectable on day 3 and remains detectable through day 8. The k_M value for enzyme 2 remains in the same order of magnitude from days 3-5 of culture. The k_M values from days 6-8 indicating that enzyme becomes less efficient at binding substrate as the culture ages. The V_{MAX} value of enzyme 2 remain consistent with culture age until senescence phase (Figure 19). There is a large increase in the V_{MAX} value of enzyme 2 on day 7 of culture (Table 3). This change as shown in Figure 19 occurs during the senescence phase of the *L. tarentolae* growth curve, and may indicate that the total amount of enzyme 2 in the culture medium increases as cells die. This suggests that the majority of enzyme 2 is stored and is secreted upon external stimulus. Incubation with a glycosidase drastically increased experimental k_M and V_{MAX} values of enzyme 2. The k_M increased by 92.5 %, and the V_{MAX} increased by 93.4 % compared to non-glycosidase incubated control.

Day in Culture	K_M (μM)	V_{MAX} (μM/24 Hr)
1	Not Detectable	Not Detectable
2	Not Detectable	Not Detectable
3	2.26±7.20E-02	1.40±2.00E-01
4	6.93±0.42	3.58±0.12
5	3.35±7.7E-02	3.51±2.9E-01
6	10.3±8.1E01	2.82±1.9E-01
7	36.6±1.8	16.2±7.0E-01
8	24.8±2.3	7.63±8.4E-01
8 + Glycosidase	331±14	115±17

Table 3. The calculated k_M or V_{MAX} values for enzyme 2 from *L. tarentolae* as a function of day in culture

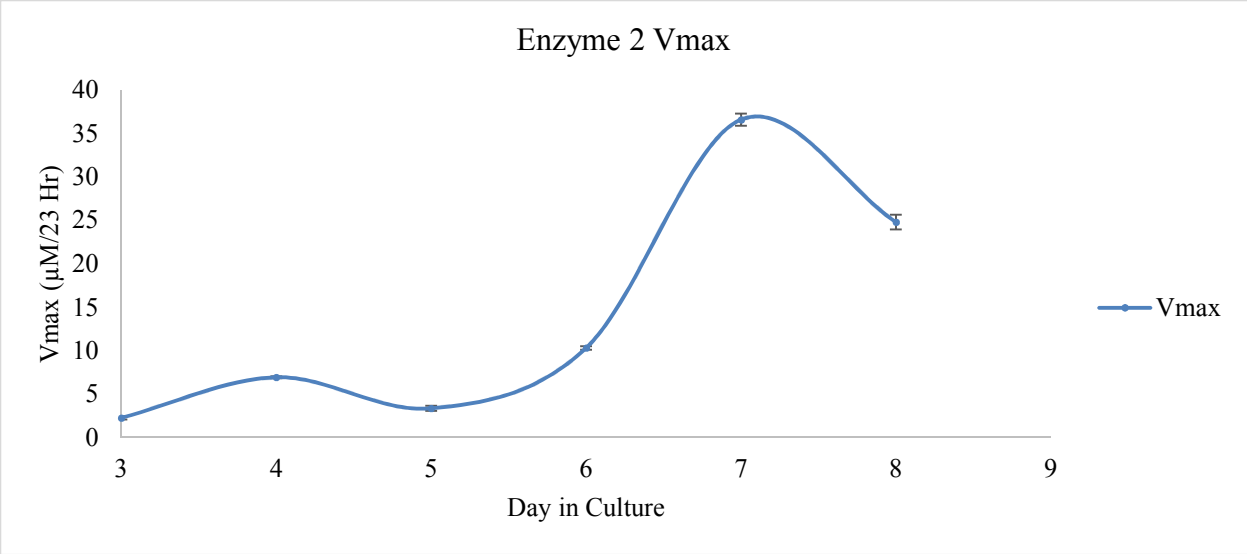

Figure 19. The calculated V_{MAX} (Y-axis) value for enzyme 2 as a function of *L. tarentolae* day in culture (X-axis). Each point is the mean ± standard deviation of n=3 replicates

Testing the Acute Effects of Electric Fields on *L. tarentolae* Growth Curves and Microscopy

The application of electric fields (50 Hz or 10,000 Hz, 100-500 µA, 30 min, cathodic, or symmetric biphasic, or anodic waveforms) to *L. tarentolae* whole cells followed by the MTT viability assay led to no statistically significant results ($p <, 0.05$ for paired, two tailed t-test; data not shown). The application of electric fields did lead to changes in cell clumping (Figures 20-25). The effect of frequency is observed by comparing Figure 20 to Figures 21 and 22. As the frequency increases from 50 Hz to 10,000 Hz, the amount of cell aggregation (clumping) drastically increases. The effect of current is observed when comparing Figure 20 to Figures 21 and 23. There are no large differences between 100 µA and 500 µA, but there is an increase in cell aggregation when comparing 50 Hz symmetric biphasic at 100 µA (Figure 23) or 500 µA (Figure 21) to control cells (Figure 20). The effect of waveform polarity is observed when comparing Figures 20 to Figures 23, 24, and 25. The application of any type of electric field causes an increase in cell aggregation. The largest effect on cell clumping caused by polarity

differences is caused by a 50 Hz, 100 µA, anodic electric field (Figure 25). The application of this electric field not only caused aggregation of cells, but also caused them to clump. We interpret cell clumping as an indication that the cells are stressed.

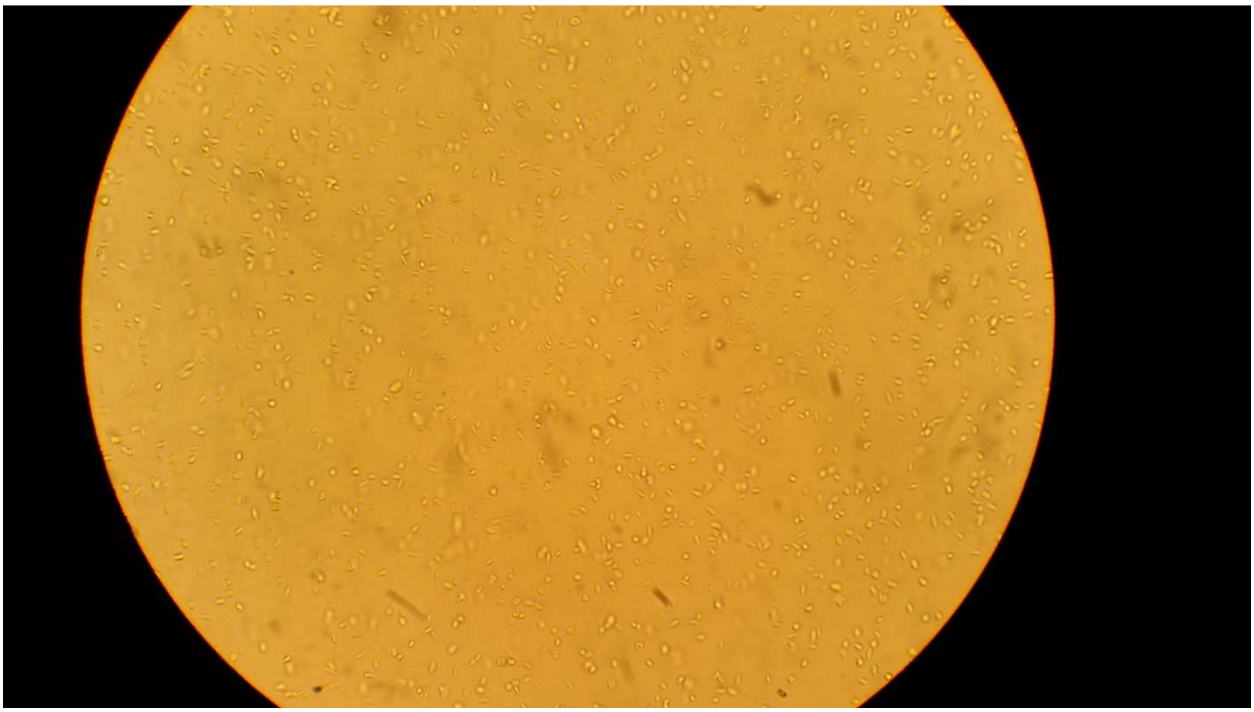

Figure 20. *L. tarentolae* lag phase control cells viewed at 400X magnification

Figure 21. *L. tarentolae* lag phase cells exposed to an electric field (50 Hz, 500 µA, 30 min, symmetric biphasic) viewed at 400X magnification. These cells exhibit several large clumps (circled areas)

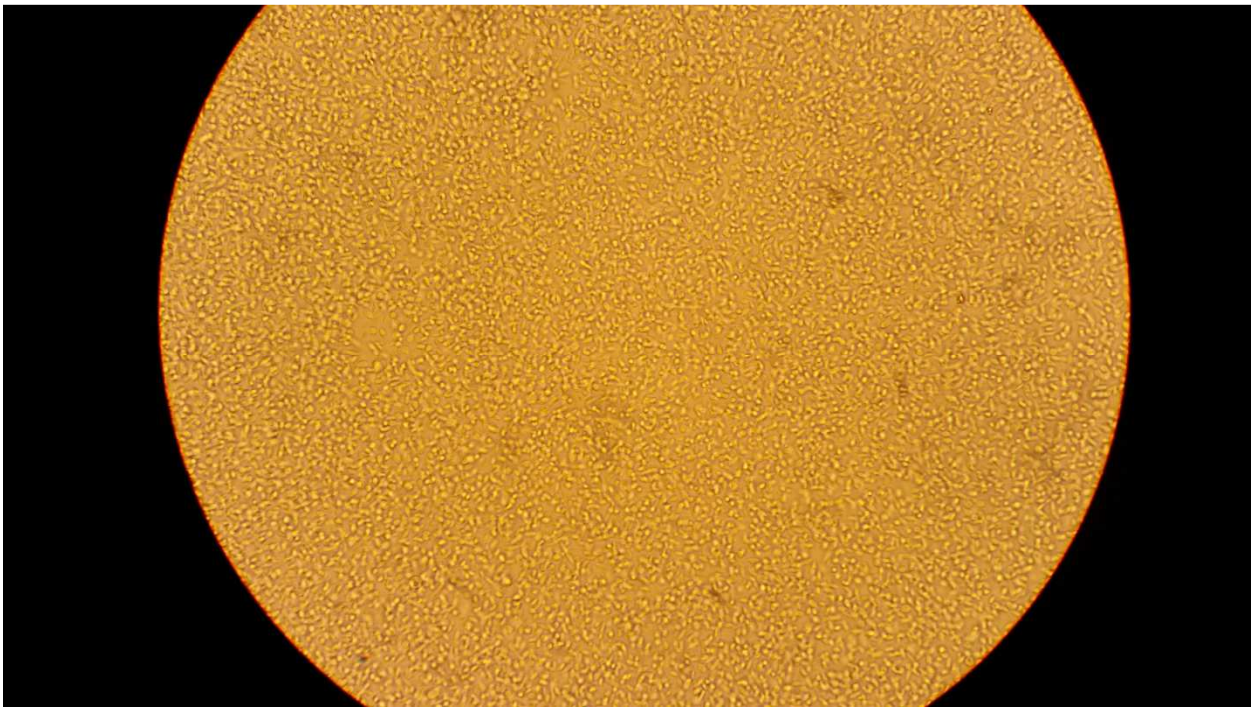

Figure 22. *L. tarentolae* lag phase cells exposed to an electric field (10,000 Hz, 500 µA, 30 min, symmetric biphasic) viewed at 400X magnification. These cells are completely packed into a single area

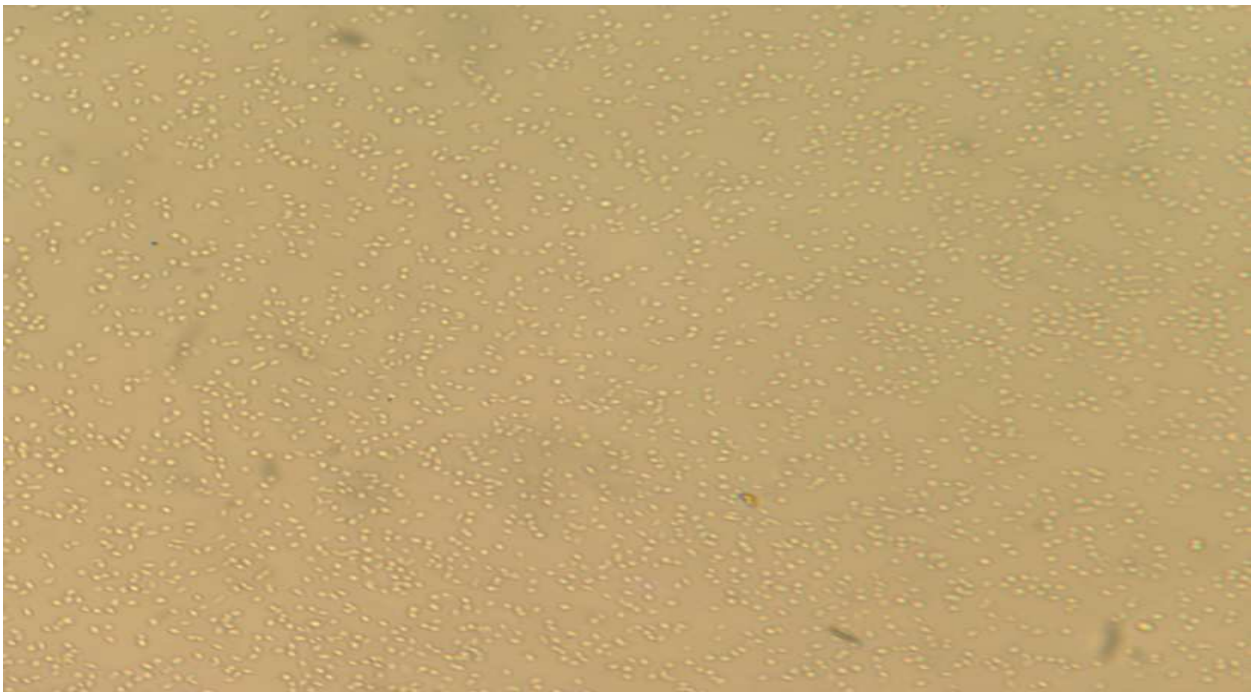

Figure 23. *L. tarentolae* lag phase cells exposed to an electric field (50 Hz, 100 µA, 30 min, symmetric biphasic) viewed at 400X magnification. These cells are more concentrated than typical *L. tarentolae* lag phase cells

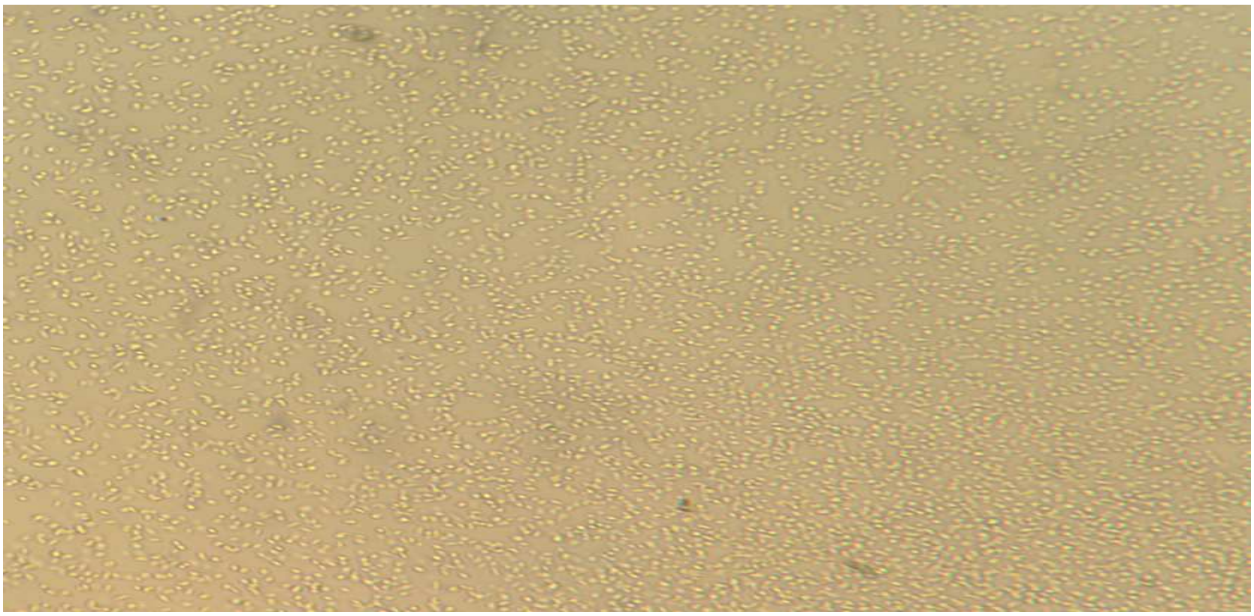

Figure 24. *L. tarentolae* lag phase cells exposed to an electric field (50 Hz, 100 µA, 30 min, cathodic) viewed at 400X magnification. These cells are more concentrated than typical *L. tarentolae* lag phase cells

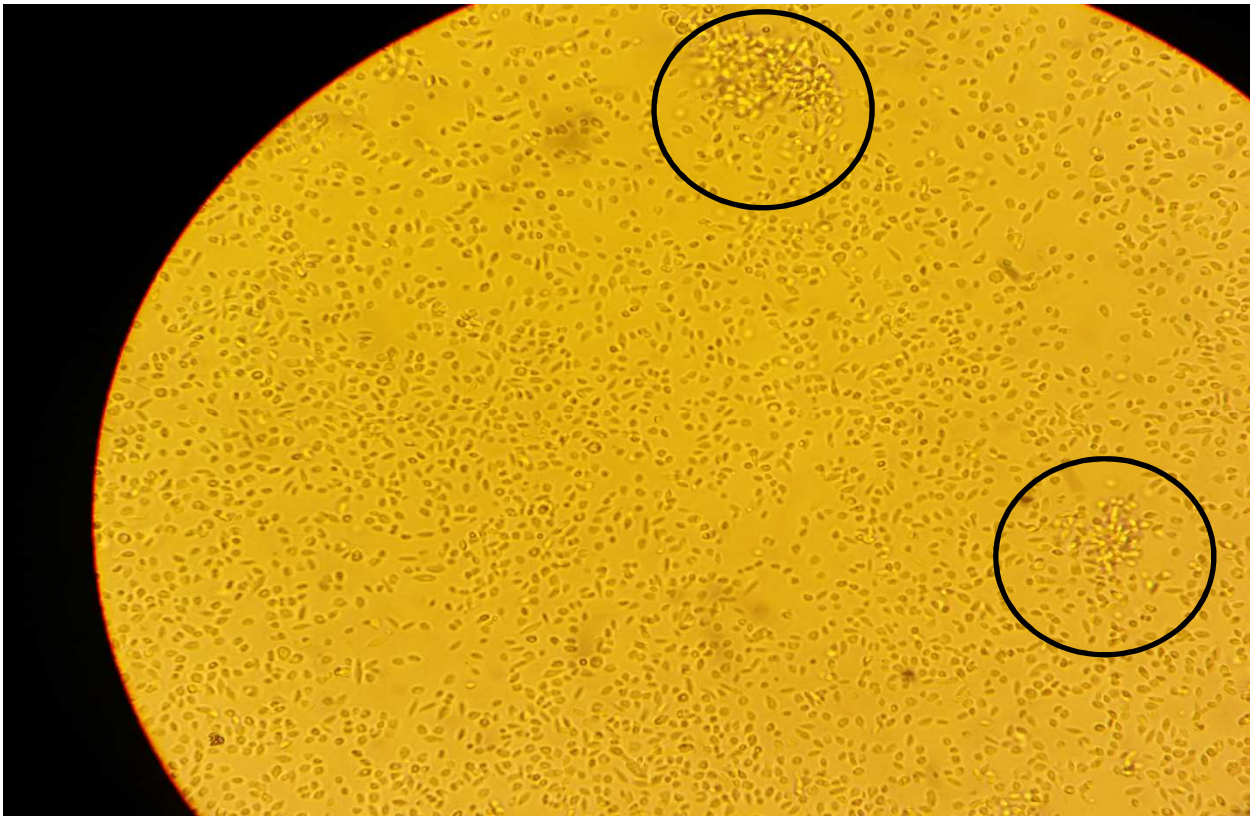

Figure 25. *L. tarentolae* lag phase cells exposed to an electric field (50 Hz, 100 µA, anodic) viewed at 400X magnification. The microscopic observations imply that the cells are moving toward the electrode during the electrode stimulation

Testing the Effects of Electric Fields on *L. tarentolae* Acid Phosphatase Activity in Supernatant or Pellet (Cells), Method 1

In method 1, the *L. tarentolae* log phase cells are separated, then electric fields (7 different current conditions, 3 different wave forms, and 2 different frequencies) were applied to small volumes (0.5–2.0 mL) of resuspended cell pellets or harvested cell supernatants. The samples were then assayed for acid phosphatase activity. For data to be shown, the experimental condition must be statistically different from the non-treated control ($p < 0.05$) in a paired, two tailed t-test. The data are plotted as percent different from same time control (Equation 8). A positive number means the treatment caused an increase in acid phosphatase activity compared

to control. A negative number means the treatment caused a decrease in acid phosphatase activity compared to control.

Equation 8.

Percent Different = (Experimental Activity – Control Activity)/(Control Activity) * 100 %

The application of a 50 Hz, cathodic electric field (7 different current conditions) to *L. tarentolae* supernatant or pellet followed by the assessment of acid phosphatase activity resulted in measurable effects in both the supernatant and pellet activity that were significantly different from their controls. Six out of seven conditions had an effect on supernatant acid phosphatase activity, but no consistent trend between current and supernatant activity was observed (Figure 26). Six out of seven conditions had an effect on pellet acid phosphatase activity, but no consistent trend between current and pellet activity was observed (Figure 27). The current conditions that affected both the supernatant and pellet acid phosphatase activity were 100, 150, 200, 250, or 400 μA. The 100, 250, or 400 μA currents caused an increase in supernatant activity, and a decrease in pellet activity. The 150 or 200 μA conditions caused an increase in both supernatant and pellet activity. All effects on either supernatant or pellet acid phosphatase activity were small (< 6 % different than control).

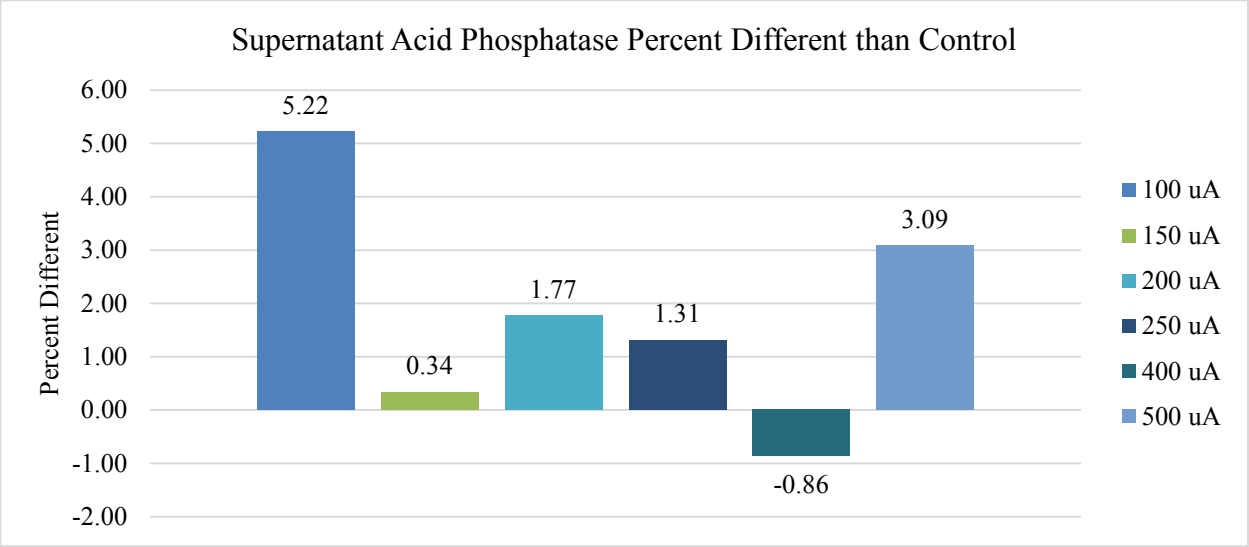

Figure 26. The effects of a 50 Hz, cathodic electric field at various current exposures on *L. tarentolae* secreted acid phosphatase are plotted as percent different from same time control

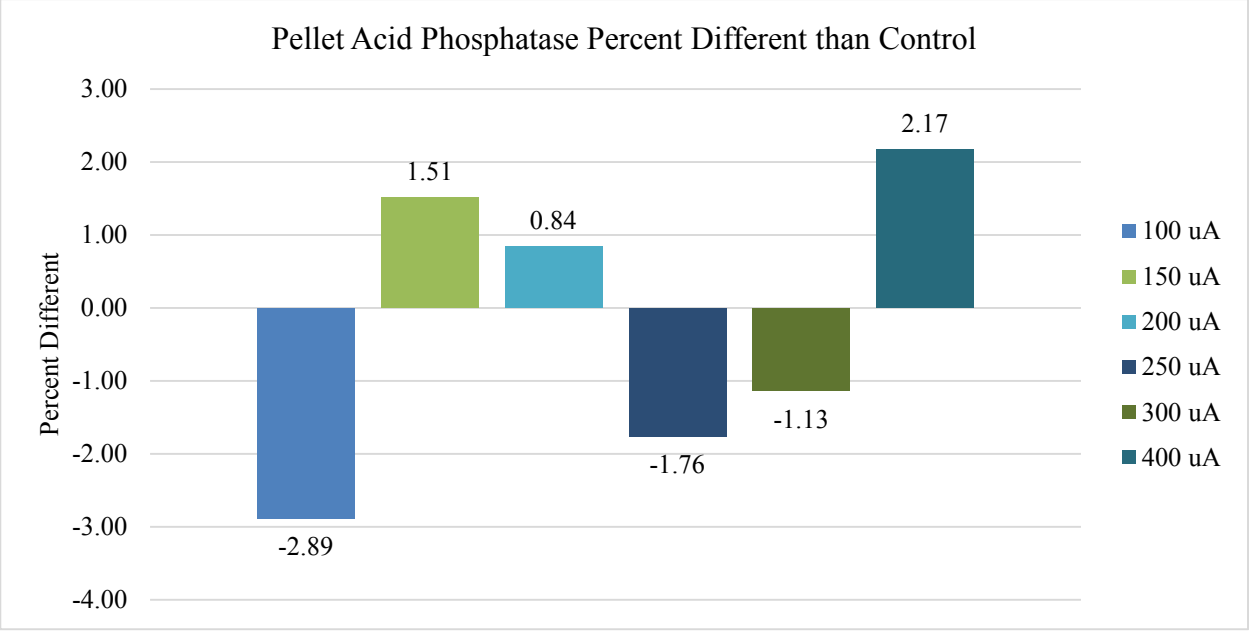

Figure 27. The effects of a 50 Hz, cathodic electric field at various current exposures on *L. tarentolae* cell pellet acid phosphatase are plotted as percent different from same time control

The application of a 50 Hz, symmetric biphasic electric field (7 different current conditions) to *L. tarentolae* supernatant or pellet followed by the assessment of acid phosphatase

activity resulted in measurable effects in both the supernatant and pellet activity that were significantly different from their controls. Six out of seven conditions had an effect on supernatant acid phosphatase activity, but no consistent trend between current and supernatant activity was observed (Figure 28). Five out of seven conditions had an effect on pellet acid phosphatase activity, but no consistent trend between current and pellet activity was observed (Figure 29). The current conditions that affected both the supernatant and pellet acid phosphatase activity were 100, 150, 200, or 400 µA. The 100 or 400 µA currents caused an increase in supernatant activity, and a decrease in pellet activity. The 150 µA condition caused an increase in both supernatant and pellet activity. The 200 µA condition caused a decrease in both supernatant and pellet activity. All effects on either supernatant or pellet acid phosphatase activity were small (< 7 % different than control).

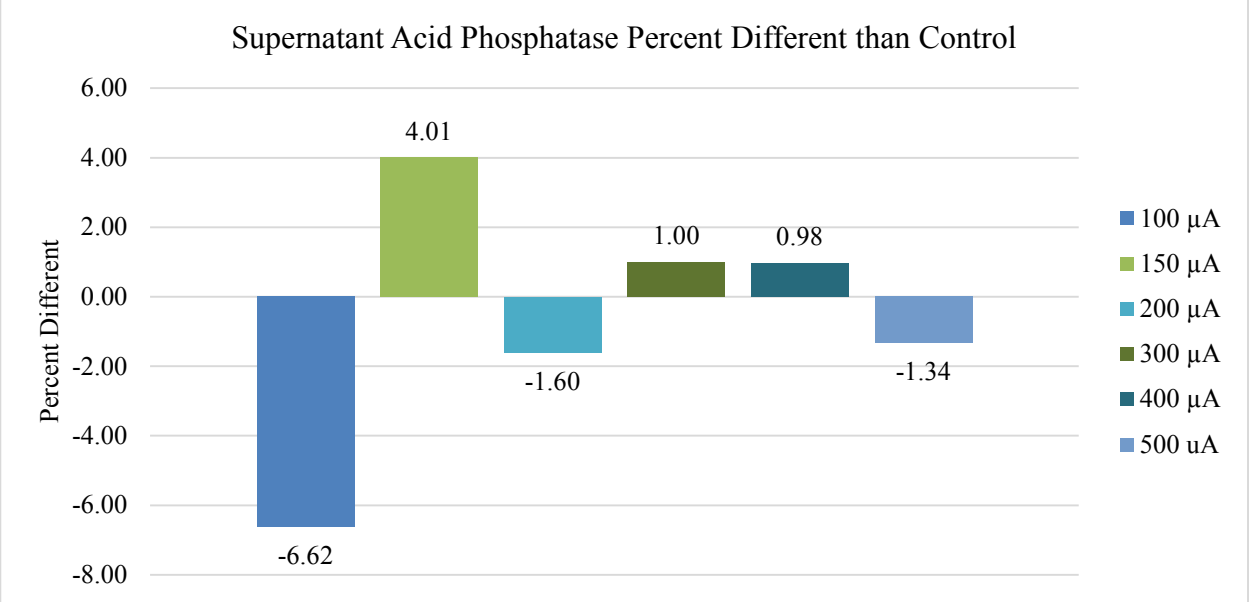

Figure 28. The effects of a 50 Hz, symmetric biphasic electric field at various current exposures on *L. tarentolae* secreted acid phosphatase are plotted as percent different from same time control

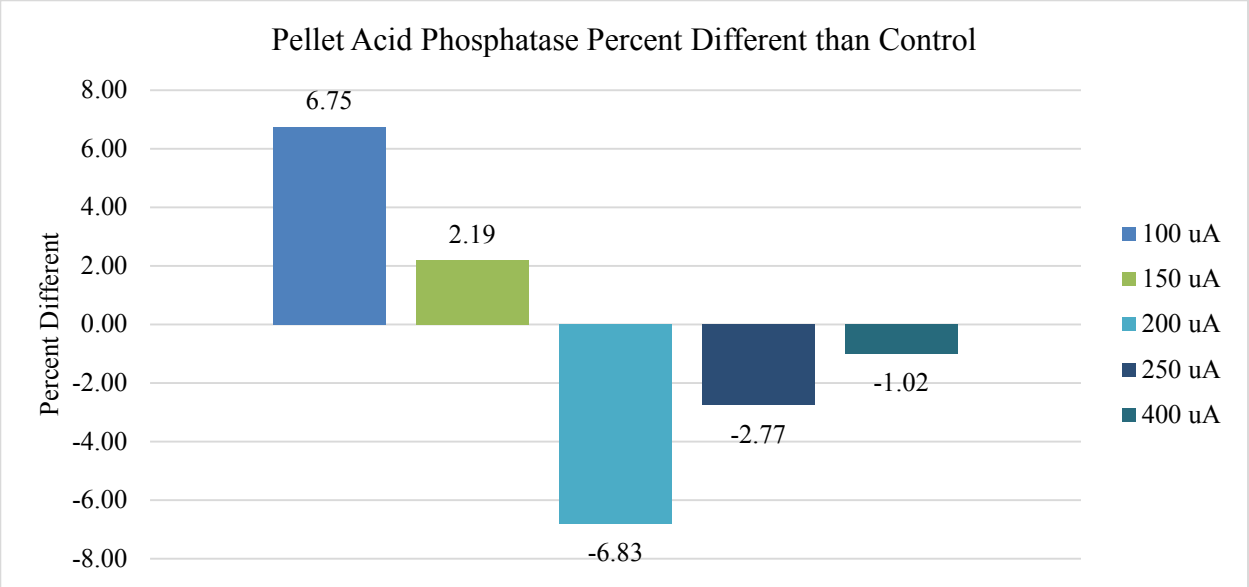

Figure 29. The effects of a 50 Hz, symmetric biphasic electric field at various current exposures on *L. tarentolae* cell pellet acid phosphatase are plotted as percent different from same time control

The application of a 50 Hz, anodic electric field (7 different current conditions) to *L. tarentolae* supernatant or pellet followed by the assessment of acid phosphatase activity resulted in measurable effects in both the supernatant and pellet activity that were different from their controls. Six out of seven conditions had an effect on supernatant acid phosphatase activity, but no consistent trend between current and supernatant activity was observed (Figure 30). Five out of seven conditions had an effect on pellet acid phosphatase activity, but no consistent trend between current and pellet activity was observed (Figure 31). The current conditions that affected both the supernatant and pellet acid phosphatase activity were 150, 200, 250, or 400 µA. The 150 µA condition caused an increase in supernatant and pellet activity. The 200 µA condition caused an increase in supernatant activity and a decrease in pellet activity. The 250 µA condition caused a decrease in both supernatant and pellet activity. The 400 µA condition caused

a decrease in supernatant activity, but an increase in pellet activity. All effects on either supernatant or pellet acid phosphatase activity were small (< 6 % different than control).

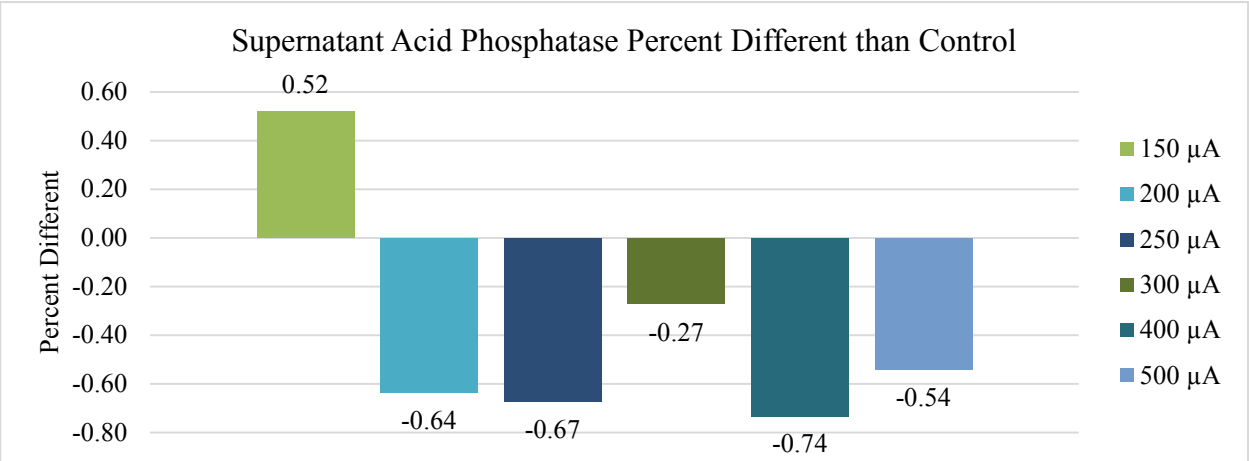

Figure 30. The effects of a 50 Hz, anodic electric field at various current exposures on *L. tarentolae* secreted acid phosphatase are plotted as percent different from same time control

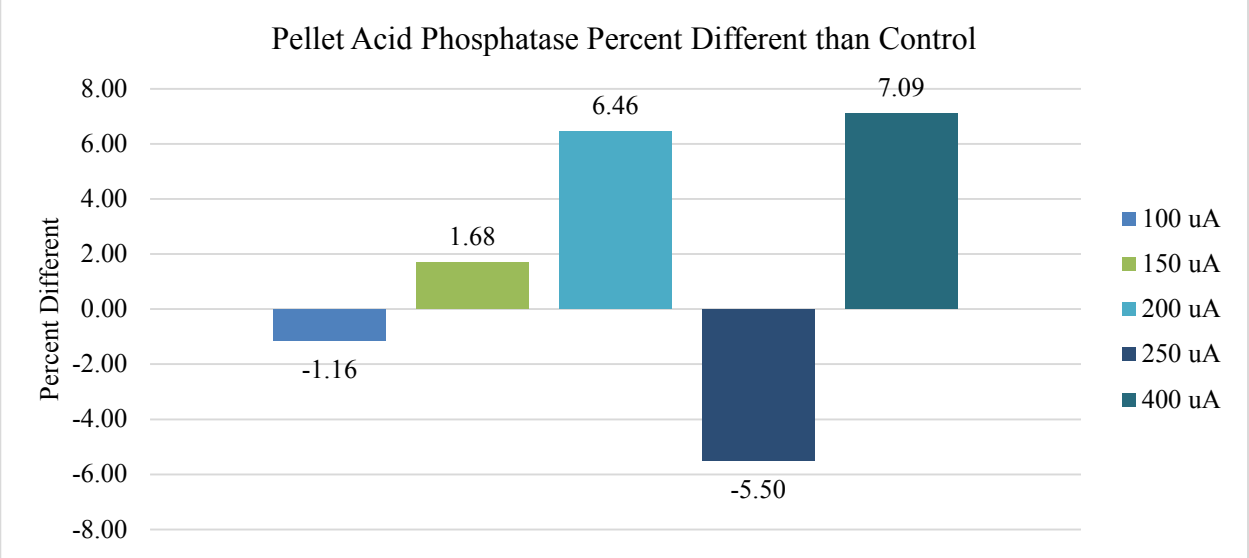

Figure 31. The effects of a 50 Hz, anodic electric field at various current exposures on *L. tarentolae* cell pellet acid phosphatase are plotted as percent different from same time control

The application of a 10,000 Hz, cathodic electric field (7 different current conditions) to *L. tarentolae* supernatant or pellet followed by the assessment of acid phosphatase activity

resulted in measurable effects in both the supernatant and pellet activity that were significantly different from their controls. Six out of seven conditions had an effect on supernatant acid phosphatase activity (Figure 32). An upward trend was observed between 100-300 µA. Under these conditions, more current application resulted in more acid phosphatase activity. Five out of seven conditions had a negative effect on pellet activity (Figure 33), suggesting a reciprocal trend between current and pellet activity was observed. The 250 or 500 µA conditions led to the largest decreases in pellet activity. The current conditions that affected both the supernatant and pellet acid phosphatase activity were 100, 150, 250, or 400 µA. All of these conditions caused an increase in supernatant activity, and a decrease in pellet activity. In general the effects of a 10,000 Hz cathodic electric field were substantially larger than the effects of a 50 Hz cathodic electric field.

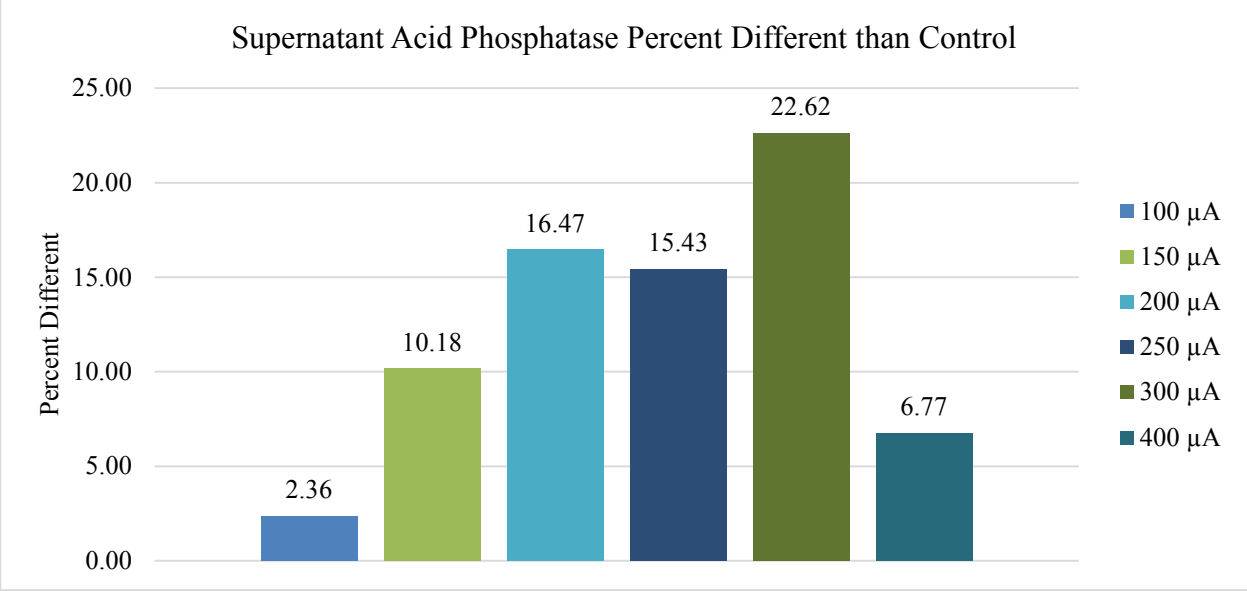

Figure 32. The effects of a 10,000 Hz, cathodic electric field at various current exposures on *L. tarentolae* secreted acid phosphatase are plotted as percent different from same time control

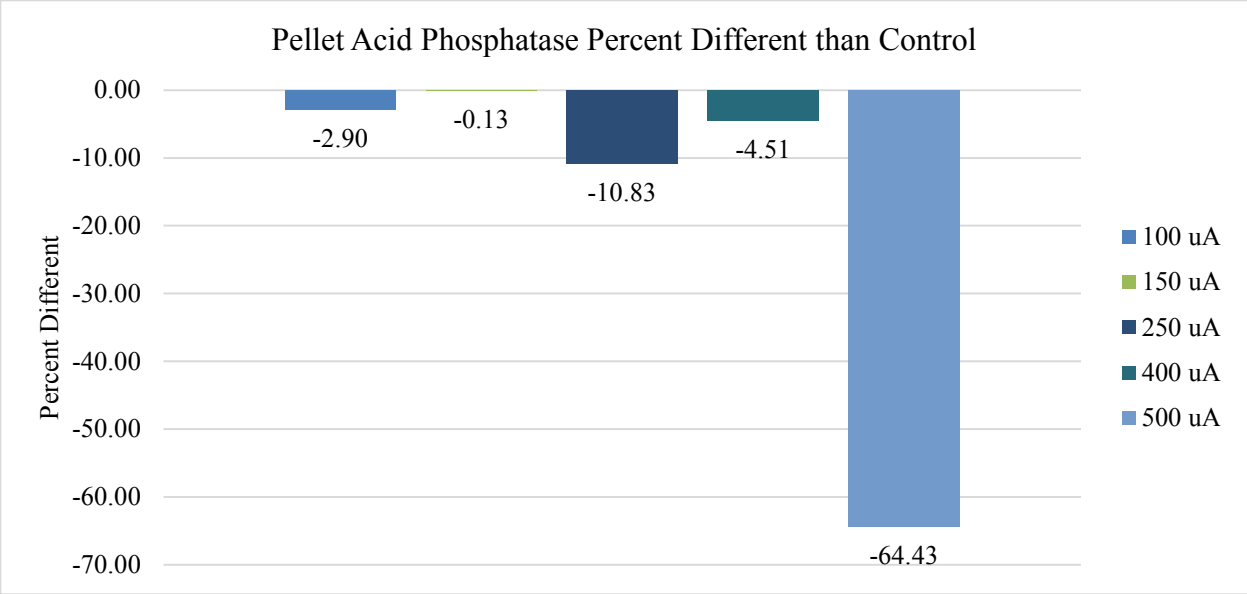

Figure 33. The effects of a 10,000 Hz, cathodic electric field at various current exposures on *L. tarentolae* cell pellet acid phosphatase are plotted as percent different from same time control

The application of a 10,000 Hz, symmetric biphasic electric field (7 different current conditions) to *L. tarentolae* supernatant or pellet followed by the assessment of acid phosphatase activity resulted in measurable effects in both the supernatant and pellet activity that were significantly different from their controls. Seven out of seven conditions had an effect on supernatant acid phosphatase activity (Figure 34). The application of 100, 150, or 200 µA resulted in greater enzyme activation than did the application of 250, 300, 400, or 500 µA. There is an apparent threshold between 200 and 250 µA current application, where by applying less current resulted in greater acid phosphatase activity. Seven out of seven conditions had an effect on pellet acid phosphatase activity (Figure 35), but no consistent trend between current and pellet activity was observed. The current conditions that affected both the supernatant and pellet acid phosphatase activity were 100, 150, 200, 250, 300, 400 or 500 µA. The 100, 150, 200, 250, 300, or 500 µA currents caused an increase in supernatant activity, and a decrease in pellet activity. The 400 µA condition caused a decrease in both supernatant and pellet activity.

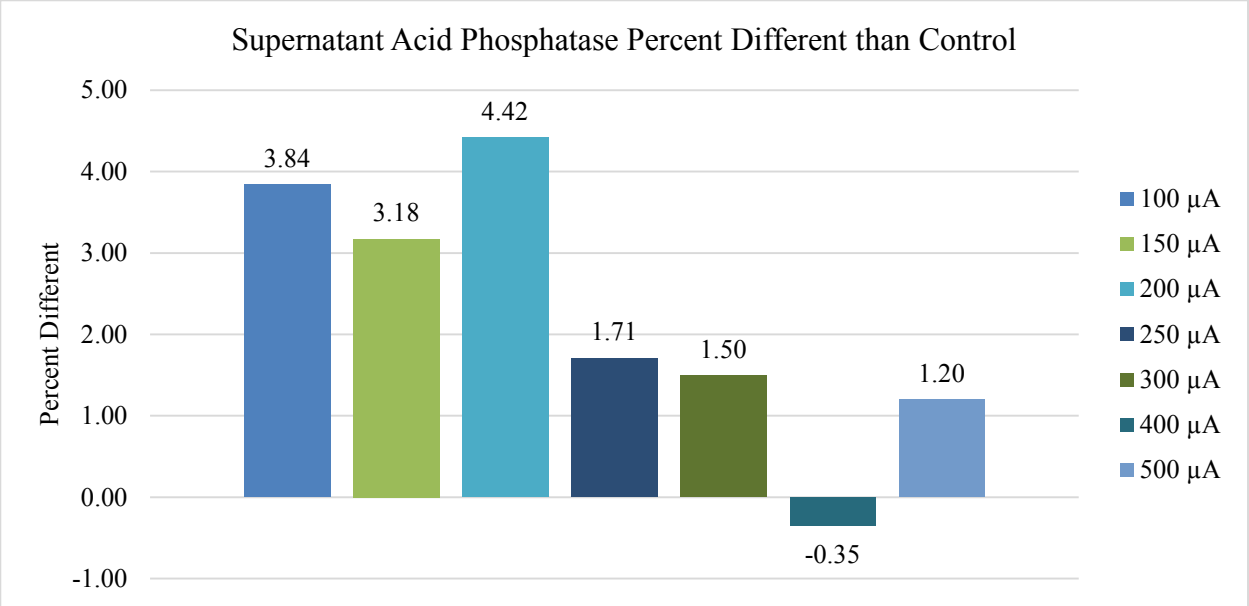

Figure 34. The effects of a 10,000 Hz, symmetric biphasic electric field at various current exposures on *L. tarentolae* secreted acid phosphatase are plotted as percent different from same time control

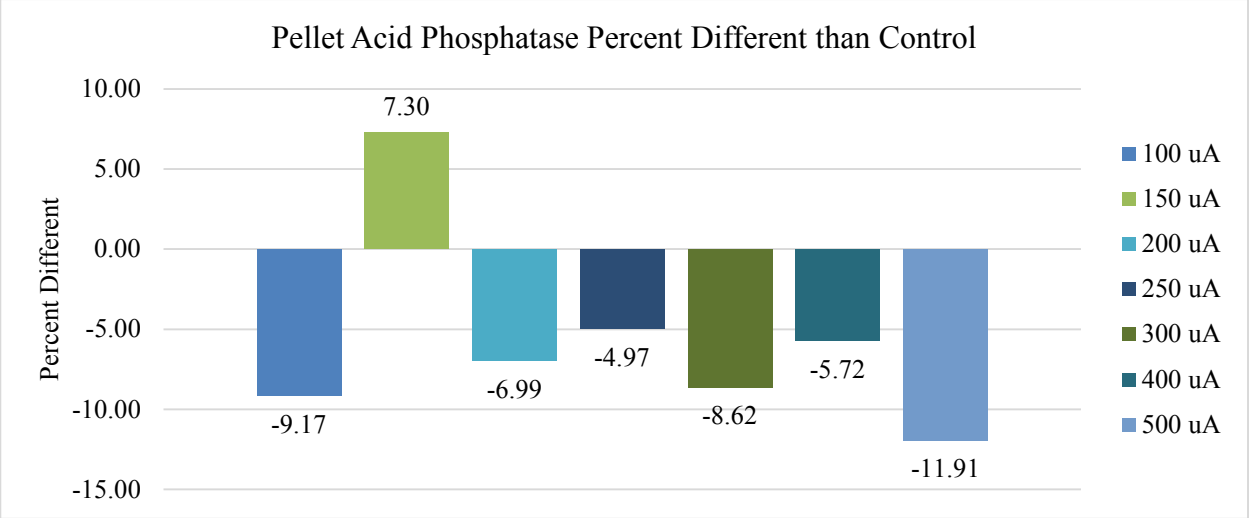

Figure 35. The effects of a 10,000 Hz, symmetric biphasic electric field at various current exposures on *L. tarentolae* cell pellet acid phosphatase are plotted as percent different from same time control

The application of a 10,000 Hz, anodic electric field (7 different current conditions) to *L. tarentolae* supernatant or pellet followed by the assessment of acid phosphatase activity resulted

in measurable effects in both the supernatant and pellet activity that were significantly different from their controls. Seven out of seven conditions had an effect on supernatant acid phosphatase activity (Figure 36). Lower current applications resulted in less detectable SAP activity. Higher current applications resulted in more detectable SAP activity. There is an apparent threshold between 200 and 250 µA, where by more current results in more SAP activity. Six out of seven conditions had an effect on pellet acid phosphatase activity (Figure 37). There is an apparent trend between 150-400 µA where by applying less current leads to greater deactivation of the enzyme activity. The current conditions that affected both the supernatant and pellet acid phosphatase activity were 100, 150, 200, 300, 400 or 500 µA. The application of currents between 100-400 µA caused an increase in supernatant and a decrease in pellet activity. The 500 µA condition caused an increase in both supernatant activity and in pellet activity.

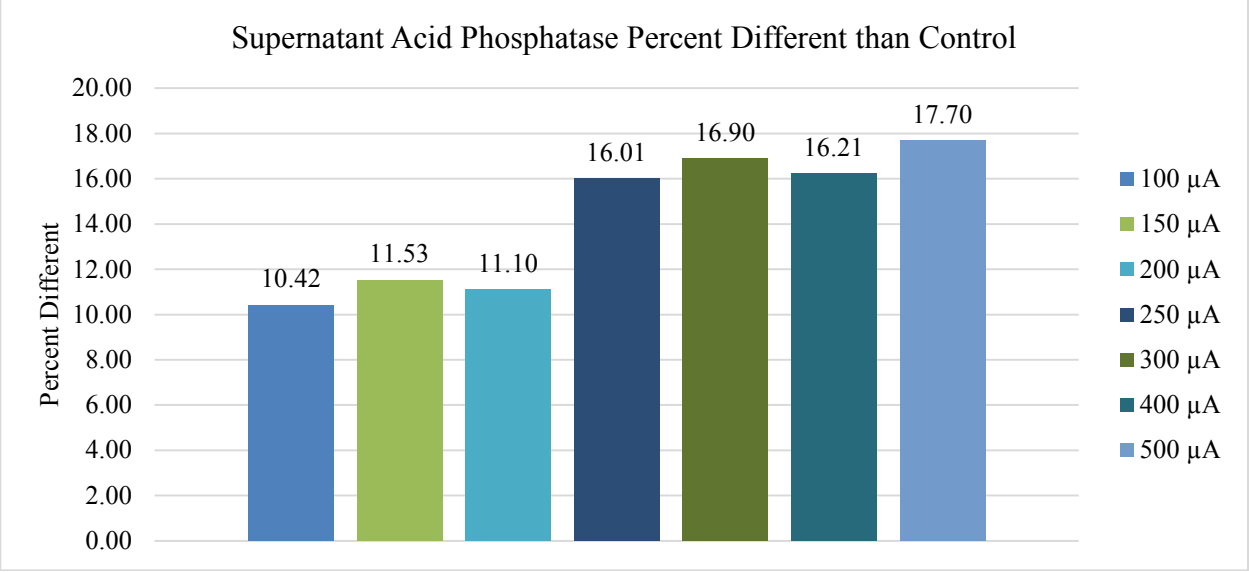

Figure 36. The effects of a 10,000 Hz, anodic electric field at various current exposures on *L. tarentolae* secreted acid phosphatase are plotted as percent different from same time control

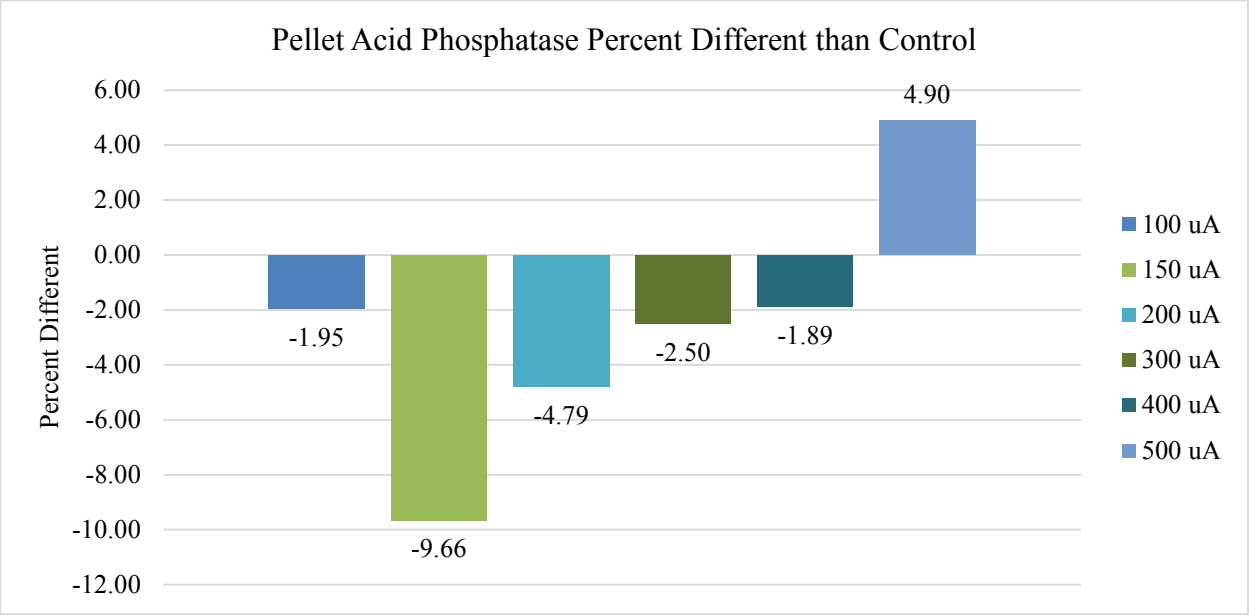

Figure 37. The effects of a 10,000 Hz, anodic electric field at various current exposures on *L. tarentolae* cell pellet acid phosphatase are plotted as percent different from same time control

Testing the Effects of Electric Fields on *L. tarentolae* Acid Phosphatase Activity in Supernatant or Pelet (Cells), Method 2

In method 2, small volumes (0.5–2.0 mL) of *L. tarentolae* log phase cells are exposed to electric fields, followed by separation, suspension of pellets, and assaying of acid phosphatase activity. For data to be shown, the experimental condition must be significantly different from the non-treated control ($p < 0.05$) in a paired, two tailed t-test. The data are plotted as percent different from same time control (Equation 8).

The application of a 50 Hz, cathodic electric field (7 different current conditions) to *L. tarentolae* whole cells followed by the separation and assessment of acid phosphatase activity resulted in measurable effects in both the supernatant and pellet activity that were significantly different from their controls. Five out of seven conditions had an effect on supernatant acid phosphatase activity (Figure 38), but there was no consistent trend between the current applied and the effect on enzyme activity. Six out of seven conditions had an effect on pellet acid

phosphatase activity (Figure 39), but there was no consistent trend between the current applied and the effect on enzyme activity. The current conditions that affected both the supernatant and pellet acid phosphatase activity were 100, 300, 400 or 500 µA. The application of 100 µA caused an increase in supernatant and a decrease in pellet activity. The application of 300 or 500 µA caused a decrease in supernatant activity and an increase in pellet activity. The application of 400 µA caused an increase in both supernatant and pellet activity.

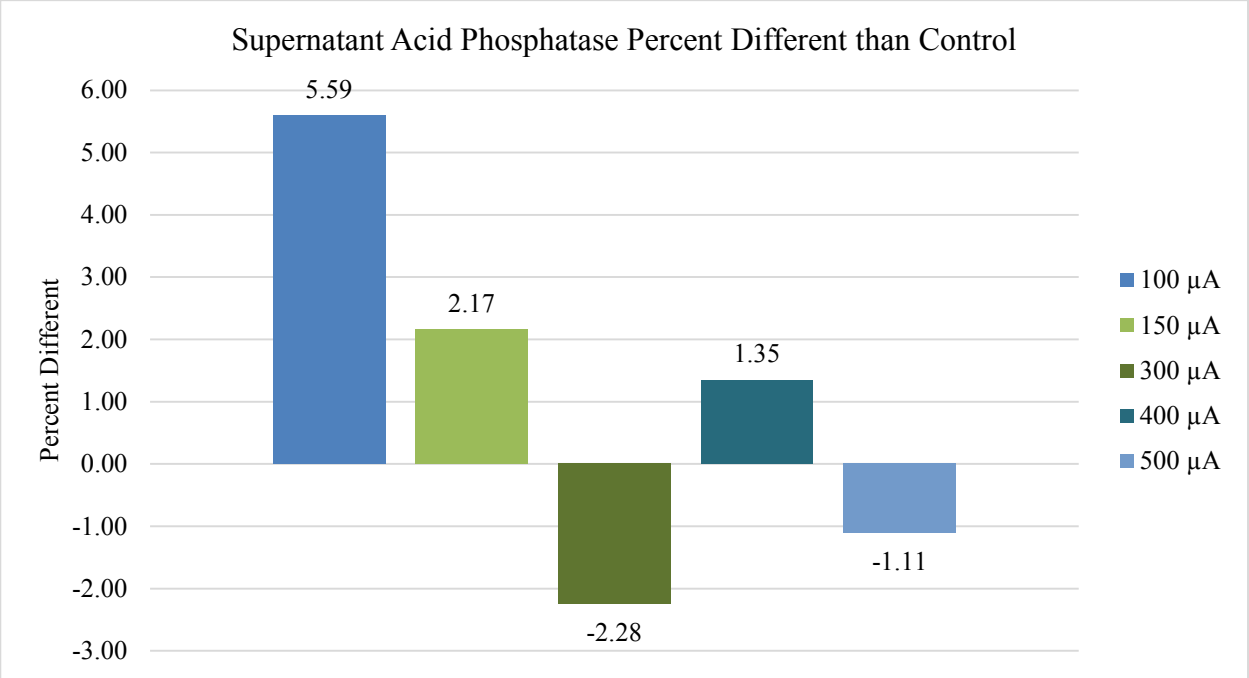

Figure 38. The effects of a 50 Hz, cathodic electric field at various current exposures on *L. tarentolae* secreted acid phosphatase are plotted as percent different from same time control

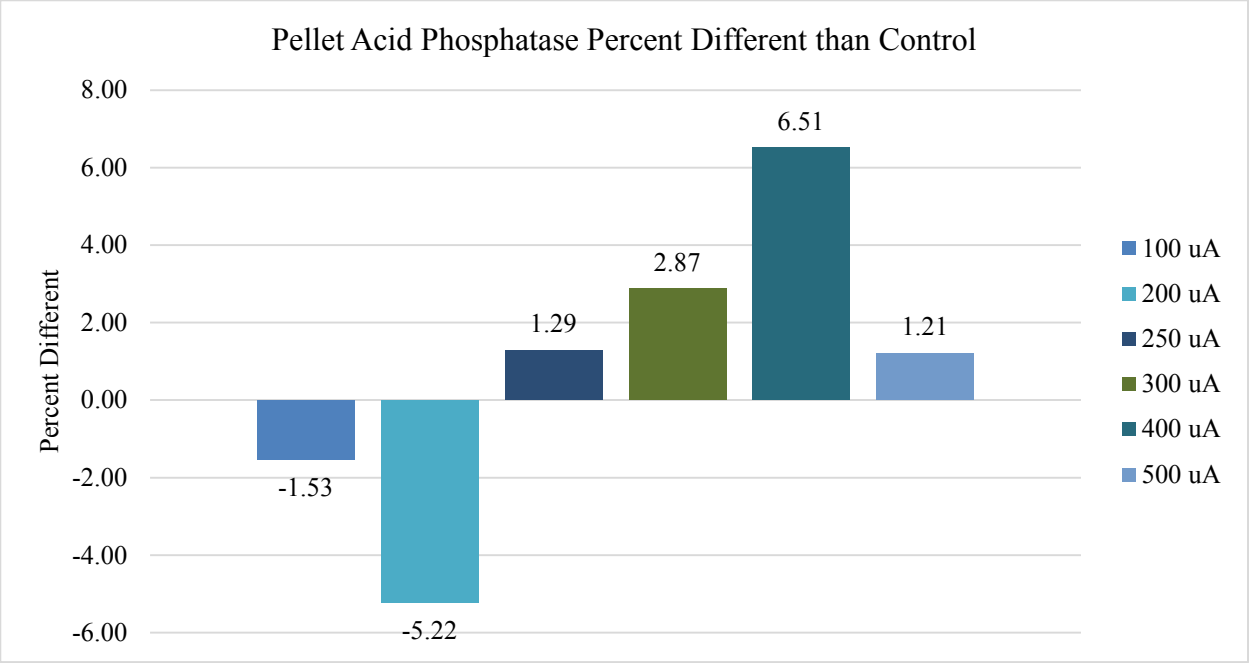

Figure 39. The effects of a 50 Hz, cathodic electric field at various current exposures on *L. tarentolae* cell pellet acid phosphatase are plotted as percent different from same time control

The application of a 50 Hz, symmetric biphasic electric fields (7 different current conditions) to *L. tarentolae* whole cells followed by the separation and assessment of acid phosphatase activity resulted in measurable effects on only the pellet activity that were significantly different from their non-treated controls. Zero out of seven conditions had an effect on supernatant acid phosphatase activity (data not shown). Two out of seven conditions had an effect on pellet acid phosphatase activity (Figure 40), but there was no obvious trend between the current applied and the effect on enzyme activity. There were no current conditions that affected both the supernatant and pellet acid phosphatase activity.

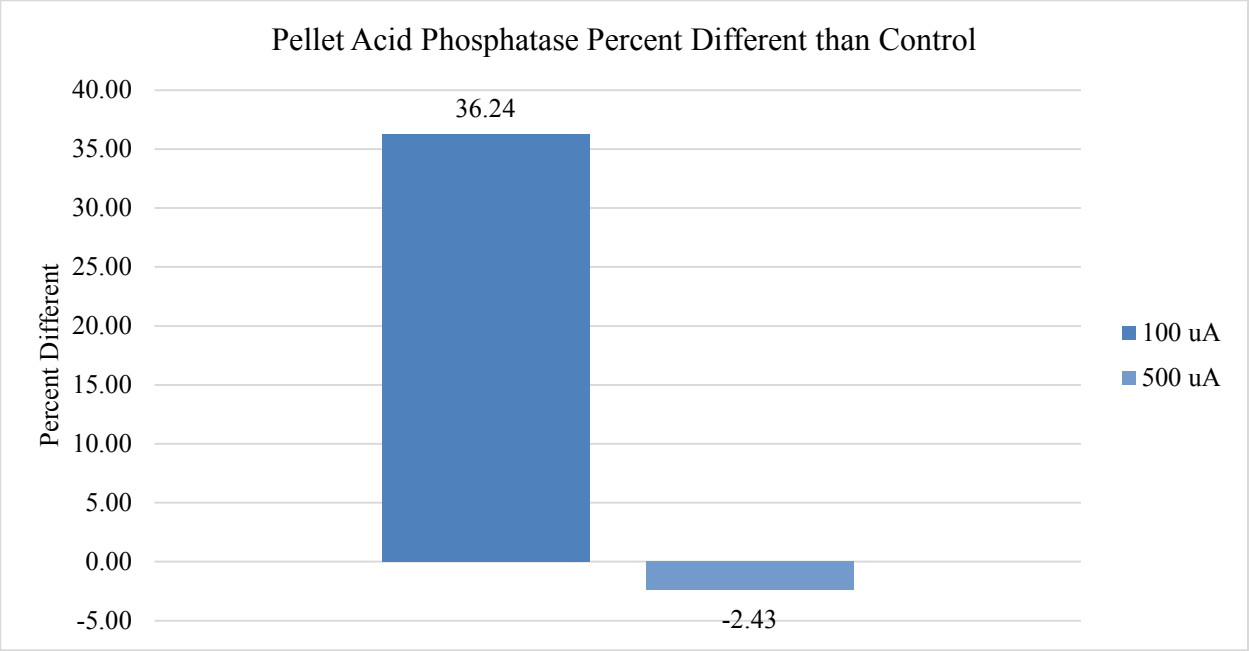

Figure 40. The effects of a 50 Hz, symmetric biphasic electric field at various current exposures on *L. tarentolae* cell pellet acid phosphatase are plotted as percent different from same time control

The application of a 50 Hz, anodic electric field (7 different current conditions) to *L. tarentolae* whole cells followed by the separation and assessment of acid phosphatase activity resulted in measurable effects in both the supernatant and pellet activity that was different from their non-treated controls. Two out of seven conditions had an effect on supernatant acid phosphatase activity (Figure 41), but there was no consistent trend between the current applied and the effect on enzyme activity. Five out of seven conditions had an effect on pellet acid phosphatase activity (Figure 42), but there was no consistent trend between the current applied and the effect on enzyme activity. The current condition that affected both the supernatant and pellet acid phosphatase activity was 400 µA, and this condition caused an increase in both the supernatant and pellet activity.

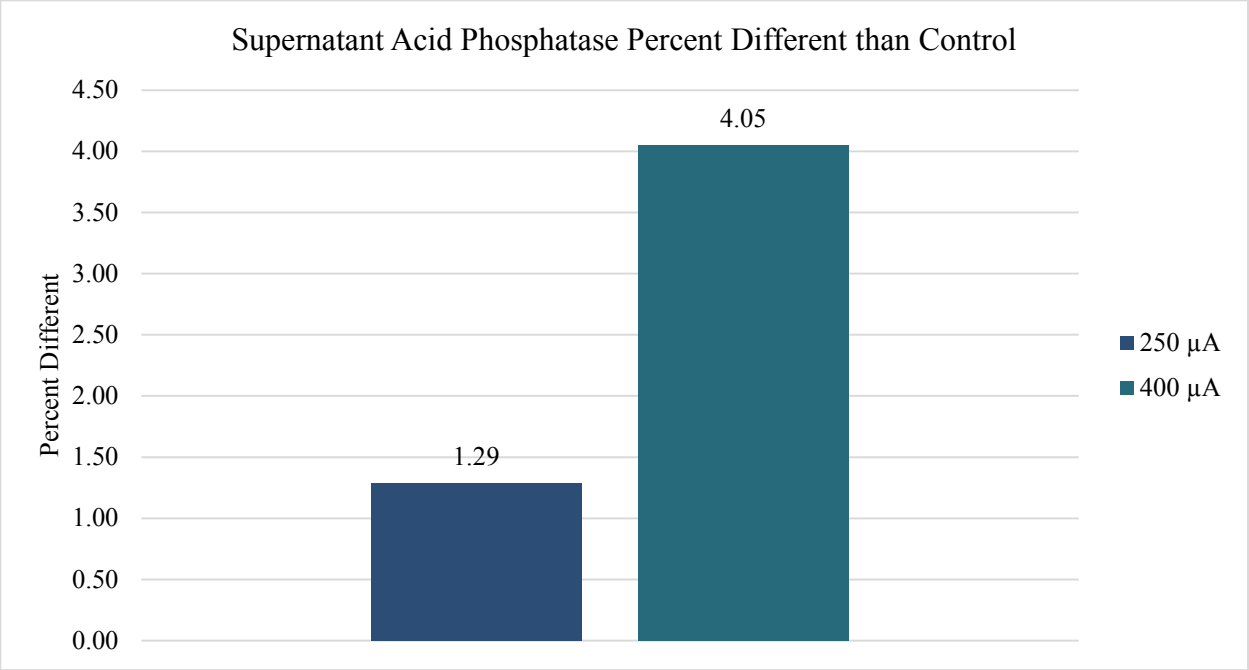

Figure 41. The effects of a 50 Hz, anodic electric field at various current exposures on *L. tarentolae* secreted acid phosphatase are plotted as percent different from same time control

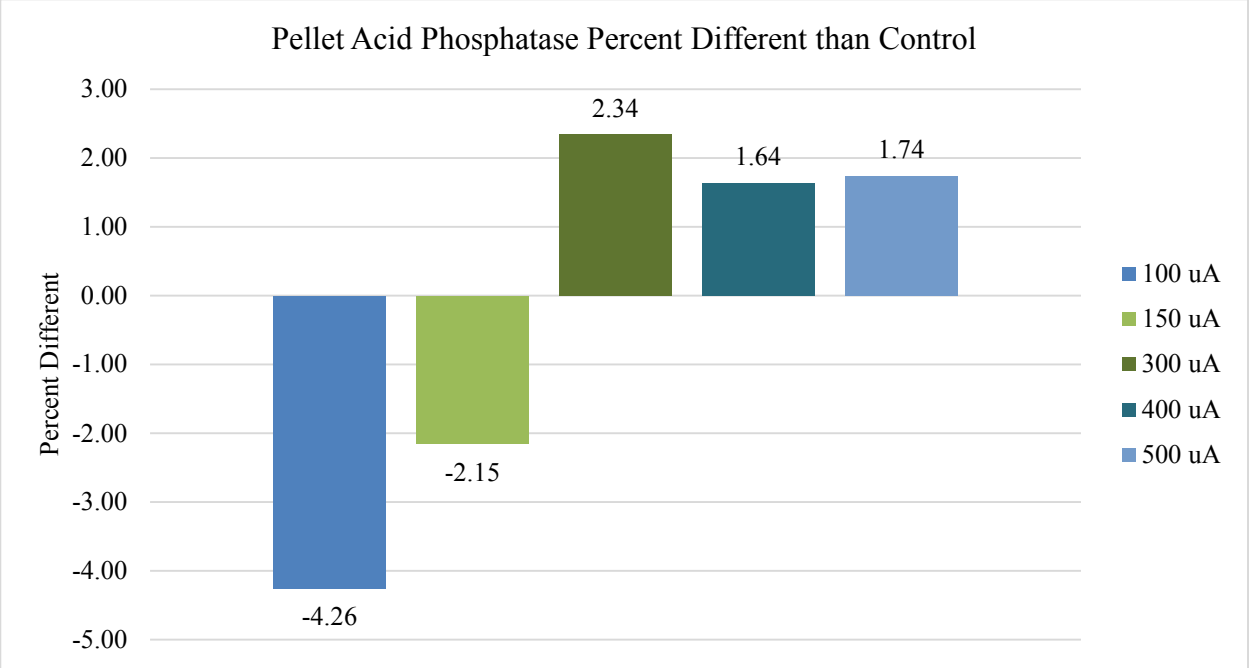

Figure 42. The effects of a 50 Hz, anodic electric field at various current exposures on *L. tarentolae* cell pellet acid phosphatase are plotted as percent different from same time control

The application of a 10,000 Hz, cathodic electric field (7 different current conditions) to *L. tarentolae* whole cells followed by the separation and assessment of acid phosphatase activity resulted in measurable effects in both the supernatant and pellet activity that were significantly different from their non-treated controls. Five out of seven conditions had an effect on supernatant acid phosphatase activity (Figure 43). An apparent trend exists between 300-500 µA where by more current leads to less enzyme activation. Five out of seven conditions had an effect on pellet acid phosphatase activity (Figure 44), but there was no consistent trend between the current applied and the effect on enzyme activity. The current conditions that affected both the supernatant and pellet acid phosphatase activity were 150, 300, or 400 µA. The application of 150 µA resulted in decreased activity in both the supernatant and pellet. The 300 µA condition caused an increase in supernatant activity and in pellet activity. The 400 µA condition caused an increase in supernatant activity, but a decrease in pellet activity.

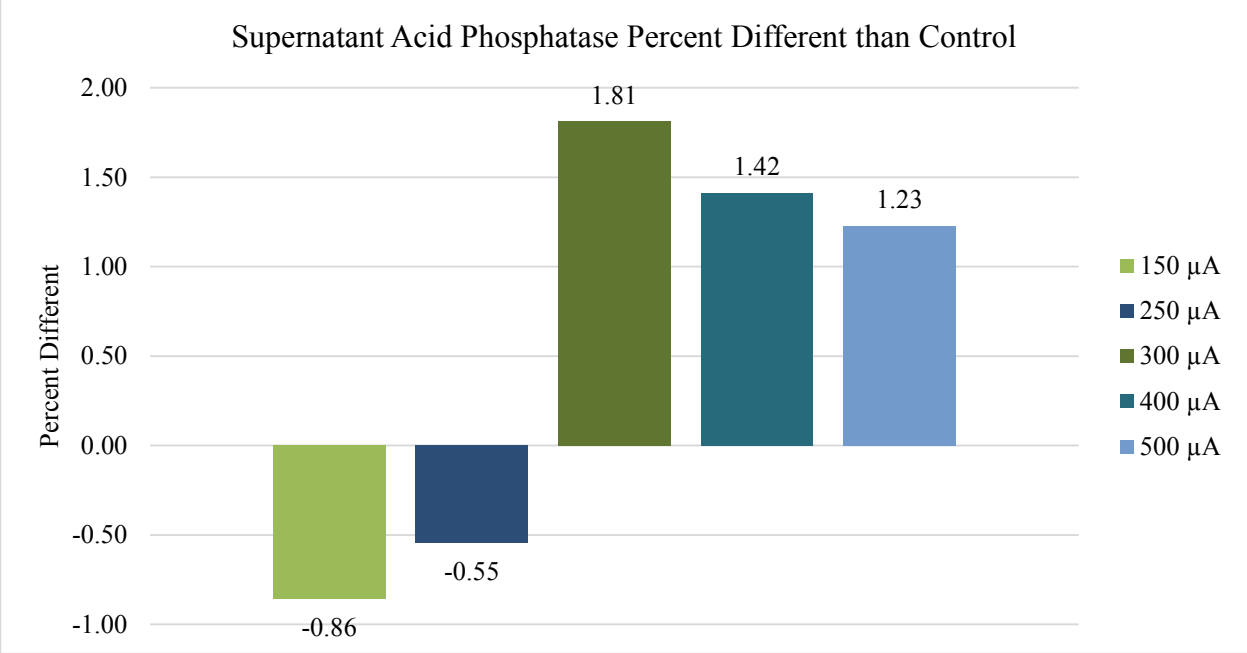

Figure 43. The effects of a 10,000 Hz, cathodic electric field at various current exposures on *L. tarentolae* secreted acid phosphatase are plotted as percent different from same time control

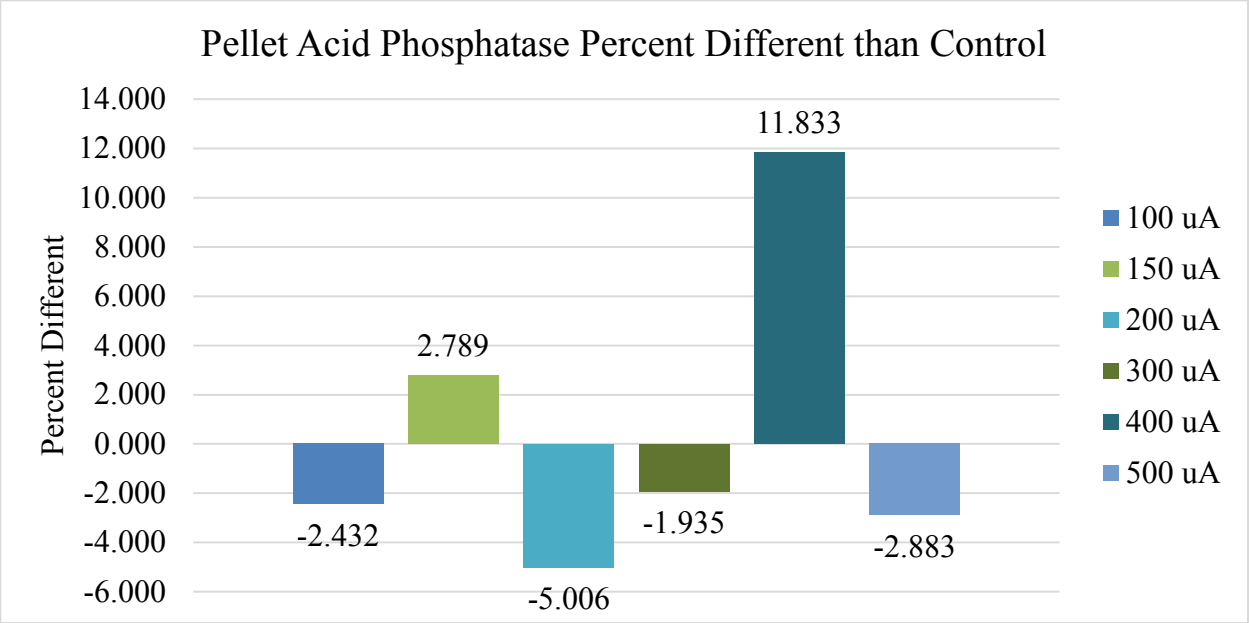

Figure 44. The effects of a 10,000 Hz, cathodic electric field at various current exposures on *L. tarentolae* cell pellet acid phosphatase are plotted as percent different from same time control

The application of a 10,000 Hz, symmetric biphasic electric field (7 different current conditions) to *L. tarentolae* whole cells followed by the separation and assessment of acid phosphatase activity resulted in measurable effects in both the supernatant and pellet activity that were different from their non-treated controls. Three out of seven conditions had an effect on supernatant acid phosphatase activity (Figure 45), but there was no consistent trend between the current applied and the effect on enzyme activity. Three out of seven conditions had an effect on pellet acid phosphatase activity (Figure 46), but there was no consistent trend between the current applied and the effect on enzyme activity. The current conditions that affected both the supernatant and pellet acid phosphatase activity were 300 or 500 µA. The application of 300 µA caused an increase in both the supernatant or pellet activity. The application of 500 µA caused a decrease in both the supernatant or pellet activity.

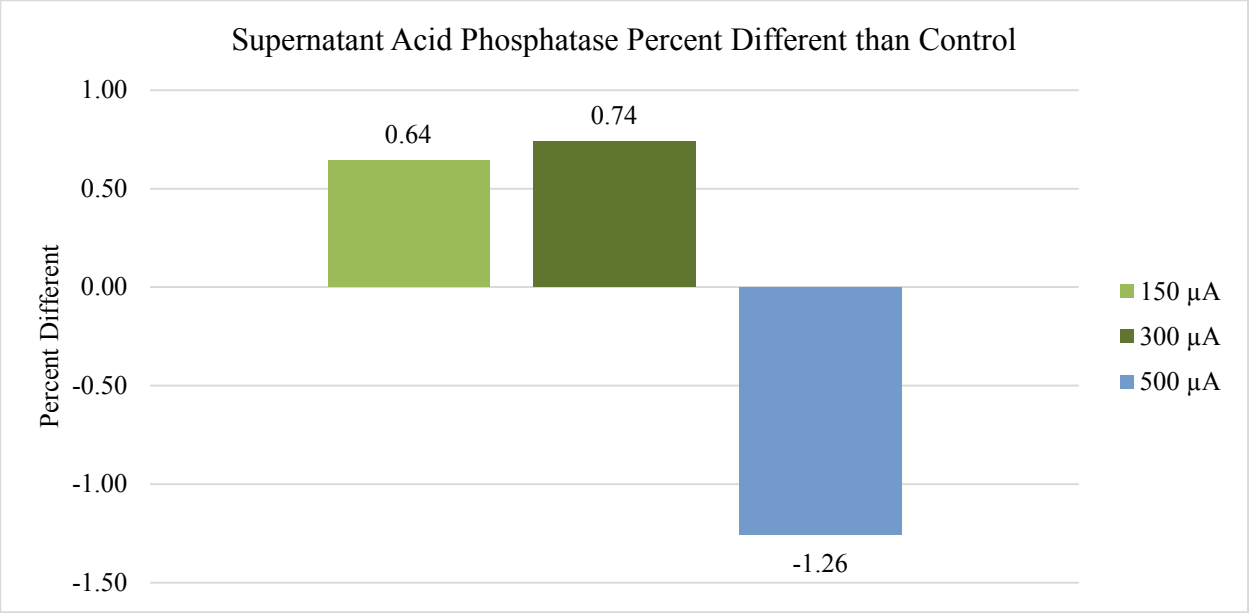

Figure 45. The effects of a 10,000 Hz, symmetric biphasic electric field at various current exposures on *L. tarentolae* secreted acid phosphatase are plotted as percent different from same time control

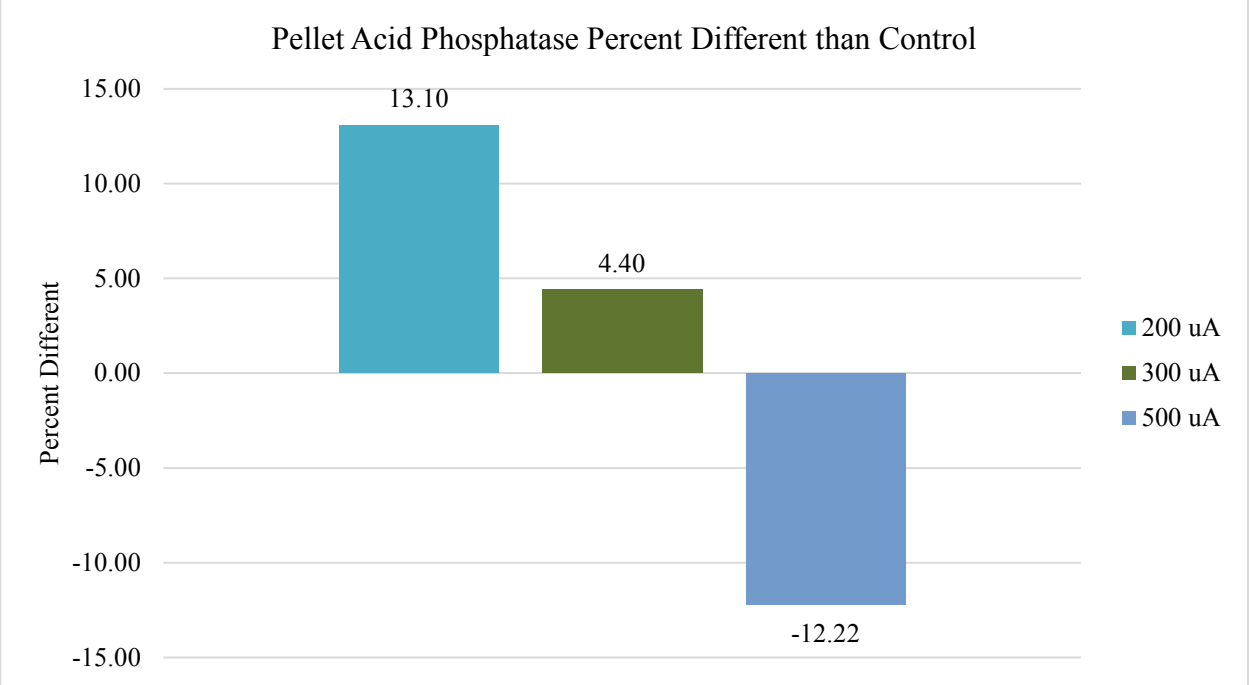

Figure 46. The effects of a 10,000 Hz, symmetric biphasic electric field at various current exposures on *L. tarentolae* cell pellet acid phosphatase are plotted as percent different from same time control

The application of a 10,000 Hz, anodic electric field (7 different current conditions) to *L. tarentolae* whole cells followed by the separation and assessment of acid phosphatase activity resulted in measurable effects in both the supernatant and pellet activity that was different from their non-treated controls. Four out of seven conditions had an effect on supernatant acid phosphatase activity (Figure 47), but there was no consistent trend between the current applied and the effect on enzyme activity. Five out of seven conditions had an effect on pellet acid phosphatase activity (Figure 48), but there was no consistent trend between the current applied and the effect on enzyme activity. The current conditions that affected both the supernatant and pellet acid phosphatase activity were 200, 250, 300 or 400 µA. The application of 200 µA caused a decrease in supernatant and an increase in pellet activity. The 250 or 400 µA conditions caused an increase in both the supernatant activity or pellet activity. The application of 300 µA resulted in decreased in both the supernatant or pellet activity.

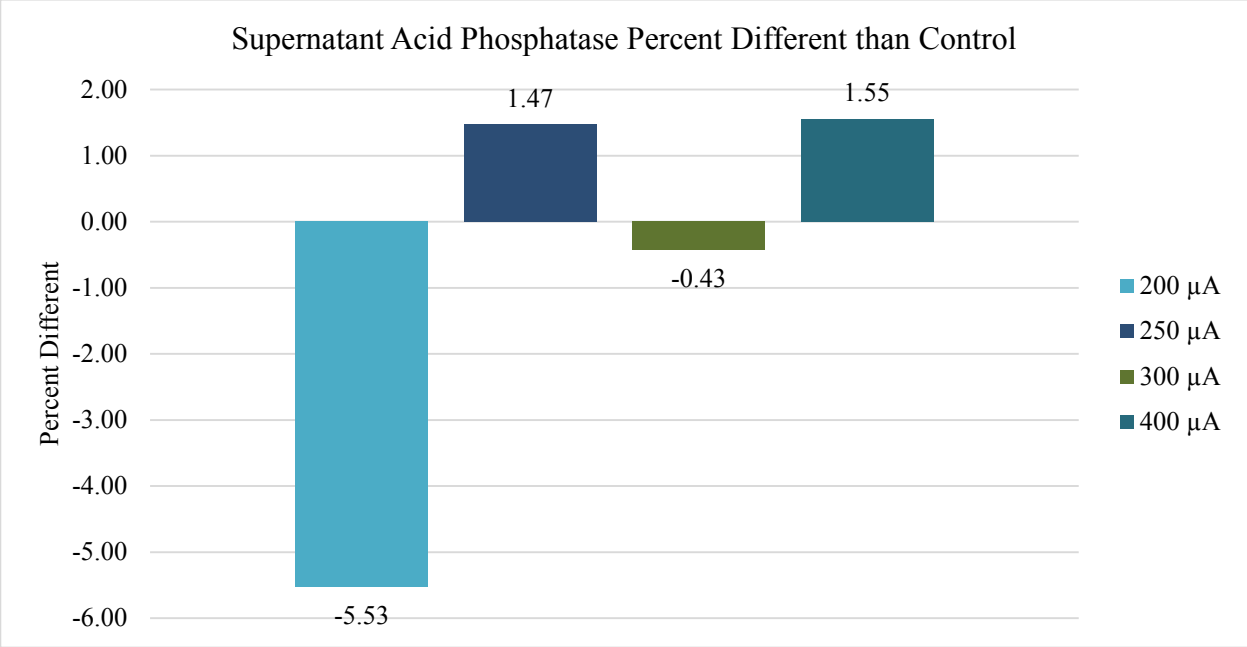

Figure 47. The effects of a 10,000 Hz, anodic electric field at various current exposures on *L. tarentolae* secreted acid phosphatase are plotted as percent different from same time control

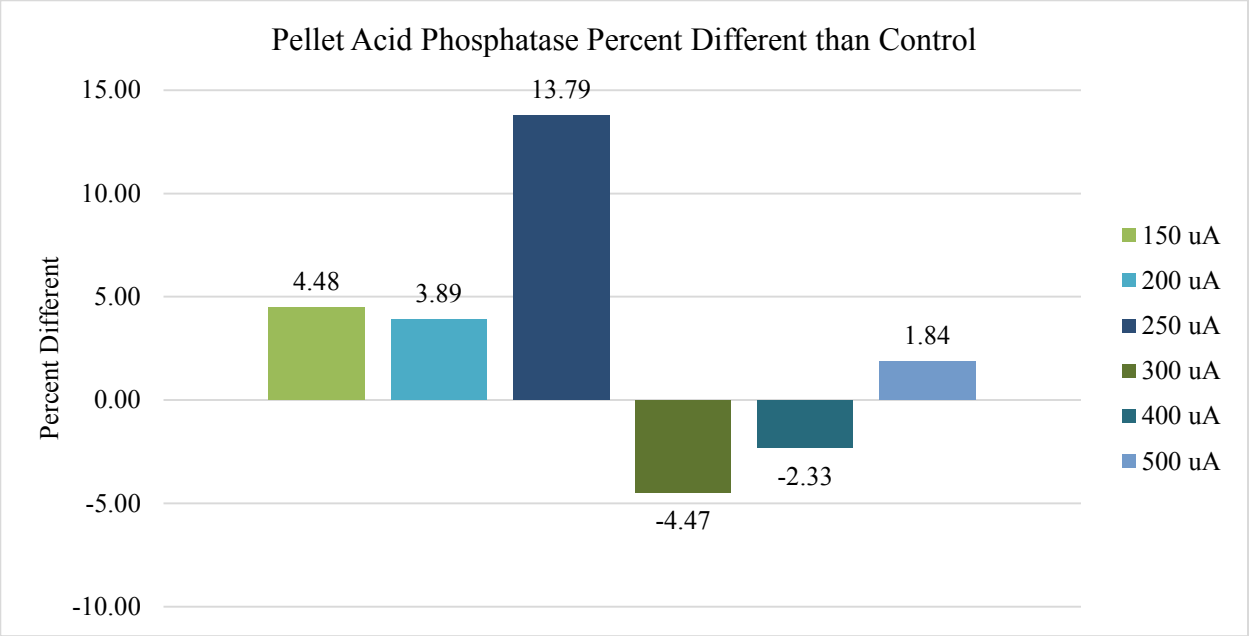

Figure 48. The effects of a 10,000 Hz, anodic electric field at various current exposures on *L. tarentolae* cell pellet acid phosphatase are plotted as percent different from same time control

Secreted Acid Phosphatase Enzyme Inhibition Assay (Following the Method of Baumhardt *et al*., 2015)

Due to the complexity of the enzyme pool, the relative amounts of mono-, di-, tri-, tetra-, octa-, or deca-nuclear vanadium present in assay are not known. Standard speciation diagrams would indicate that under secreted acid phosphatase assay conditions, the main form of vanadium present is decavanadate (Figure 1, Baes, mesmer, 1976). When plotting (Figure 49) *L. tarentolae* secreted acid phosphatase enzyme activity (y-axis) incubated with V_{10} (red curve) or VO_4^{3-} (blue curve) as a function of log [S]/[I] (x-axis), where [I] is either total moles of V_{10} or VO_4^{3-}, there are three conditions where decavanadate or orthovanadate resulted in different effects from control and each other. These conditions are statistically significant ($p < 0.05$ in a paired, two-tailed t-test). These conditions occur when the log[S]/[I] ratio is equal to -0.5, 1.5, or 2.0. Orthovanadate is a better inhibitor in two of these conditions (log[S]/[I] = -0.5 or 2.0), and

decavanadate is a better inhibitor in one condition (log [S]/[I] = 1.5). Plotting the data in this manner assumes that no vanadium speciation occurs. When plotting (Figure 50) *L. tarentolae* secreted acid phosphatase enzyme activity (y-axis) incubated with V_{10} (red curve) or VO_4^{3-} (blue curve) as a function of log [S]/[I] (x-axis), where [I] is total moles of vanadium, there are six conditions where decavanadate or orthovanadate resulted in different effects from control and each other. These conditions are statistically significant ($p < 0.05$ in a paired, two-tailed t-test). These conditions occur when the log[S]/[I] ratio is equal to -1.5, -1.0, -0.5, 0.0, 0.5, or 1.0. Orthovanadate is a better inhibitor in all six of these conditions. Plotting the data in this manner attempts to compensate for the uncertainty associated with vanadium speciation and takes into account only the total moles of vanadium present. Under this assumption, orthovanadate is consistently better at inhibiting secreted acid phosphatase activity, on a mole of vanadium basis compared to decavanadate for an enzyme pool collected from *L. tarentolae* log phase cells.

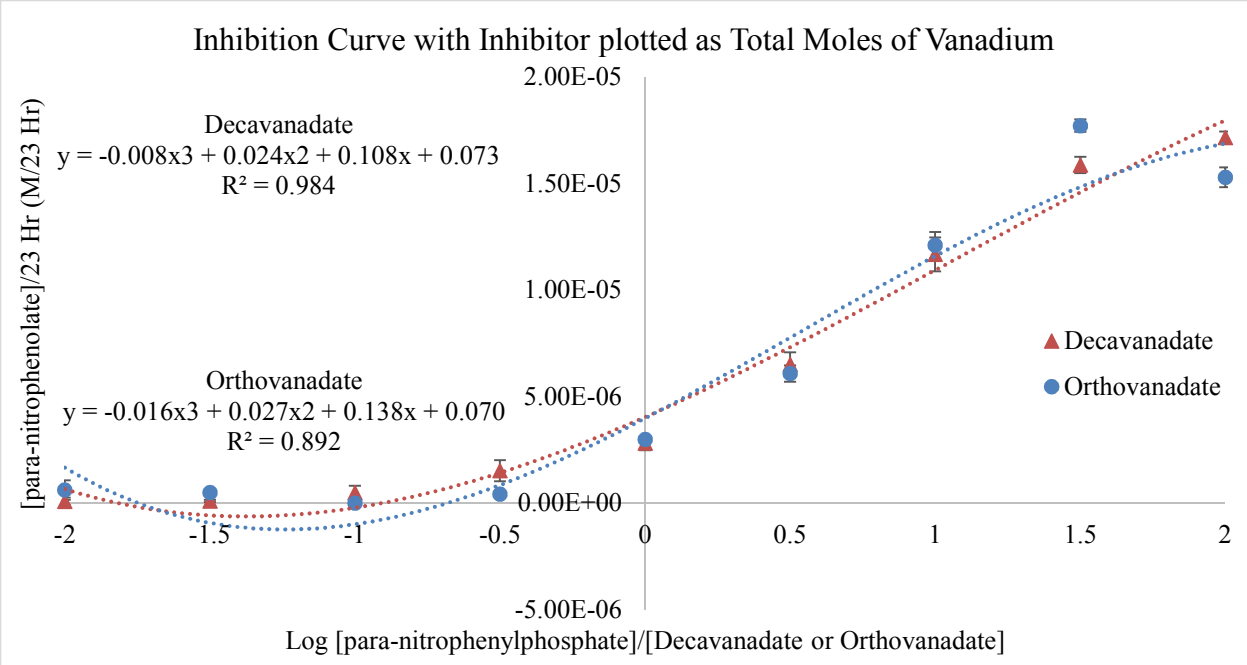

Figure 49. *L. tarentolae* secreted acid phosphatase enzyme activity (Y-axis) when incubated with decavanadate (red curve) or orthovanadate (blue curve) plotted as a function of log [S]/[I] (X-axis). [I] is either total moles of decavanadate or orthovanadate

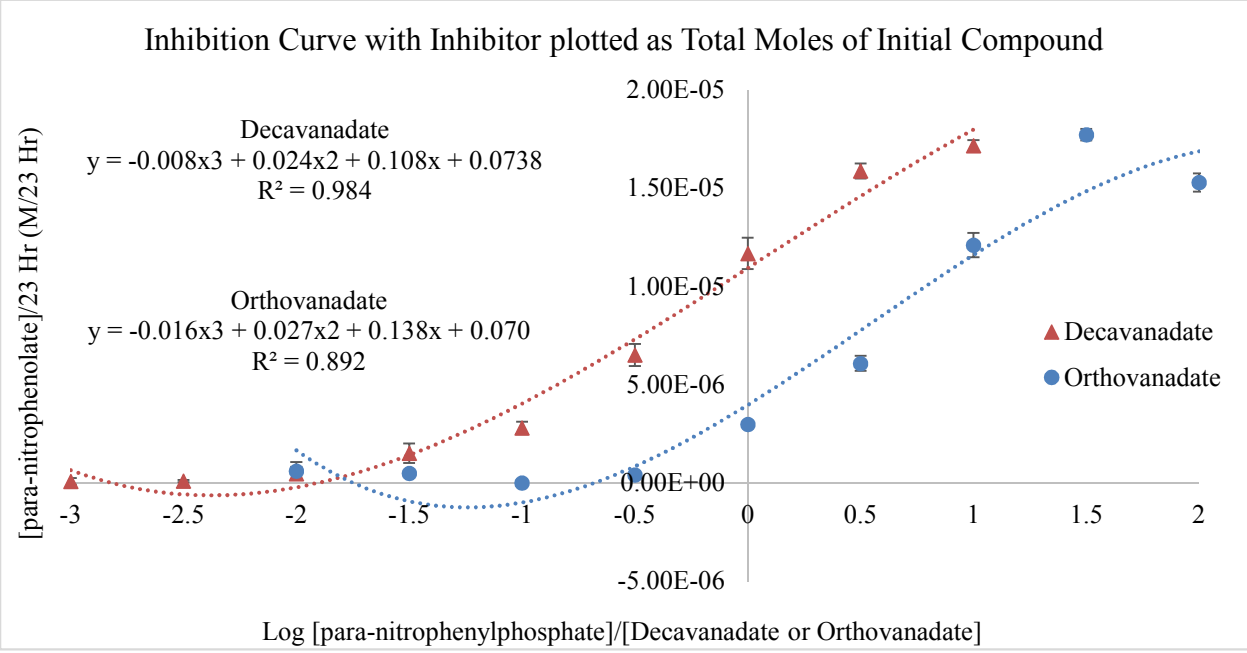

Figure 50. *L. tarentolae* secreted acid phosphatase enzyme activity (Y-axis) when incubated with decavanadate (red curve) or orthovanadate (blue curve) plotted as a function of log [S]/[I] (X-axis). [I] is total moles of vanadium

Secreted Acid Phosphatase Enzyme Inhibition Assays with Pretreatment with Electric Fields Followed by Incubation with and without Orthovanadate (25 µM or LOG [S]/[I] = 1.19)

The pretreatment of *L. tarentolae* log phase supernatant with a 50 Hz, cathodic electric field at various current amplitudes resulted in three conditions (150, 200, or 250 µA) that are different from control (Figure 51). These three conditions are statistically significant ($p < 0.05$ for a paired, two tailed t-test). There is no consistent trend between current and secreted acid phosphatase inhibition greater than orthovanadate alone. The synergistic effect (more inhibition) of pretreatment with electric field followed by orthovanadate incubation is small.

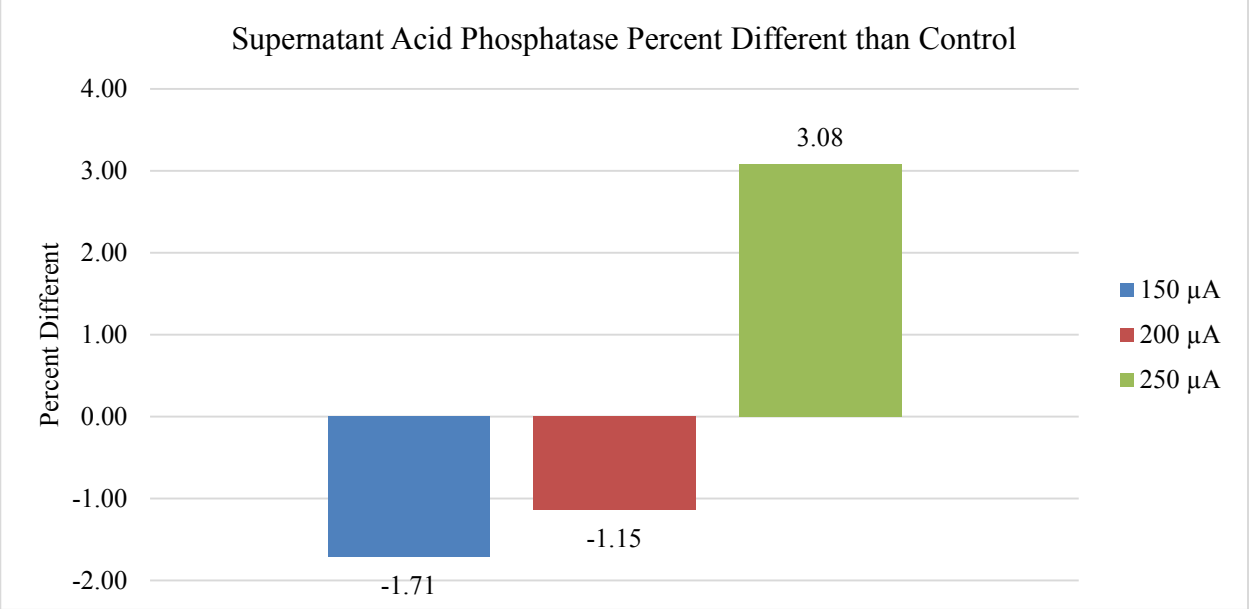

Figure 51. The effects, plotted as percent different from control, of pretreating the log phase *L. tarentolae* secreted acid phosphatase enzyme pool with 50 Hz, cathodic electric field at various current exposures followed by orthovanadate (25 µM) incubation compared to same time control (25 µM orthovanadate exposure only) are shown

The pretreatment of *L. tarentolae* log phase supernatant with a 50 Hz, symmetric biphasic electric field at various current amplitudes resulted in three conditions (200, 300, or 500 µA) that

are significantly different from control (Figure 52). These three conditions are statistically significant ($p < 0.05$ for a paired, two tailed t-test). Under these conditions more current leads to greater inhibition compared to orthovanadate only incubation. The synergistic effect of pretreatment with electric field followed by orthovanadate incubation is, however, small.

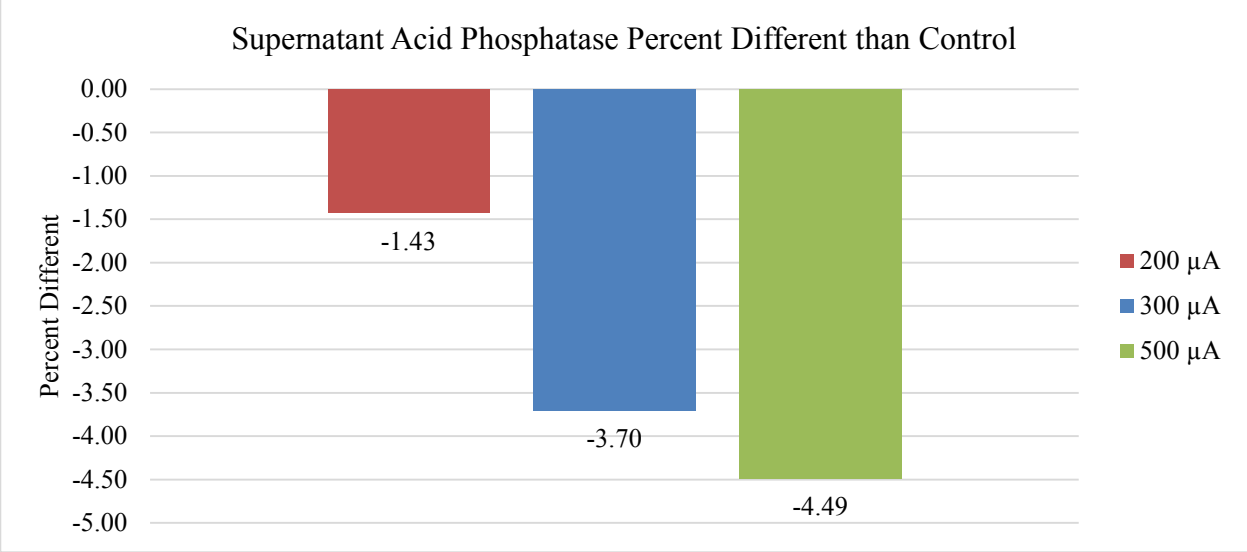

Figure 52. The effects, plotted as percent different from control, of pretreating the log phase *L. tarentolae* secreted acid phosphatase enzyme pool with 50 Hz, symmetric biphasic electric field at various current exposures followed by orthovanadate (25 µM) incubation compared to same time control (25 µM orthovanadate exposure only) are shown

The pretreatment of *L. tarentolae* log phase supernatant with a 50 Hz, anodic electric field at various current amplitudes resulted in three conditions (150, 200, or 250 µA) that are different from control (Figure 53). These three conditions are statistically significant ($p < 0.05$ for a paired, two tailed t-test). There is no apparent trend between current and inhibition. The synergistic effect of pretreatment with electric field followed by orthovanadate incubation is small.

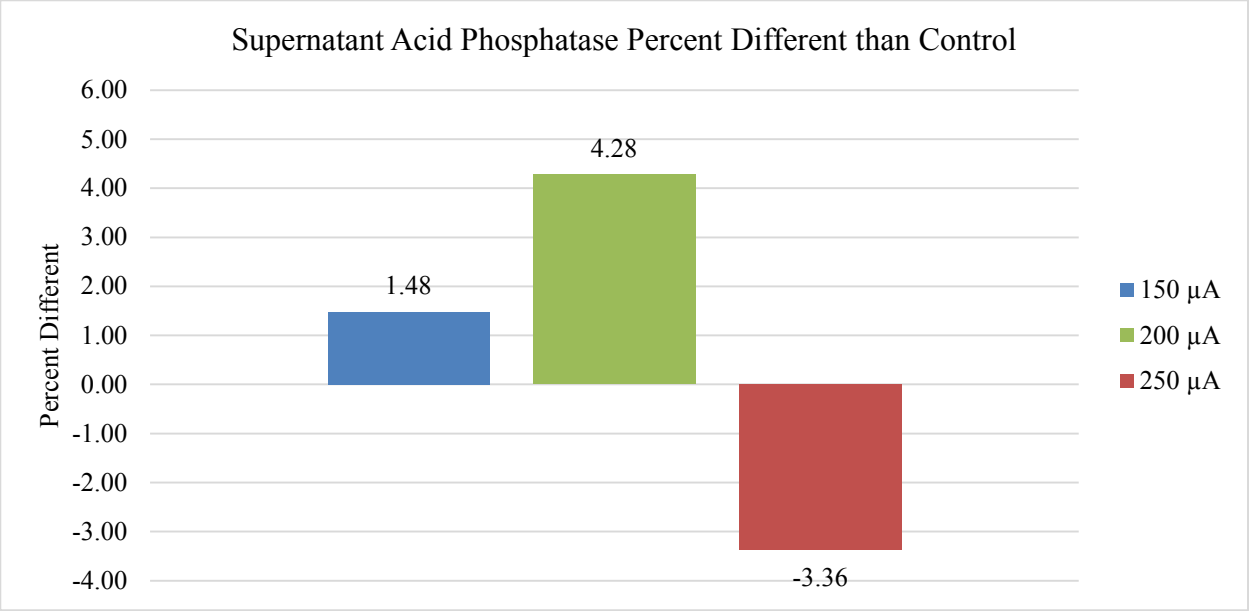

Figure 53. The effects, plotted as percent different from control, of pretreating the log phase *L. tarentolae* secreted acid phosphatase enzyme pool with 50 Hz, anodic electric field at various current exposures followed by orthovanadate (25 µM) incubation compared to same time control (25 µM orthovanadate exposure only) are shown

The pretreatment of *L. tarentolae* log phase supernatant with a 10,000 Hz, cathodic electric field at various current amplitudes resulted in five conditions (150, 250, 300, 400, or 500 µA) that are different from control (Figure 54). These five conditions are statistically significant ($p < 0.05$ for a paired, two tailed t-test). There is no apparent trend between current and inhibition. The synergistic effect of pretreatment with electric field followed by orthovanadate incubation is small, but more substantial than with 50 Hz, cathodic treatment.

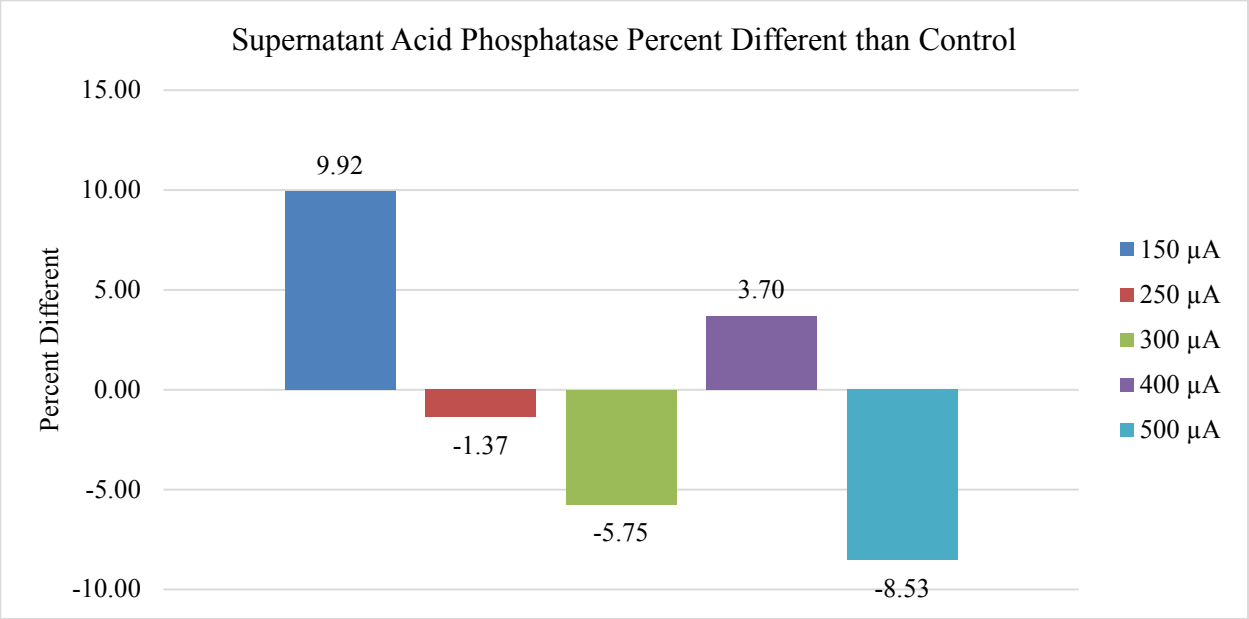

Figure 54. The effects, plotted as percent different from control, of pretreating the log phase *L. tarentolae* secreted acid phosphatase enzyme pool with 10,000 Hz, cathodic electric field at various current exposures followed by orthovanadate (25 µM) incubation compared to same time control (25 µM orthovanadate exposure only) are shown

The pretreatment of *L. tarentolae* log phase supernatant with a 10,000 Hz, symmetric biphasic electric field at various current amplitudes resulted in five conditions (150, 200, 250, 300, or 400 µA) that are different from control (Figure 55). These five conditions are statistically significant ($p < 0.05$ for a paired, two tailed t-test). There is no apparent trend between current and inhibition. The synergistic effect of pretreatment with electric field followed by orthovanadate incubation is small, and moderately smaller than shown by the 50 Hz, symmetric biphasic treatment.

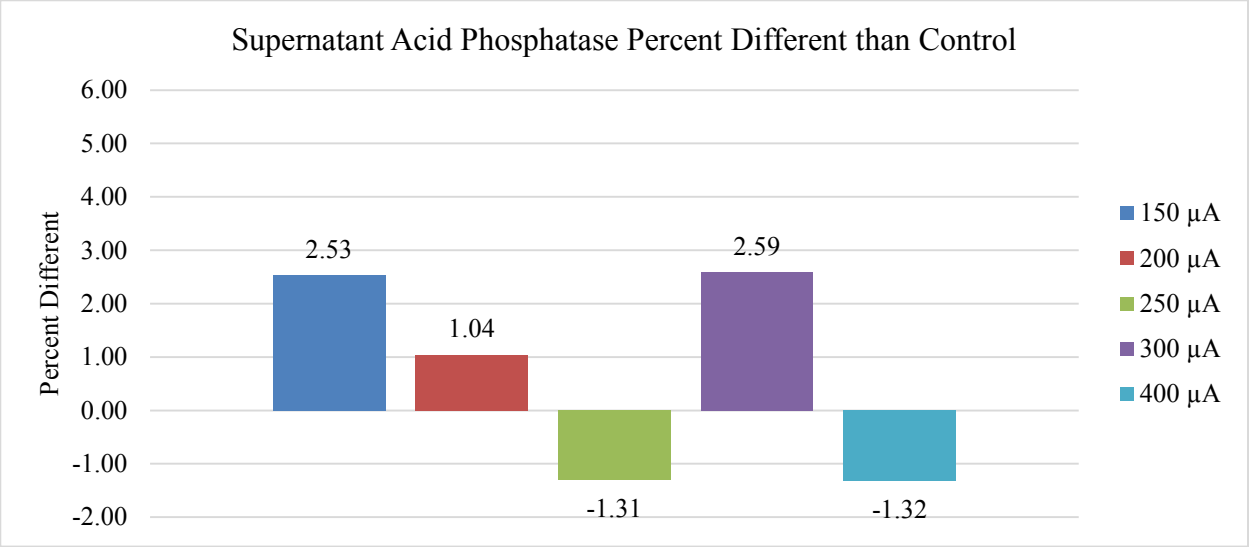

Figure 55. The effects, plotted as percent different from control, of pretreating the log phase *L. tarentolae* secreted acid phosphatase enzyme pool with 10,000 Hz, symmetric biphasic electric field at various current exposures followed by orthovanadate (25 µM) incubation compared to same time control (25 µM orthovanadate exposure only) are shown

The pretreatment of *L. tarentolae* log phase supernatant with a 10,000 Hz, anodic electric field at various current amplitudes resulted in six conditions (100, 150, 200, 250, 300, or 500 µA) that are different from control (Figure 56). These six conditions are statistically significant ($p < 0.05$ for a paired, two tailed t-test). There is no apparent trend between current and inhibition. The synergistic effect of pretreatment with electric field followed by orthovanadate incubation is small, and in the range observed with the 50 Hz, anodic treatment.

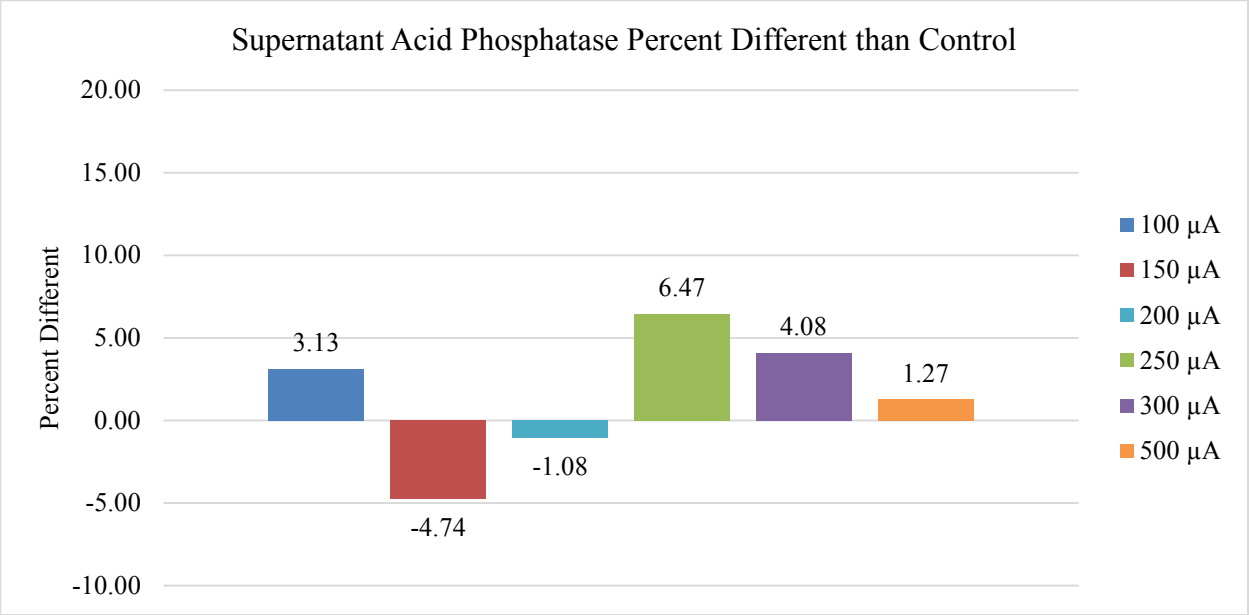

Figure 56. The effects, plotted as percent different from control, of pretreating the log phase *L. tarentolae* secreted acid phosphatase enzyme pool with 10,000 Hz, anodic electric field at various current exposures followed by orthovanadate (25 µM) incubation compared to same time control (25 µM orthovanadate exposure only) are shown

Secreted Acid Phosphatase Kinetics Assay with and without the Preincubation with a Glycosidase, Followed by Pretreatment with and without Electric Fields

The pretreatment of log phase *L. tarentolae* enzyme pool with the glycosidase, PNGase F, resulted in a 5.00 % decrease in the k_M value of enzyme 1 compared to control, but no statistically significant difference in the V_{MAX} value of enzyme 1 compared to control (Table 4). The pretreatment of log phase *L. tarentolae* enzyme pool with PNGase F resulted in a 36.49 % decrease in the k_M value of enzyme 2 compared to control, but no statistically significant difference in the V_{MAX} value of enzyme 2 compared to control (Table 5). The pretreatment of log phase *L. tarentolae* enzyme pool with PNGase F followed by the application of 10,000 Hz, 100 µA, anodic electric field resulted in an 8.33 percent decrease in k_M value of enzyme 1 compared to control, and a 12. 57 increase in the V_{MAX} value of enzyme 1 compared to control. The pretreatment of log phase *L. tarentolae* enzyme pool with PNGase F followed by the application

of 10,000 Hz, 100 μA, anodic electric field resulted in no changes in either k_M or V_{MAX} value of enzyme 2 that were statistically different compared to control.

Conditions	k_M (μM)	V_{MAX} (μM/23 Hr)	k_M Percent different versus control	V_{MAX} Percent different versus control
24 Hour incubation with PNGase F	0.114 ± 0.030	55.866 ± 1.616	-5.00	Not statistically different from control
24 Hour incubation with PNGase F followed by 30 min exposure to 10,000 Hz, 100 μA, anodic electric field	0.130 ± 0.011	62.500 ± 1.937	-8.33	12.57

Table 4. Enzyme 1 kinetic parameters k_M and V_{MAX} under different conditions compared to control. Negative percentages indicate a decrease in value compared to control. Positive percentages indicate an increase in value compared to control

Conditions	k_M (μM)	V_{MAX} (μM/23 Hr)	k_M Percent different versus control	V_{MAX} Percent different versus control
24 Hour incubation with PNGase F	1.480 E-04 ± 0.033 E-04	30.647 ± 0.688	-34.69	Not statistically different from control
24 Hour incubation with PNGase F followed by 30 min exposure to 10,000 Hz, 100 μA, anodic electric field	4.926 E-04 ± 2.440 E-04	33.818 ± 1.891	Not statistically different from control	Not statistically different from control

Table 5. Enzyme 2 kinetic parameters k_M and V_{MAX} under different conditions compared to control. Negative percentages indicate a decrease in value compared to control. Positive percentages indicate an increase in value compared to control

CHAPTER IV

CONCLUSIONS AND FUTURE WORK

Cell Culture and Microscopy of *L. tarentolae* and Assessment of Cell Viability by the MTT Assay

Using *L. tarentolae* promastigotes as a model system to probe potential Leishmania therapeutics continues to prove itself useful, especially in the context of this work. The capacity for these cells to be easily grown, assessed by multiple metrics (MTT assay and microscopy), and their predictable behavior make them a valuable tool as a model system.

Secreted Acid or Alkaline Phosphatase Enzyme Assay

Secreted acid phosphatase activity for *L. tarentolae* supernatant is detectable on all eight days of a typical *L. tarentolae* growth curve. Because the log phase is likely the most relevant phase to the *Leishmania* infection cycle, log phase whole cells or cell supernatant should be used in all future studies for this work. Secreted alkaline phosphatase activity is not detectable on any of the eight days of the *L. tarentolae* growth curve. Therefore, secreted alkaline phosphatase activity should not be assayed in any future studies of this work.

Kinetic Enzyme Assay

Supernatant enzyme source collected from *L. tarentolae* log phase cells gives an apparent typical Michaelis-Menten type response to increasing substrate concentrations. However, the Lineweaver-Burk linear transformation of the V versus S curve of the *L. tarentolae* log phase supernatant produced two straight lines (Figures 15, 16, and 17). Thus, two enzymes with different k_M or V_{MAX} values are detectable in the *L. tarentolae* log phase cell supernatant (Figures 18 and 19, and Tables 2 and 3) using this kinetic approach. These kinetic data correlate with the gene data indicating two separate enzymes as reported by Shakariana *et al*., 1997.

Enzyme 1 has a larger k_M and larger V_{MAX} (Table 2) than enzyme 2. Enzyme 2 has a smaller k_M and smaller V_{MAX} (Table 3) than enzyme 1. Enzyme 1 binds substrate less effectively than enzyme 2, but enzyme 1 makes product at a larger velocity than enzyme 2. The capacity of enzyme 1 to be detected on all eight days of the *L. tarentolae* growth curve suggests this enzyme may play a role beyond that of aiding in survival of the parasite in the sand fly or aiding in human infectivity. The inability for enzyme 2 to be detected on days one and two of the *L. tarentolae* growth curve, followed by its lower V_{MAX} value on days three to six, then a large apparent increase in V_{MAX} as the culture appears to enter the senescence phase (Figure 19, Day 7) suggests that enzyme 2 may be stored and released for a specific function. This interpretation assumes V_{MAX} is only increasing because the concentration of enzyme 2 is increasing, and that V_{MAX} is equal to $k_2[E_{total}]$ for a Michaelis-Menten type enzyme.

Testing the Acute Effects of Electric Fields on *L. tarentolae* Growth Curves and Microscopy

L. tarentolae MTT response was unaffected by treatment with any of the tested electric fields. However, the cells do appear to respond to electric fields since *L. tarentolae* cell clumping is differentially affected by electric field frequency, polarity, and current. As the electric field frequency increases, *L. tarentolae* cell clumping increases. Effect of polarity is such that the application of any electric field causes aggregation of *L. tarentolae* underneath the electrode, with cell population density decreasing as a function of distance away from the electrode. Furthermore, the application of anodic electric fields causes the cells not only to aggregate, but also to clump. We interpret this clumping as a stress response from *L. tarentolae*. As current amplitude increases, *L. tarentolae* cell clumping increases. The interpretation of a treatment causing cell clumping is that said treatment is stressing the cells. In cell clumps, *L. tarentolae* may exhibit a behavior identified as quorum sensing. During quorum sensing, cells restrict the

expression of specific genes to the high cell densities at which the resulting phenotypes will be most beneficial to survival (Miller, Bassler, 2001). Therefore, the conditions of electric fields could be optimized such that maximum cell aggregation occurs in one area, thus making effective dosing of a topical therapeutic more easily accomplished.

Testing the Effects of Electric Fields on *L. tarentolae* Acid Phosphatase Activity in Supernatant or Pellet (Cells), Method 1

Method 1 was used to investigate eighty-four different experimental conditions and Figure 57 is a summary. Seventy-two of the eighty-four experimental conditions were different than control and statistically significant ($p < 0.05$ for a paired, two tailed t-test). Thirty-eight of the forty-two conditions tested with the supernatant enzymes were statistically different from controls ($p < 0.05$ for a paired, two tailed t-test). Thirty-four of the forty-two conditions tested on the cell pellets were statistically different from controls ($p < 0.05$ for a paired, two tailed t-test). Thirty of the eighty-four tested conditions affected both the supernatant and the cell pellet acid phosphatase activity. Twenty-one of the thirty conditions caused an increase in supernatant activity and a decrease in pellet activity. Five of the thirty conditions increased both supernatant and pellet activity. Two of the thirty conditions decreased the supernatant or pellet activity. Two of the thirty conditions decreased supernatant activity or increased pellet activity.

Thirty-four of the forty-two 50 Hz conditions tested were statistically significant ($p < 0.05$ for a paired, two tailed t-test). Eighteen of the thirty-four significant results were from applying electric fields to *L. tarentolae* log phase cell supernatant. The magnitude of the average effect from a 50 Hz cathodic electric field is 2.10 % different from control (2.35 % activation, 0.86 % inhibition). The magnitude of the average effect from a 50 Hz symmetric biphasic electric field is 2.59 % different from control (2.00 % activation, 3.19 % inhibition). The

magnitude of the average effect from a 50 Hz anodic electric field is 0.56 % different from control (0.52 % activation, 0.57 % inhibition). Sixteen of the thirty-four significant results were from applying electric fields to *L. tarentolae* log phase cell pellets. The magnitude of the average effect from a 50 Hz cathodic electric field is 1.72 % different from control (1.51 % activation, 1.93 % inhibition). The magnitude of the average effect from a 50 Hz symmetric biphasic electric field is 3.91 % different from control (4.47 % activation, 3.54 % inhibition). The magnitude of the average effect from a 50 Hz anodic electric field is 4.38 % different from control (5.08 % activation, 3.33 % inhibition). Within the 50 Hz frequency, the largest activation effect on average is seen from the application of 50 Hz anodic electric fields to *L. tarentolae* cell pellets. The greatest average inhibition caused by 50 Hz is the application of 50 Hz symmetric biphasic electric fields to *L. tarentolae* log phase cell pellets.

Thirty-eight of the forty-two 10,000 Hz conditions tested were statistically significant ($p < 0.05$ for a paired, two tailed t-test). Twenty of the thirty-eight significant results were from applying electric fields to *L. tarentolae* log phase cell supernatant. The magnitude of the average effect from a 10,000 Hz cathodic electric field is 12.31 % different from control (12.31 % activation, 0.00 % inhibition). The magnitude of the average effect from a 10,000 Hz symmetric biphasic electric field is 2.31 % different from control (2.64 % activation, 0.35 % inhibition). The magnitude of the average effect from a 10,000 Hz anodic electric field is 14.27 % different from control (14.27 % activation, 0.00 % inhibition). Eighteen of the thirty-eight significant results were from applying electric fields to *L. tarentolae* log phase cell pellets. The magnitude of the average effect from a 10,000 Hz cathodic electric field is 16.56 % different from control (0.00 % activation, 16.56 % inhibition). The magnitude of the average effect from a 10,000 Hz symmetric biphasic electric field is 7.81 % different from control (7.30 % activation, 7.90 %

inhibition). The magnitude of the average effect from a 10,000 Hz anodic electric field is 4.28 % different from control (4.90 % activation, 4.16 % inhibition). Within the 10,000 Hz frequency, the largest activation effect on average is seen from the application of 10,000 Hz cathodic electric fields to *L. tarentolae* cell pellets. The greatest average activation caused by 10,000 Hz is the application of 10,000 Hz anodic electric fields to *L. tarentolae* log phase cell supernatant. The greatest average inhibition caused by 10,000 Hz is the application of 10,000 Hz cathodic electric fields to *L. tarentolae* log phase cell pellets.

Testing the Effects of Electric Fields on *L. tarentolae* Acid Phosphatase Activity in Supernatant or Pellet (Cells), Method 2

Method 2 was used to investigate eighty-four different experimental conditions and Figure 58 is a summary. Forty-five of the eighty-four experimental conditions were different than control and statistically significant ($p < 0.05$ for a paired, two tailed t-test). Nineteen of the forty-two conditions tested with the supernatant enzymes were statistically different from controls ($p < 0.05$ for a paired, two tailed t-test). Twenty-six of the forty-two conditions tested on the pellets were statistically different from controls ($p < 0.05$ for a paired, two tailed t-test). Fourteen of the eighty-four tested conditions affected both the supernatant and the pellet acid phosphatase activity. Two of the fourteen conditions caused an increase in supernatant activity and a decrease in pellet activity. Six of the fourteen conditions increased both supernatant and pellet activity. Three of the fourteen conditions decreased both the supernatant and pellet activity. Three of the fourteen conditions decreased supernatant activity or increased pellet activity.

Twenty of the forty-two 50 Hz conditions tested were statistically significant ($p < 0.05$ for a paired, two tailed t-test). Seven of the twenty significant results were from applying electric

fields to *L. tarentolae* log phase cell supernatant. The magnitude of the average effect from a 50 Hz cathodic electric field is 2.50 % different from control (3.04 % activation, 1.70 % inhibition). The magnitude of the average effect from a 50 Hz symmetric biphasic electric field cannot be discussed due to these data not being statistically different from control. The magnitude of the average effect from a 50 Hz anodic electric field is 2.67 % different from control (2.67 % activation, 0.00 % inhibition). Thirteen of the twenty significant results were from applying electric fields to *L. tarentolae* log phase cell pellets. The magnitude of the average effect from a 50 Hz cathodic electric field is 3.11 % different from control (3.38 % activation, 2.97 % inhibition). The magnitude of the average effect from a 50 Hz symmetric biphasic electric field is 19.34 % different from control (36.2 % activation, 2.43 % inhibition). The magnitude of the average effect from a 50 Hz anodic electric field is 2.43 % different from control (1.91 % activation, 3.21 % inhibition). Within the 50 Hz frequency, the largest effect on average is seen from the application of 50 Hz symmetric biphasic electric fields to *L. tarentolae* cell pellets. The greatest average activation caused by 50 Hz is the application of 50 Hz cathodic electric fields to *L. tarentolae* log phase cell supernatant. The greatest average inhibition caused by 50 Hz is the application of 50 Hz symmetric biphasic electric fields to *L. tarentolae* log phase cell pellets.

Twenty-five of the forty-two 10,000 Hz conditions tested were statistically significant ($p < 0.05$ for a paired, two tailed t-test). Twelve of the twenty-five significant results were from applying electric fields to *L. tarentolae* log phase cell supernatant. The magnitude of the average effect from a 10,000 Hz cathodic electric field is 1.17 % different from control (1.49 % activation, 0.71 % inhibition). The magnitude of the average effect from a 10,000 Hz symmetric biphasic electric field is 0.88 % different from control (0.69 % activation, 1.26 % inhibition). The magnitude of the average effect from a 10,000 Hz anodic electric field is 2.25 % different

from control (1.51 % activation, 2.98 % inhibition). Thirteen of the twenty-five significant results were from applying electric fields to *L. tarentolae* log phase cell pellets. The magnitude of the average effect from a 10,000 Hz cathodic electric field is 4.48 % different from control (7.31 % activation, 3.07 % inhibition). The magnitude of the average effect from a 10,000 Hz symmetric biphasic electric field is 9.91 % different from control (8.75 % activation, 12.22 % inhibition). The magnitude of the average effect from a 10,000 Hz anodic electric field is 5.13 % different from control (6.00 % activation, 3.35 % inhibition). Within the 10,000 Hz frequency, the largest effect on average is seen from the application of 10,000 Hz symmetric biphasic electric fields to *L. tarentolae* cell pellets. The greatest average activation caused by 10,000 Hz is the application of 10,000 Hz symmetric biphasic electric fields to *L. tarentolae* log phase cell supernatant. The greatest average inhibition caused by 10,000 Hz is the application of 10,000 Hz symmetric biphasic electric fields to *L. tarentolae* log phase cell pellets. This apparent discrepancy can be explained by understanding that different currents within a single frequency and polarity had different effects on acid phosphatase enzyme activity.

Comparing the Effectiveness of Method 1 to Method 2

When comparing the effectiveness of method 1 (separating supernatant from pellet then applying electric fields directly to enzyme pools) to method 2 (applying electric fields to whole cells followed by separation of supernatant from pellet), the number of total experiments that produced statistically different enzyme activity compared to control are seventy-two (method 1) compared to forty-five (method 2). As shown in Figures 57 and 58, the total number of statistically significant supernatant experiments is thirty-eight (method 1) compared to nineteen (method 2). The total number of statistically significant pellet experiments is thirty-four (method 1) compared to twenty-six (method 2). Comparing the average effect from a 50 Hz waveform on

L. tarentolae cell supernatant acid phosphatase activity, utilizing either method 1 or method 2, method 2 (2.59 % different than control) produced a larger effect, on average, than method 1 (1.75 % different than control). Comparing the activating effect from a 50 Hz waveform on *L. tarentolae* cell supernatant acid phosphatase activity, utilizing either method 1 or method 2, method 2 (2.86 % different than control) is more effective than method 1 (1.62 % different than control). Comparing the inhibition effect from a 50 Hz waveform on *L. tarentolae* cell supernatant acid phosphatase activity, utilizing either method 1 or method 2, method 1 (1.54 % different than control) is more effective than method 2 (0.85 % different than control). Thus, while the total number of statistically significant results is larger when using method 1, the overall magnitude of the effect, or the activation effect, of the application of 50 Hz electric fields is larger on *L. tarentolae* cell supernatant when using method 2. The magnitude of the inhibition effect on *L. tarentolae* cell supernatant caused by the application of 50 Hz magnetic fields is largest when using method 1.

Comparing the average effect from a 10,000 Hz waveform on *L. tarentolae* cell supernatant acid phosphatase activity, utilizing either method 1 or method 2, method 1 (9.63 % different than control) is more effective than method 2 (1.43 % different than control). Comparing the activating effect from a 10,000 Hz waveform on *L. tarentolae* cell supernatant acid phosphatase activity, utilizing either method 1 or method 2, method 1 (9.74 % different than control) is more effective than method 2 (1.23 % different than control). Comparing the inhibition effect from a 10,000 Hz waveform on *L. tarentolae* cell supernatant acid phosphatase activity, utilizing either method 1 or method 2, method 2 (1.65 % different than control) is more effective than method 1 (0.12 % different than control). Thus, the total number of statistically significant results is larger when using method 1, and the overall magnitude of the effect, or the

activation effect, of the application of 10,000 Hz electric fields is larger on *L. tarentolae* cell supernatant when using method 1. The magnitude of the inhibition effect on *L. tarentolae* cell supernatant caused by the application of 10,000 Hz magnetic fields is largest when using method 2.

Comparing the average effect from a 50 Hz waveform on *L. tarentolae* cell pellet acid phosphatase activity, utilizing either method 1 or method 2, method 2 (8.29 % different than control) is more effective than method 1 (3.34 % different than control). Comparing the activating effect from a 50 Hz waveform on *L. tarentolae* cell pellet acid phosphatase activity, utilizing either method 1 or method 2, method 2 (13.84 % different than control) is more effective than method 1 (3.69 % different than control). Comparing the inhibition effect from a 50 Hz waveform on *L. tarentolae* cell supernatant acid phosphatase activity, utilizing either method 1 or method 2, method 1 (2.93 % different than control) is more effective than method 2 (2.87 % different than control). Thus, while the total number of statistically significant results is larger when using method 1, the overall magnitude of the effect, or the activation effect, of the application of 10,000 Hz electric fields is larger on *L. tarentolae* cell pellets when using method 2. The magnitude of the inhibition effect on *L. tarentolae* cell pellets caused by the application of 50 Hz magnetic fields is largest when using method 1.

Comparing the average effect from a 10,000 Hz waveform on *L. tarentolae* cell pellet acid phosphatase activity, utilizing either method 1 or method 2, method 1 (9.55 % different than control) is more effective than method 2 (6.51 % different than control). Comparing the activating effect from a 10,000 Hz waveform on *L. tarentolae* cell pellet acid phosphatase activity, utilizing either method 1 or method 2, method 2 (7.35 % different than control) is more effective than method 1 (4.07 % different than control). Comparing the inhibition effect from a

10,000 Hz waveform on *L. tarentolae* cell supernatant acid phosphatase activity, utilizing either method 1 or method 2, method 1 (9.54 % different than control) is more effective than method 2 (6.21 % different than control). Thus, both the total number of statistically significant results is larger when using method 1, and the overall magnitude, or inhibition effect, of the application of 10,000 Hz electric fields is larger on *L. tarentolae* cell pellets when using method 1. The magnitude of the activation effect on *L. tarentolae* cell pellets caused by the application of 10,000 Hz magnetic fields is largest when using method 2.

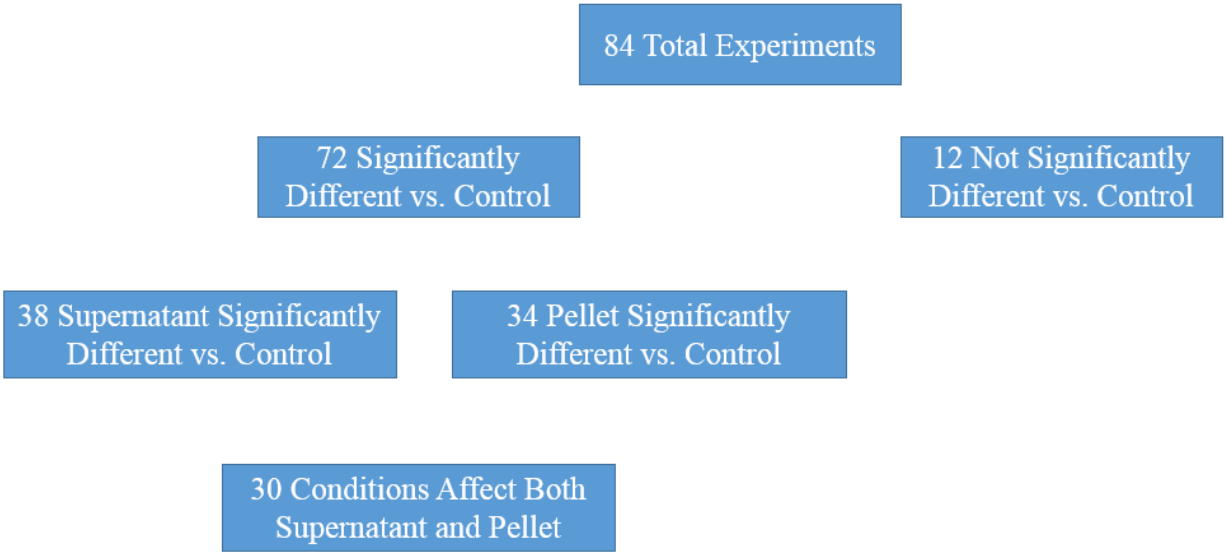

Figure 57. A summary of the results from method 1

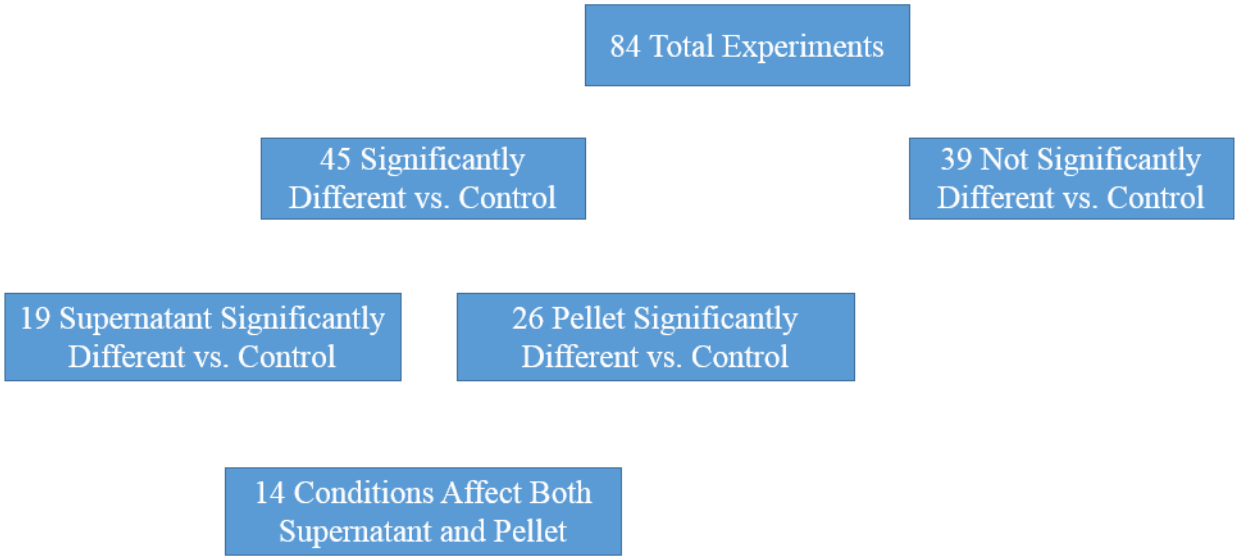

Figure 58. A summary of the results from method 2

Secreted Acid Phosphatase Enzyme Inhibition Assay (Following the Method of Baumhardt *et al*., 2015)

Using Baumhardt *et al*., 2015 as model system, it is clear that when comparing the inhibitory effects of decavanadate to orthovanadate on *L. tarentolae* log phase supernatant acid phosphatase activity, orthovanadate is a better inhibitor than decavanadate on a mole of total vanadium basis (Figure 50). These data correlate with the x-ray diffraction data in the studies reviewed by McLauchlan *et al*. (2015). Therefore, orthovanadate was used as an inhibitor at the log[S]/[I] ratio = 1.19 in most of this thesis work. This ratio is selected because it inhibits acid phosphatase activity but does not completely shut down the enzyme. Thus, any potential synergistic effect caused by electric field treatment followed by orthovanadate exposure can be observed.

Secreted Acid Phosphatase Enzyme Inhibition Assays with Pretreatment with Electric Fields Followed by Incubation with and without Orthovanadate (25 μM)

Pretreatment of *L. tarentolae* log phase supernatant with 50 Hz electric fields followed by incubation with competitive inhibitor orthovanadate (25 μM, log [S]/[I] = 1.19) resulted in nine out of the twenty-one tested conditions being statistically different ($p < 0.05$ for a paired, two tailed t-test) than control (incubation with orthovanadate, 25 μM, only). The average magnitude of the 50 Hz cathodic electric field is 1.98 % different from control (3.08 % activation, 1.43 % inhibition). The average magnitude of the 50 Hz symmetric biphasic electric field is 3.21 % different from control (0.00 % activation, 3.21 % inhibition). The average magnitude of the 50 Hz anodic electric field is 3.04 % different from control (2.88 % activation, 3.36 % inhibition).

Pretreatment of *L. tarentolae* log phase supernatant with 10,000 Hz electric fields followed by incubation with competitive inhibitor orthovanadate (25 μM) resulted in seventeen out of the twenty-one tested conditions being statistically different ($p < 0.05$ for a paired, two tailed t-test) than control (incubation with orthovanadate, 25 μM, only). The average magnitude of the 10,000 Hz cathodic electric field is 5.85 % different from control (6.81 % activation, 5.22 % inhibition). The average magnitude of the 10,000 Hz symmetric biphasic electric field is 1.76 % different from control (2.05 % activation, 1.32 % inhibition). The average magnitude of the 10,000 Hz anodic electric field is 3.46 % different from control (3.74 % activation, 2.91 % inhibition).

The total average effect from the application of electric fields to *L. tarentolae* log phase cell supernatant is larger for 10,000 Hz electric fields (3.69 %) compared to 50 Hz electric fields (2.74 %). The average activation from the application of electric fields to *L. tarentolae* log phase cell supernatant is larger for 10,000 Hz electric fields (4.20 %) compared to 50 Hz electric fields

(1.99 %). The average deactivation from the application of electric fields to *L. tarentolae* log phase cell supernatant is larger for 10,000 Hz electric fields (3.15 %) compared to 50 Hz electric fields (2.67 %). Therefore, the greatest antagonistic effects that occur from pretreatment by electric fields followed by orthovanadate incubation are with 10,000 Hz electric fields. The largest synergistic effect between electric fields and orthovanadate incubation also comes from 10,000 Hz electric fields. This apparent discrepancy can be explained by the fact that different current amplitudes or electric field polarities within the 10,000 Hz frequency have different effects, some activate secreted acid phosphatase activity (antagonistic effect with orthovanadate inhibitor), some inhibit secreted acid phosphatase activity (synergistic effect with orthovanadate inhibitor).

Secreted Acid Phosphatase Kinetic Assay with and without the Preincubation with a Glycosidase, Followed by Pretreatment with and without Electric Fields

The importance of carbohydrate attachment to *L. tarentolae* SAP1 or SAP2 becomes apparent when the enzyme source was incubated with PNGase F. The capacity of the PNGase F incubation with *L. tarentolae* enzyme pool to alter kinetic parameters of enzyme 1 and enzyme 2 indicates that the N-linked carbohydrates of enzyme 1 and enzyme 2 are of importance to these enzymes to bind substrate (k_M values of enzyme 1 and enzyme 2 are affected by PNGase F incubation). Furthermore, enzyme 1 is more sensitive to the application of a 10,000 Hz, 100 μA, anodic electric field after preincubation of the *L. tarentolae* enzyme pool with PNGase F. These data further support the idea that there are two isoforms of SAP secreted by *L. tarentolae* into the culture medium, and that their responses to PNGase F incubation and electric field application are different and thus may have different roles in successful infections.

Final Global Conclusions and Recommendations for Future Work

L. tarentolae secrete two detectable acid phosphatases into the culture medium, enzyme 1 and enzyme 2. These two isoforms have different kinetic parameters, k_M and V_{MAX}, such that enzyme 1 binds substrate less tightly than enzyme 2, but enzyme 1 also produces product more quickly than does enzyme 2. Furthermore, *L. tarentolae* has utility as a model system for assessing the effects applying electric fields have on cell viability and enzyme activity of enzyme 1 and enzyme 2. The application of electric fields does not affect cell viability of *L. tarentolae*, but does have a large effect on *L. tarentolae* cell clumping. Increasing frequency, or current, or applying anodic electric fields leads to increased *L. tarentolae* cell clumping compared to control. Applying electric fields to *L. tarentolae* cell supernatant (method 1) produced more statistically significant results than did applying electric fields to whole cells followed by separation and collection of supernatant (method 2). The application of 10,000 Hz electric fields produced larger effects on *L. tarentolae* cell supernatant on average than did the application of 50 Hz electric fields (9.63 % different from control vs. 1.75 % different from control). The application of 10,000 Hz electric fields produced larger activation effects on *L. tarentolae* cell supernatant than did the application of 50 Hz electric fields (9.74 % different from control vs. 2.86 % different from control). The application of 10,000 Hz electric fields produced larger inhibition effects on *L. tarentolae* cell supernatant than did the application of 50 Hz electric fields (1.65 % different from control vs. 1.54 % different from control). Overall, electric fields had the effect of increasing SAP activity from *L. tarentolae* log or stationary phase enzyme pools. The method of Baumhardt *et al*. proved useful for determining which of the two tested inhibitors were better on a mole of vanadium basis, orthovanadate or decavanadate. By this method, orthovanadate was a better inhibitor of *L. tarentolae* SAP activity than was

decavanadate. Following through with this result, the application of electric fields to *L. tarentolae* followed by incubation with orthovanadate (25 μM) did not lead to a consistent synergistic effect on *L. tarentolae* SAP activity. Incubation of *L. tarentolae* stationary phase SAP enzyme pool with PNGase F did lead to changes in k_M values of both enzyme 1 and enzyme 2. The incubation of *L. tarentolae* stationary phase SAP enzyme pool followed by the application of 10,000 Hz, 100 μA, anodic electric field had an effect on k_M and V_{MAX} values of enzyme 1, but no effect on enzyme 2.

Based on these global conclusions this author recommends the following when working under the conditions of the methods presented here. To investigate SAP activity from *L. tarentolae*, collection of the supernatant from the log phase or stationary phase of the *L. tarentolae* growth curve will result in the greatest amount of activity from enzyme 1. To investigate enzyme 2, collection of the *L. tarentolae* stationary or senescence phase supernatant will result in the greatest activity from enzyme 2. To investigate both enzymes, collection of *L. tarentolae* log or stationary phase supernatant will suffice, as both enzymes are present and detectable during these phases of the *L. tarentolae* growth curve. To further investigate the effect of electric field on *L. tarentolae* cell aggregation and/or cell clumping, use larger frequencies (10,000 Hz), larger currents (500 μA), and anodic polarities for thirty minute exposures. These conditions will result in a large clumping effect, but will also not lead to *L. tarentolae* cell death due to electric field exposure. To further investigate, or to begin probing the mechanism, of how the application of electric fields modulates log or stationary phase *L. tarentolae* SAP activity, the 10,000 Hz frequency is most useful as it has produced the greatest measurable effects thus far. To further investigate any potential synergism between the application of electric fields followed by incubation with a competitive inhibitor, the method of Baumhardt *et al*., with experiments performed under the same

assay conditions as electric field experiments, proves very useful. This method allows the determination of which of any potential competitive inhibitor is most effective at enzyme inhibition on a stoichiometric basis of inhibitor to substrate (log[S]/[I]). This work suggests that the application of electric fields followed by incubation with orthovanadate does not produce a large synergistic effect. The following method is recommended for future work on synergism between orthovanadate and electric fields for the purpose of inhibiting *L. tarentolae* SAP activity. A master pool of assay buffer, enzyme source and orthovanadate should be produced such that buffer occupies 55.56 % of the volume of the master pool, enzyme source occupies 33.33 % of the volume of the master pool, orthovanadate (25 μM) is added to the master pool, and aliquots (2.00 mL) of this master pool are then exposed to electric fields. After electric field exposure, aliquots of the master pool will be added to 1.5 mL polypropylene tubes, and *P*NPP will be added (100 μL of 1.347 mM) to give a final assay volume of 0.9 mL. Assays will be stopped with the addition of NaOH (0.1 mL, 10 M), and product will be measured by spectroscopy (A405 nm). Results from this thesis do now suggest that the therapeutic response reported by Hejazi *et al*. (1972), using electrical treatment of mice, may involve the direct as well as indirect effects of electricity on the activity of secreted acid phosphatases. Clearly more work is needed to sort out the full mechanism of action of electric fields on *Leishmania* secreted acid phosphatases.

REFERENCES

Abbott, S. J., Jones, S. R., Weinman, S. A., Bockhoff, F. M., McLafferty, F. W., Knowles, J. R. (1979). Chiral[16O, 17O, 18O]phosphate monoesters. Asymmetric synthesis and stereochemical analysis of [1(R)-16O, 17O, 18O]phosphor-(S)-propane-1,2-diol. *Journal of the American Chemical Society,* 101, 4323-4332.

Agency for Toxic Substances and Disease Registry, (2016). https://www.atsdr.cdc.gov/phs/phs.asp?id=274&tid=50 (accessed 29 Dec. 2016).

Baghaei, M., BAGHAEI, M. (2003). Characterization of acid phosphatase in the promastigotes of three isolates of *Leishmania major*. *Iranian Journal of Medical Sciences,* 28(1),1-8.

Baumhardt, J. M., Dorsey, B. M., McLauchlan, C. C., Jones, M. A. (2015). An additional method for analyzing the reversible inhibition of an enzyme using acid phosphatase as a model. *Current Enzyme Inhibition,* (11), 140-146.

Baes, J., Charles F., Mesmer, R. E. (1976). In The Hydrolysis of Cations, Baes, J., Charles F., Mesmer, R. E., Eds., New York: John Wiley & Sons.

Biophysics of Membrane Potential, (2017). https://www.cise.ufl.edu/~arunava/Teaching/Lectures-CN/neuroelectronics.pdf (accessed 21 June. 2017).

Box Shade Server, (2017). http://www.ch.embnet.org/software/BOX_form.html (accessed 21 June. 2017).

Chawla, B., and Madhubala, R. (2010). Drug targets in *Leishmania Journal of Parasitic Diseases, Dis,* 34(1),1-13.

Corigliano, F., Pasquale, S. D. (1975). Comparative IR study of solid hydrate decavanadates and polyvanadates in acidic aqueous solution. *Inorganica Chimica Acta*, (12), 99-101.

Enslen, H., Tokumitsu, H., Stork, P. J. S., Davis, R. J., Soderling, T. R. (1996). Regulation of mitogen-activated protein kinases by a calcium/ calmodulin-dependent protein kinase cascade. *Proceedings of the National Academy of Sciences, Sci,* (93), 10803-10808.

ExPASy, (2016). http://enzyme.expasy.org/EC/3.1. (accessed 8 Jan 2016).

Fernandes, A. C., Soares, D. C., Saraiva, E. M., Meyer-Fernandez, J. R., Souto-Padron, T. (2013). Different secreted phosphatase activites in *Leishmania amazonensis*. *FEMS Microbiology Letters,* 340(2),117-128.

Gani, D., Wilkie, J. (1997). Metal Sites in Proteins and Models, Structure and Bonding. (89): 133-175. In Metal Ions in The Mechanism of Enzyme-Catalyzed Phosphate Monoester Hydrolysis. Sadler, PJ., Thomson, AJ., Berlin Heidelberg: Eds, Springer.

Gordon, J. A. (1991). Use of vanadate as Protein-Phosphotyrosine phosphatase inhibitor. *Methods in Enzymology*, (201), 477-482.

Gressor, M. J., Tracey, A. S., Stankiewwicz, P. J., (1987). In Advances in protein phosphatases, Merlev, W., DiSalvo, J.Eds.,Leuven University Press: Belgum.

Hejazi, H., Eslami, G., Dalimi, A. (1972). The parasiticidal effect of electricity on *Leishmania major*, both *in vitro* and *in vivo*. *Annals of Tropical Medicine & Parasitology*, 98(1), 37-42.

Henneberry, M. O., Engel, G., Grayhack, J. T. (1979). Acid phosphatase. *Urologic Clinics of North America,* 6(3), 629-641.

Holden, K. R. Biological effects of pulsed electromagnetic field (PEMF) therapy, (2017). http://www.ondamed.net/us/biological-effects-of-pulsed-electromagnetic-field-pemf-therapy (Accessed 2 Feb. 2017).

Ilg, T., Stierhof,Y-D., Etges, R., Adrian, M., Harbecke, D. (1991). Secreted acid phosphatase of *Leishmania Mexicana*: A filamentous phosphoglycoprotein polymer. *Proceedings of the National Academy of Sciences,* (88), 8774-8778.

Isnard, A., Shio, M. T., Oliver, M. (2012). Impact of *Leishmania* metalloprotease GP63 on macrophage signaling. *Frontiers in Cellular and Infection Microbiology,* (2), 72.

Kalign, (2016). http://www.ebi.ac.uk/Tools/msa/kalign/ (accessed 20 Dec 2016).

King, M. W. The Medicinal Biochemistry Page. Introduction to cholesterol metabolism, (2017). http://themedicalbiochemistrypage.org/cholesterol.php (accessed 5 Feb. 2017).

Knowles, J. R. (1980). Enzyme-catalyzed phosphoryl transfer reactions. *Annual Review of Biochemistry,* (49), 877-919.

Leishmaniasis, (2016). https://www.cdc.gov/parasites/leishmaniasis/epi.html (accessed 20 Dec. 2016).

Leishmaniasis Professionals, (2016). https://www.cdc.gov/parasites/leishmaniasis/health_professionals/index.html#tx (accessed 20 Dec. 2016).

Li, M., Ding, W., Baruah, B., Crans, D. C., Wang, R., (2008). Inhibition of protein tyrosine phosphatases 1B and alkaline phosphatase by bis(maltolato)oxovanadium (IV). *BioMetals,* (102), 1846-1853.

Lippert, D. N., Dwyer, D. W., Li, F., Olafson, R. W. (1999). Phosphoglycosylation of a secreted acid phosphatase from *Leishmania donovani*. *Glycobiology,* 9(6), 627-636.

McLauchlan, C. C., Peters, B. J., Willsky, G. R., Crans, D. C. (2015). Vanadium-phosphatse complexes: Phosphatase inhibitors favor the trigonal bipyramidal transition state geometries. *Coordination Chemistry Reviews,* (301-302), 163-199.

Mendez, R. S., Dorsey, B. M., McLauchlan, C. C., Beio, M., Turner, T. L., Nguyen, V. H., Su, A., Beynon, W., Friesen, J. A., Jones, M. A. (2014). Vanadium complexes are *in vitro* inhibitors of leishmania secreted acid phosphatases. *International journal of Chemistry,* 6(1), 35-49.

Merril, D. R., Bikson, M., Jefferys, J. G. R. (2005). Electrical stimulation of excitable tissue: design of efficatious and safe protocols. *Journal of Neuroscience Methods,* (141), 171-198.

Miller, M. B., Bassler, B. L. (2001). Quorum sensing in bacteria. *Annual Review of Microbiology,* (55), 165-199.

Mojtahedi Z, Clos J, Kamali-Sarvestani E. (2008). Leishmania major: identification of developmentally regulated proteins in procyclic and metacyclic promastigotes. *Experimental Parasitology*, 119(3), 422–429.

Morgenthaler, J. B., Peters, S. J., Cedeno, D. L., Constantino, M. H., Edwards, K. A., Kamowski, E. M., Jones, M. A. (2008). Carbaporphyrin ketals as potential agents for a new photodynamic therapy treatment of leishmaniasis. *Bioorganic and Medicinal Chemistry,* 16(4), 7033-7038.

Mosmann, T. (1983). Rapid colorimetric assay for cellular growth and survival: Application to proliferation and cytotoxicity assays. *Journal of Immunological Methods,* 65(1-2), 55-63.

Navabi, A., Soleimanifard, S. (2015) Enzymatic characterization of acid phosphatase in the logarithmic and stationary phase of *Ieishmania major* promastagotes. *Shiraz E-Medical Journal*, 16(1), e26246-.

PNGase F, (2017). http://www.sigmaaldrich.com/life-science/proteomics/post-translational-analysis/phosphorylation/pngase-f.html (accessed 18 October. 2017).

Rehder, D. (2013). Vanadium. Its role for humans. *Metal Ion in Life Sciences,* (13), 139-169.

Rigden, D. J., Littlejohn, J. E., Henderson, K., Jedrzejas, M. J. (2003). Structures of phosphate and trivanadate of Bacillus stearothermophilus phosphatase PhoE: structural and functional analysis in the cofactor-dependent phosphoglycerate mutase superfamily. *Journal of Molecular Biology,* (325), 411-420.

Rossotti, F. J. C., Rossotti, H. (1956). Equilibrium studies of polyanions. *Acta Chemica Scandinavica*, (10), 957-984.

Shakariana, A. M., Ellisa, S. L., Mallinsonac, D. J., Olafsonb, R. W., Dwyera, D. M. (1997). Two tandemly arrayed genes encode the (histidine) secretory acid phosphatases of *Leishmania donovani*. *Gene*, 196 (1-2), 127-137.

Taylor, V. M., Munoz, D. L., Cedeno, D. L., Velez, I. V., Jones, M. A., Robledo, S. M. (2010). *Leishmania tarentolae*: Utility as an *in vitro* model for screening of antileishmanial agents. *Experimental Parasitology*, (126), 471-475.

VanEtten, R. L., Waymack, P. P., Rehkop, D. M. (1974). Inhibition of myosin ATPase by vanadate ion. *Journal of the American Chemical Society,* (96), 6782-6785.

Vannier-Stantos, M.A., Martiny, A., & de Souza W. (2002). Cell biology of Leishmania spp.: Invading and evading. *Current Pharmaceutical Design,* 8(4), 297-318. http://dx.doi.org/10.2174/138161202339623

Vincent, JB., Crowder, MW., Averill, BA. (1992). Hydrolysis of phosphate monoesters: a biological problemwith multiple chemical solutions. *Trends in Biochemical. Sciences,* 17(3), 105-110.

World Health Organization Leishmaniasis Treatment Cost, (2017). http://www.who.int/leishmaniasis/research/978_92_4_12_949_6_Annex6.pdf (accessed 21 June. 2017).

APPENDIX A

THE INDIVIDUAL LINEWEAVER-BURK PLOTS AND DATA POINTS

CORRESPONDING TO THE TEXT (TABLE 2, FIGURE 18,

TABLE 3, AND FIGURE 19).

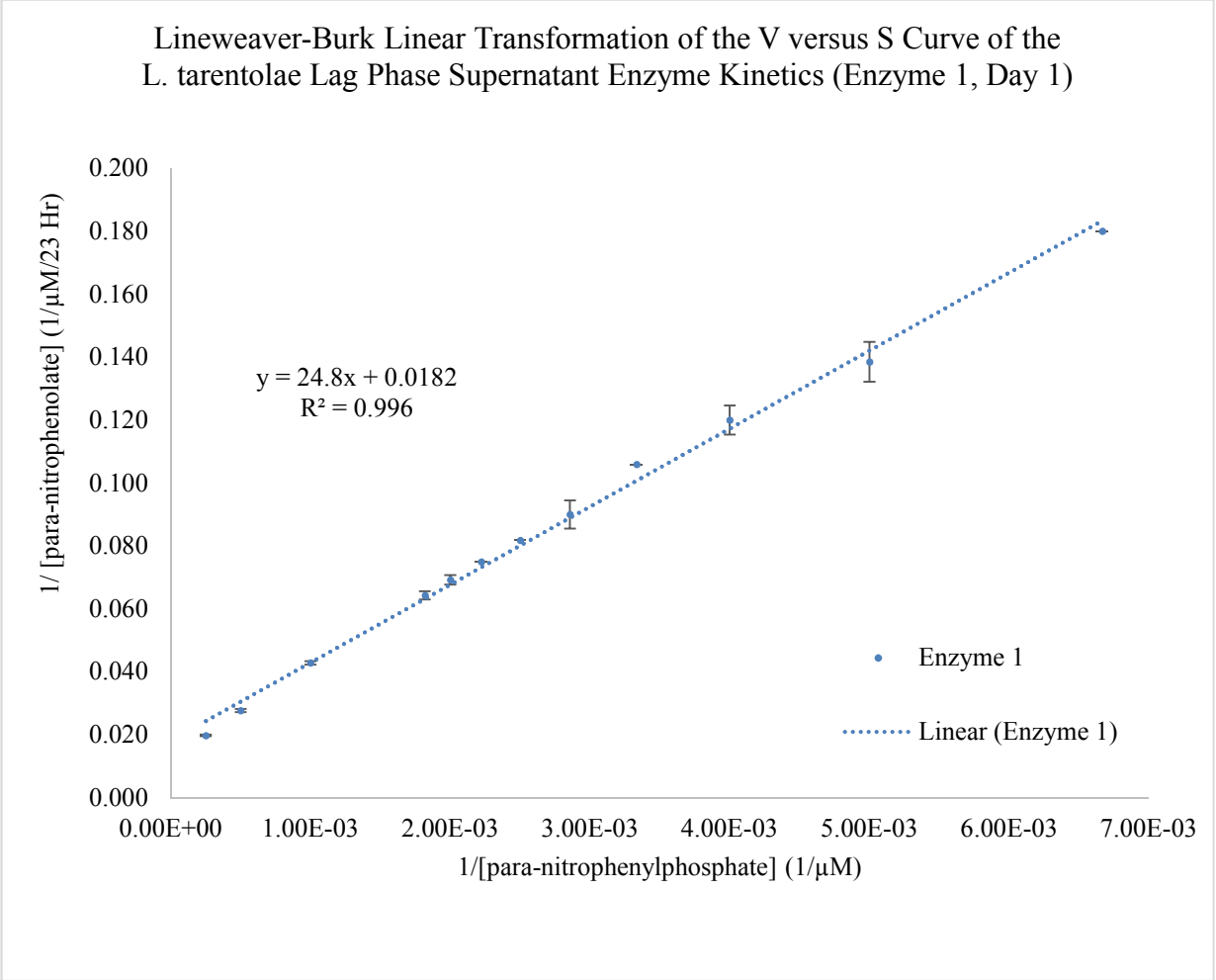

Day 1
Enzyme 1
K_M (µM):
1.36E03±1.3E02
V_{MAX} (µM/23 Hr):
54.9±1.1E-01

[para-nitrophenylphosphate] (µM)	Average [*para*-nitrophenolate] (µM/23 Hr)	1/[*para*-nitrophenolate] (1/µM/23 Hr)	1/[*para*-nitrophenyl phosphate] (1/µM)	standard deviation [*para*-nitrophenol] (1/µM/23 Hr)
150	5.56	0.180	6.67E-03	0.00E+00
200	7.22	0.138	5.00E-03	6.31E-03
250	8.33	0.120	4.00E-03	4.62E-03
300	9.44	0.106	3.33E-03	0.00E+00
350	11.1	9.00E-02	2.86E-03	4.50E-03
400	12.2	8.18E-02	2.50E-03	1.26E-17
450	13.3	7.50E-02	2.22E-03	0.00E+00
500	14.4	6.92E-02	2.00E-03	1.52E-03
550	15.6	6.43E-02	1.82E-03	1.31E-03
1.00E+03	23.3	4.29E-02	1.00E-03	5.84E-04
2.00E+03	36.1	2.77E-02	5.00E-04	4.89E-04
4.00E+03	50.6	1.98E-02	2.50E-04	2.51E-04

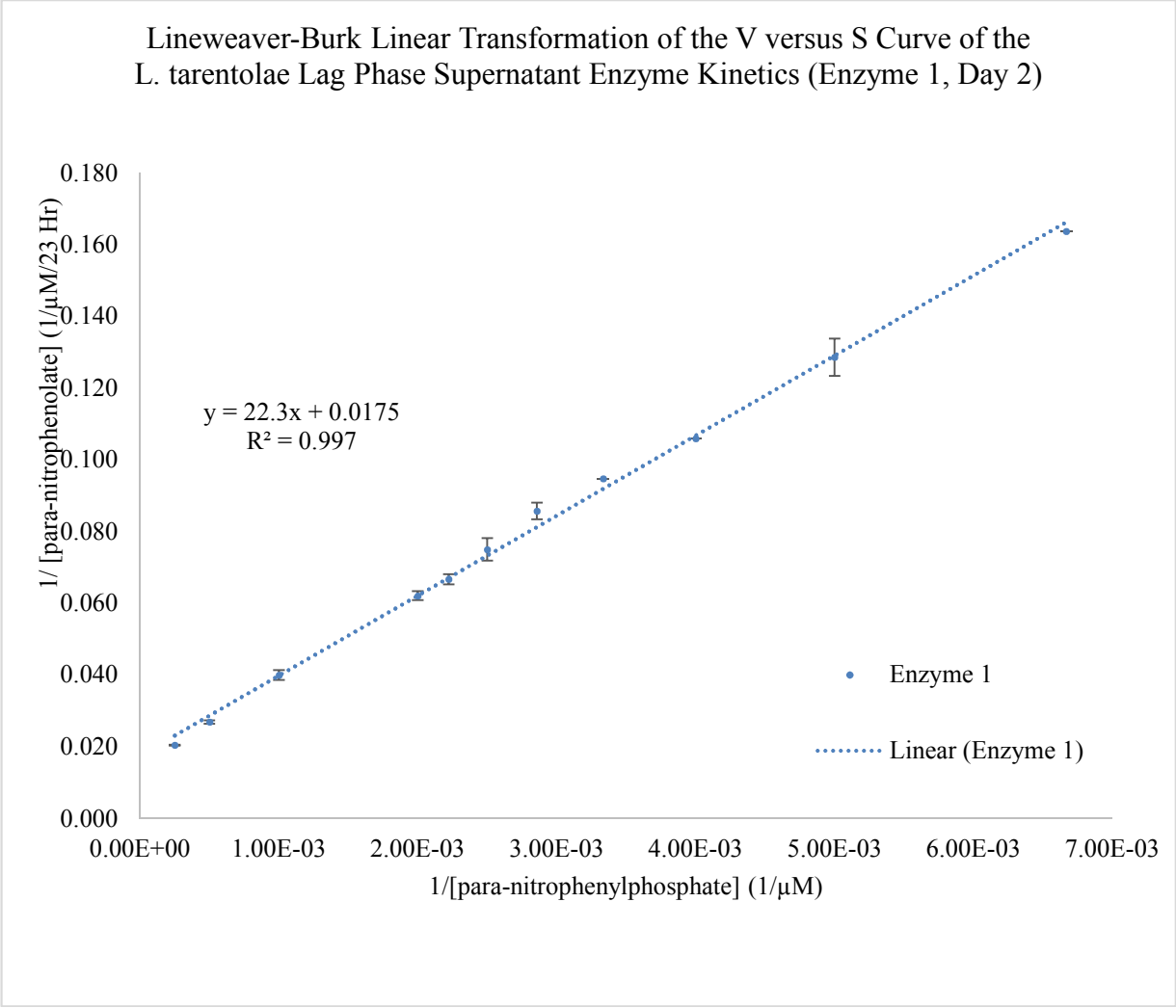
Lineweaver-Burk Linear Transformation of the V versus S Curve of the L. tarentolae Lag Phase Supernatant Enzyme Kinetics (Enzyme 1, Day 2)
1/ [para-nitrophenolate] (1/µM/23 Hr)
0.180
0.160
0.140
0.120
0.100
0.080
0.060
0.040
0.020
0.000
y = 22.3x + 0.0175
R² = 0.997
Enzyme 1
Linear (Enzyme 1)
0.00E+00
1.00E-03
2.00E-03
3.00E-03
4.00E-03
5.00E-03
6.00E-03
7.00E-03
1/[para-nitrophenylphosphate] (1/µM)

Day 2
Enzyme 1
K_M (µM):
1.27E03±1.0E02
V_{MAX} (µM/23 Hr):
57.1±1.0E-01

[para-nitrophenylphosphate] (µM)	Average [*para*-nitrophenolate] (µM/23 Hr)	1/[*para*-nitrophenolate] (1/µM/23 Hr)	1/[*para*-nitrophenyl phosphate] (1/ µM)	standard deviation [*para*-nitrophenol] (1/µM/23 Hr)
150	6.11	0.164	6.67E-03	0.00E+00
200	7.78	0.129	5.00E-03	5.18E-03
250	9.44	0.106	4.00E-03	0.00E+00
300	10.6	9.47E-02	3.33E-03	1.69E-17
350	11.7	8.57E-02	2.86E-03	2.32E-03
400	13.3	7.50E-02	2.50E-03	3.13E-03
450	15.0	6.67E-02	2.22E-03	1.44E-03
500	16.1	6.21E-02	2.00E-03	1.25E-03
1.00E+03	25.0	4.00E-02	1.00E-03	1.39E-03
2.00E+03	37.2	2.69E-02	5.00E-04	4.61E-04
4.00E+03	48.9	2.05E-02	2.50E-04	1.34E-04

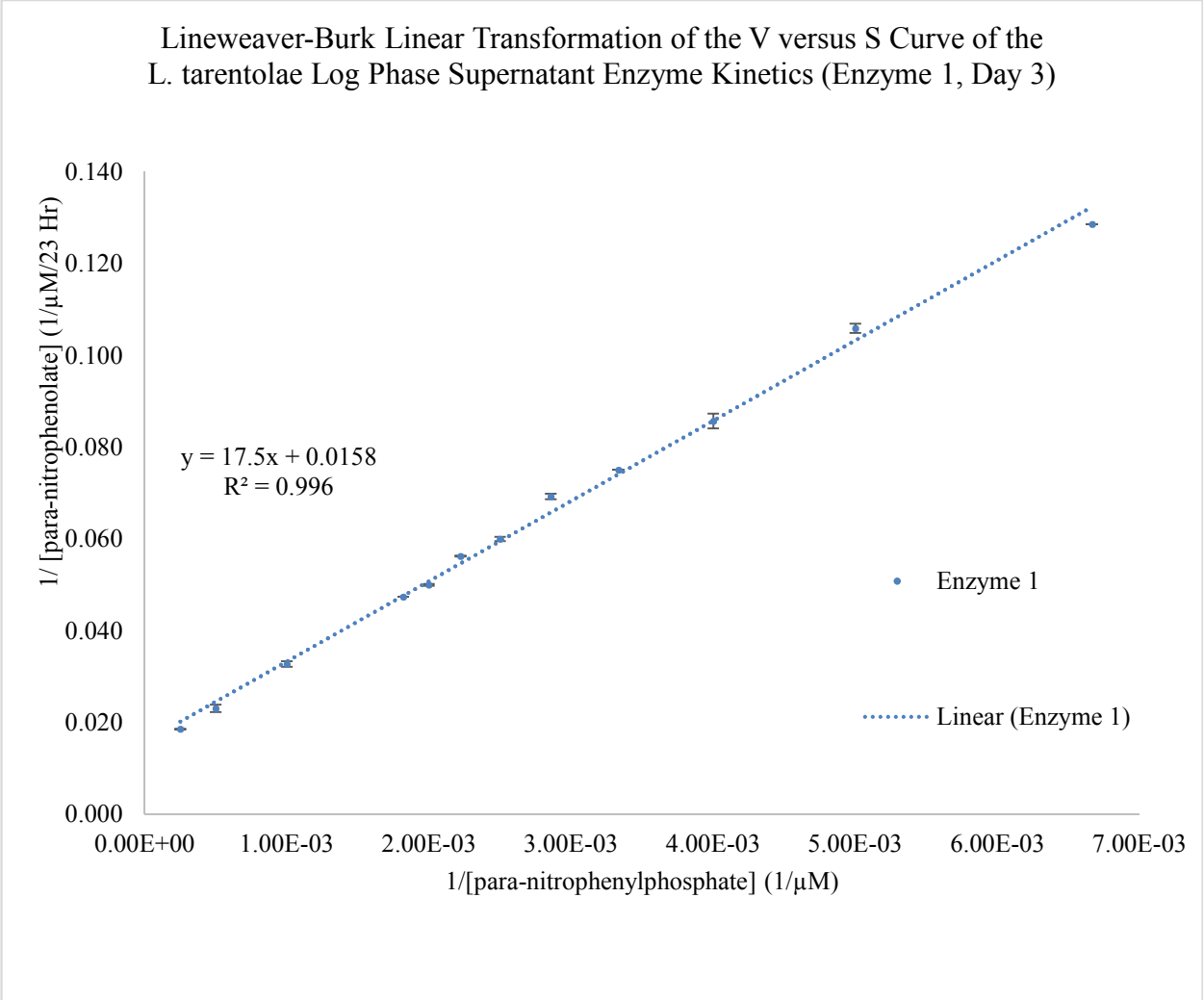
Lineweaver-Burk Linear Transformation of the V versus S Curve of the L. tarentolae Log Phase Supernatant Enzyme Kinetics (Enzyme 1, Day 3)
1/ [para-nitrophenolate] (1/µM/23 Hr)
0.140
0.120
0.100
0.080
0.060
0.040
0.020
0.000
y = 17.5x + 0.0158
R² = 0.996
Enzyme 1
Linear (Enzyme 1)
0.00E+00
1.00E-03
2.00E-03
3.00E-03
4.00E-03
5.00E-03
6.00E-03
7.00E-03
1/[para-nitrophenylphosphate] (1/µM)

Day 3
Enzyme 1
K_M (µM):
1.11E03±9.1E01
V_{MAX} (µM/23 Hr):
63.3±9.0E-01

[para-nitrophenylphosphate] (µM)	Average [*para*-nitrophenolate] (µM/23 Hr)	1/[*para*-nitrophenolate] (1/µM/23 Hr)	1/[*para*-nitrophenyl phosphate] (1/µM)	standard deviation [*para*-nitrophenol] (1/µM/23 Hr)
150	7.78	0.129	6.67E-03	0.00E+00
200	9.44	0.106	5.00E-03	1.00E-03
250	11.7	8.57E-02	4.00E-03	1.62E-03
300	13.3	7.50E-02	3.33E-03	8.47E-18
350	14.4	6.92E-02	2.86E-03	5.95E-04
400	16.7	6.00E-02	2.50E-03	4.54E-04
450	17.8	5.63E-02	2.22E-03	1.11E-04
500	20.0	5.00E-02	2.00E-03	2.00E-04
550	21.1	4.74E-02	1.82E-03	0.00E+00
1.00E+03	30.6	3.27E-02	1.00E-03	6.00E-04
2.00E+03	43.3	2.31E-02	5.00E-04	8.00E-04
4.00E+03	53.9	1.86E-02	2.50E-04	1.00E-04

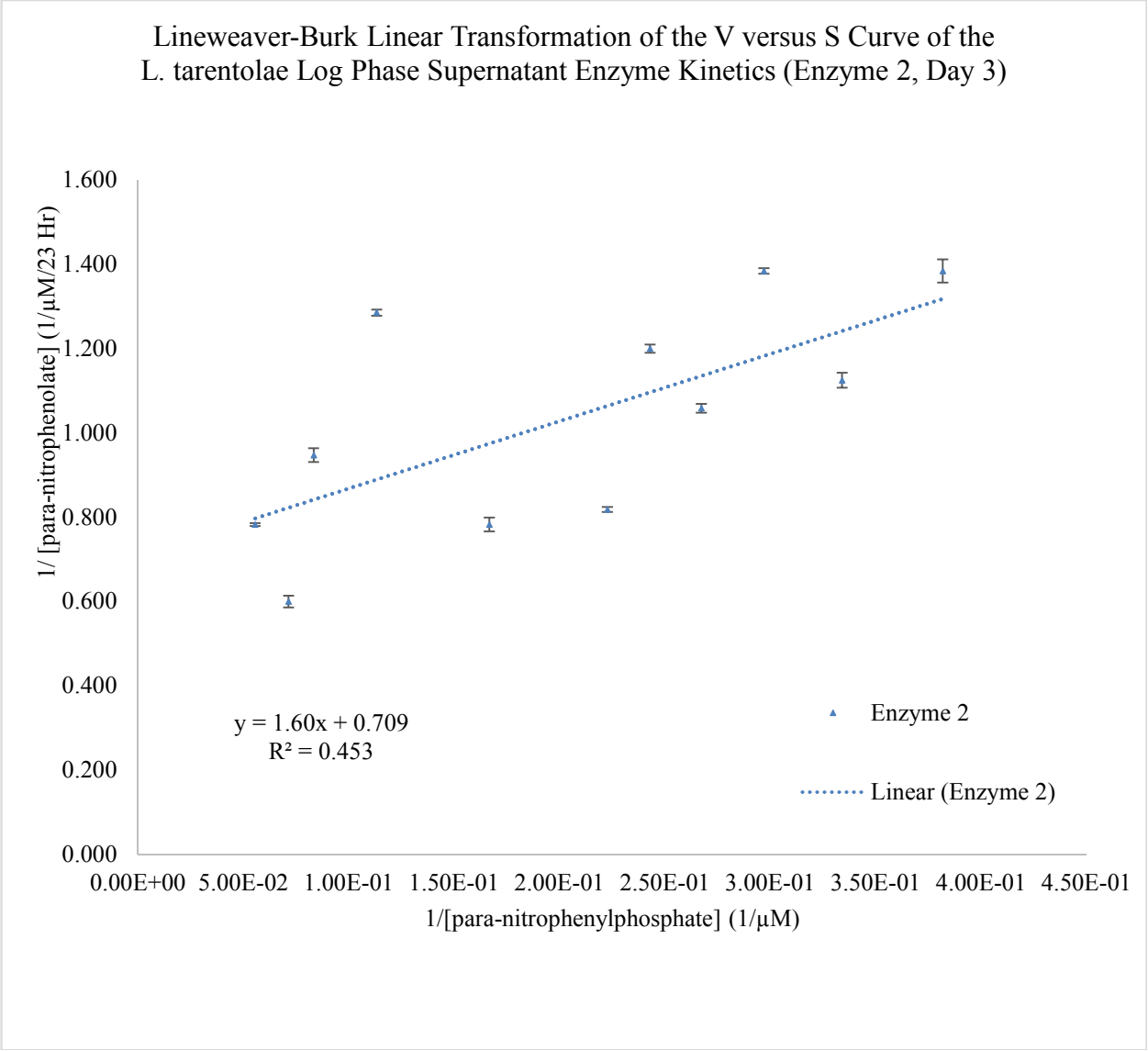
Lineweaver-Burk Linear Transformation of the V versus S Curve of the L. tarentolae Log Phase Supernatant Enzyme Kinetics (Enzyme 2, Day 3)
1/ [para-nitrophenolate] (1/µM/23 Hr)
1.600
1.400
1.200
1.000
0.800
0.600
0.400
0.200
0.000
0.00E+00
5.00E-02
1.00E-01
1.50E-01
2.00E-01
2.50E-01
3.00E-01
3.50E-01
4.00E-01
4.50E-01
1/[para-nitrophenylphosphate] (1/µM)
y = 1.60x + 0.709
R² = 0.453
Enzyme 2
Linear (Enzyme 2)

Day 3 **Enzyme 2** **K_M (µM):** **2.26±7.20E-02** **V_{MAX} (µM/23 Hr):** **1.40±2.00E-01**				
[para-nitrophenylphosphate] (µM)	**Average [*para*-nitrophenolate] (µM)**	**1/[*para*-nitrophenolate] (1/µM/23 Hr)**	**1/[*para*-nitrophenyl phosphate] (1/µM)**	**standard deviation [*para*-nitrophenol] (1/µM/23 Hr)**
2.62	0.722	1.38	3.82E-01	2.73E-02
2.99	0.889	1.13	3.34E-01	1.78E-02
3.37	0.722	1.38	2.97E-01	6.84E-03
3.74	0.944	1.06	2.67E-01	1.03E-02
4.12	0.833	1.20	2.43E-01	9.72E-03
4.49	1.22	0.818	2.23E-01	5.95E-03
6.00	1.28	0.783	1.67E-01	1.64E-02
8.83	0.778	1.29	1.13E-01	7.18E-03
1.20E+01	1.06	0.947	8.33E-02	1.65E-02
1.40E+01	1.67	0.600	7.14E-02	1.39E-02
1.80E+01	1.28	0.783	5.56E-02	3.74E-03

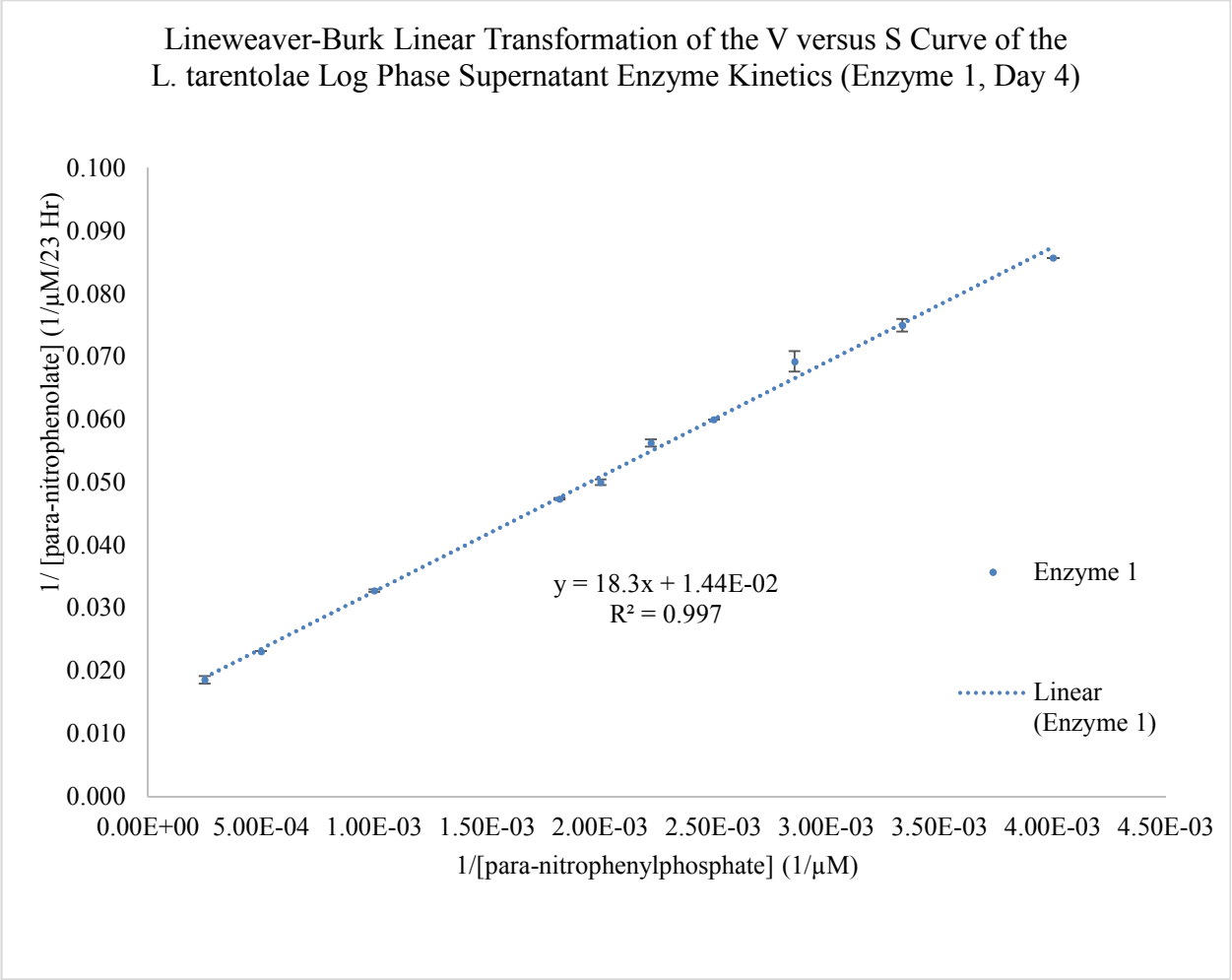
Lineweaver-Burk Linear Transformation of the V versus S Curve of the L. tarentolae Log Phase Supernatant Enzyme Kinetics (Enzyme 1, Day 4)
1/ [para-nitrophenolate] (1/µM/23 Hr)
0.100
0.090
0.080
0.070
0.060
0.050
0.040
0.030
0.020
0.010
0.000
0.00E+00
5.00E-04
1.00E-03
1.50E-03
2.00E-03
2.50E-03
3.00E-03
3.50E-03
4.00E-03
4.50E-03
1/[para-nitrophenylphosphate] (1/µM)
y = 18.3x + 1.44E-02
R² = 0.997
Enzyme 1
Linear (Enzyme 1)

Day 4
Enzyme 1
K_M (µM):
1.27E03±9.0E01
V_{MAX} (µM/23 Hr):
69.4±6.1E-01

[para-nitrophenylphosphate] (µM)	Average [*para*-nitrophenolate] (µM/23 Hr)	1/[*para*-nitrophenolate] (1/µM/23 Hr)	1/[*para*-nitrophenyl phosphate] (1/µM)	standard deviation [*para*-nitrophenol] (1/µM/23 Hr)
250	11.7	8.57E-02	4.00E-03	4.60E-03
300	13.3	7.50E-02	3.33E-03	7.36E-03
350	14.4	6.92E-02	2.86E-03	2.81E-03
400	16.7	6.00E-02	2.50E-03	2.71E-03
450	17.8	5.62E-02	2.22E-03	1.19E-03
500	20.0	5.00E-02	2.00E-03	9.56E-04
550	21.1	4.74E-02	1.82E-03	0.00E+00
1.00E+03	30.6	3.27E-02	1.00E-03	0.00E+00
2.00E+03	43.3	2.31E-02	5.00E-04	4.86E-04
4.00E+03	53.9	1.86E-02	2.50E-04	0.00E+00

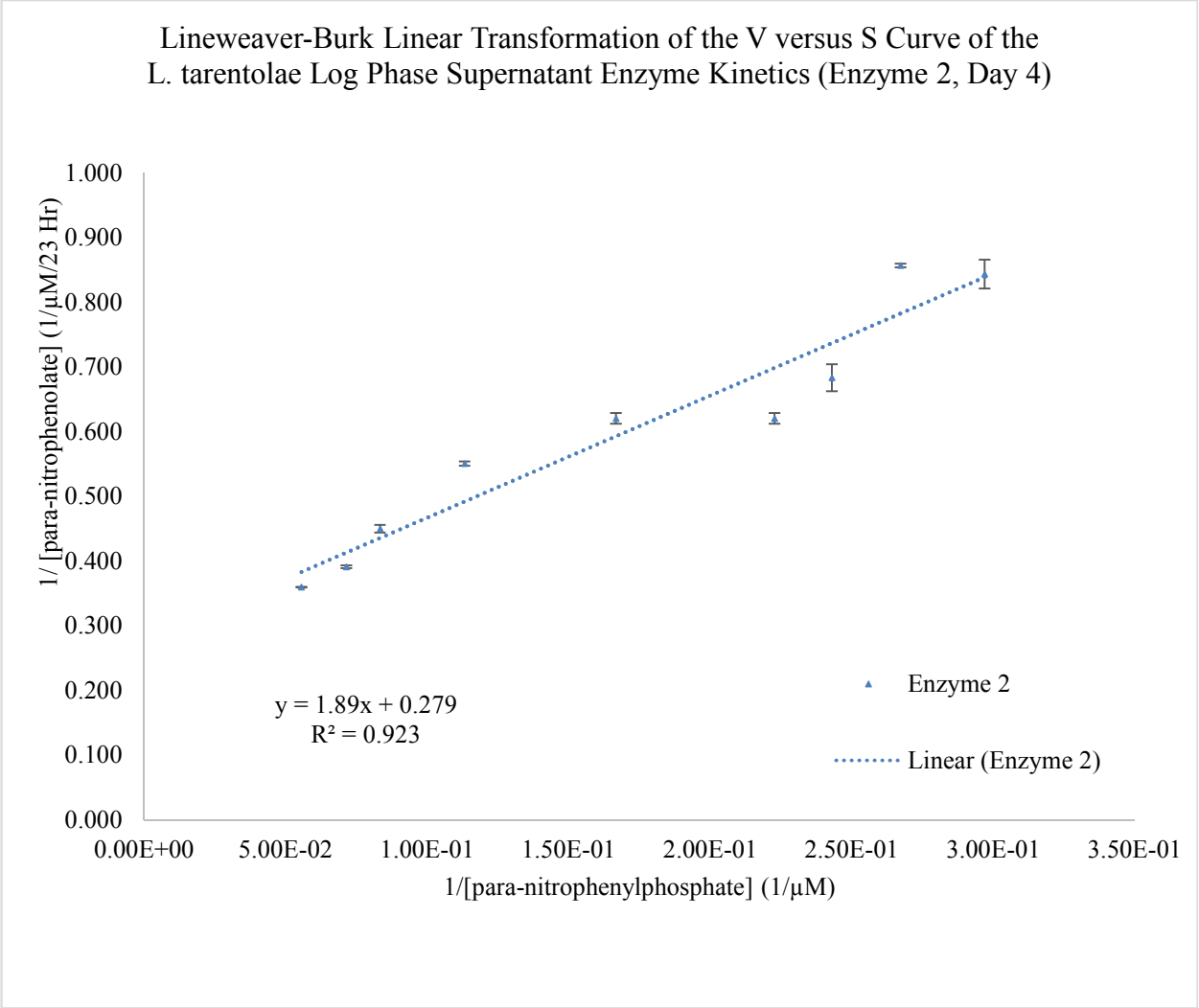
Lineweaver-Burk Linear Transformation of the V versus S Curve of the L. tarentolae Log Phase Supernatant Enzyme Kinetics (Enzyme 2, Day 4)
1/ [para-nitrophenolate] (1/µM/23 Hr)
1.000
0.900
0.800
0.700
0.600
0.500
0.400
0.300
0.200
0.100
0.000
0.00E+00
5.00E-02
1.00E-01
1.50E-01
2.00E-01
2.50E-01
3.00E-01
3.50E-01
1/[para-nitrophenylphosphate] (1/µM)
y = 1.89x + 0.279
R² = 0.923
Enzyme 2
Linear (Enzyme 2)

Day 4
Enzyme 2
K_M (µM): 6.93±0.42
V_{MAX} (µM/23 Hr): 3.58±0.12

[para-nitrophenylphosphate] (µM)	Average [*para*-nitrophenolate] (µM/23 Hr)	1/[*para*-nitrophenolate] (1/µM/23 Hr)	1/[*para*-nitrophenyl phosphate] (1/µM)	standard deviation [*para*-nitrophenol] (1/µM/23 Hr)
3.37	1.19	0.844	2.97E-01	2.23E-02
3.74	1.17	0.857	2.67E-01	2.94E-03
4.12	1.46	0.684	2.43E-01	2.09E-02
4.49	1.61	0.621	2.23E-01	8.32E-03
6.00	1.61	0.621	1.67E-01	8.32E-03
8.83	1.81	0.551	1.13E-01	3.29E-03
1.20E+01	2.22	0.450	8.33E-02	5.98E-03
1.40E+01	2.56	0.391	7.14E-02	2.25E-03
1.80E+01	2.78	0.360	5.56E-02	5.68E-04

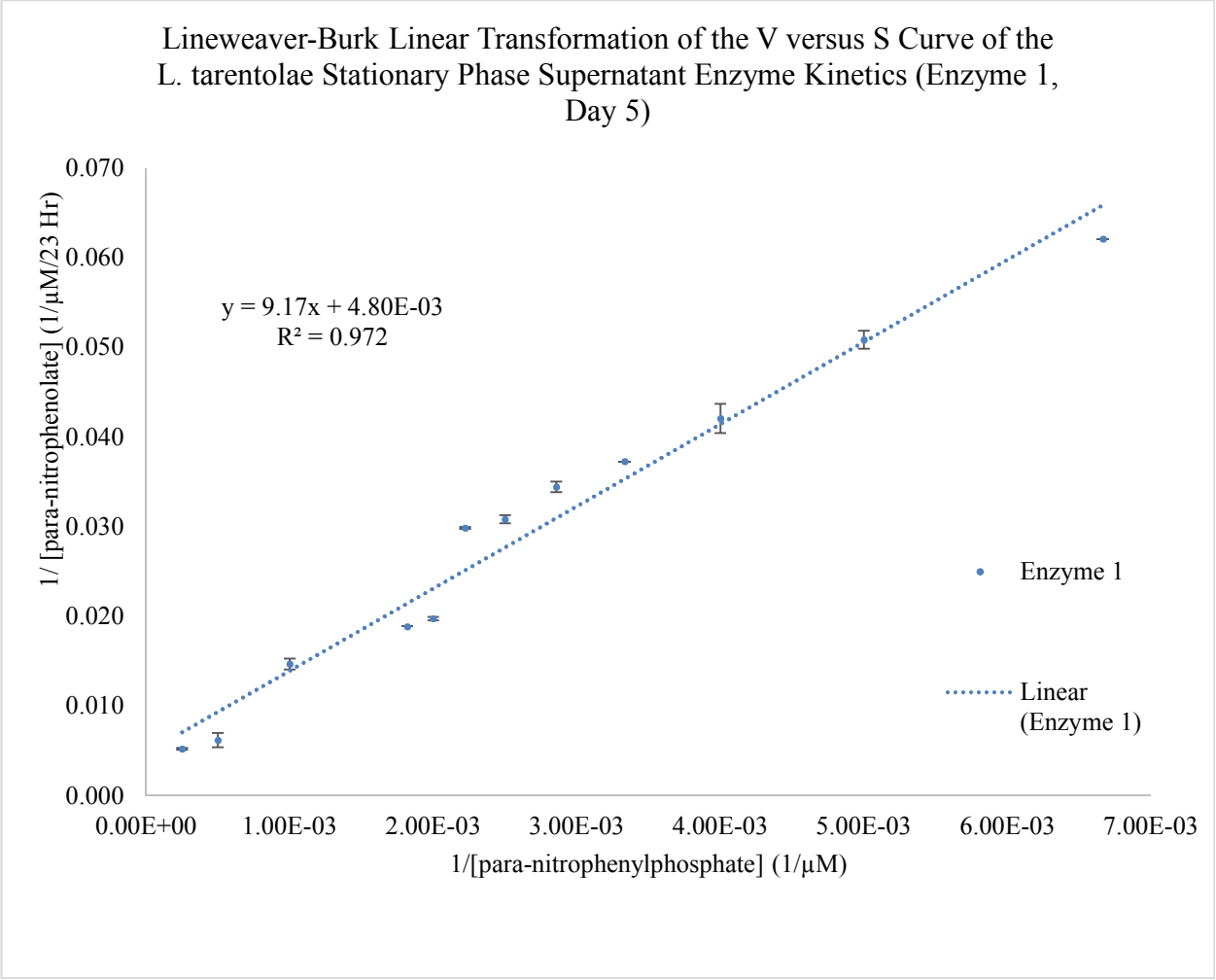
Lineweaver-Burk Linear Transformation of the V versus S Curve of the L. tarentolae Stationary Phase Supernatant Enzyme Kinetics (Enzyme 1, Day 5)
y = 9.17x + 4.80E-03
R² = 0.972
1/ [para-nitrophenolate] (1/µM/23 Hr)
0.070
0.060
0.050
0.040
0.030
0.020
0.010
0.000
0.00E+00
1.00E-03
2.00E-03
3.00E-03
4.00E-03
5.00E-03
6.00E-03
7.00E-03
1/[para-nitrophenylphosphate] (1/µM)
Enzyme 1
Linear (Enzyme 1)

Day 5
Enzyme 1
K_M (µM):
1.91E03±1.3E02
V_{MAX} (µM/23 Hr):
208±1.0E01

[para-nitrophenylphosphate] (µM)	Average [*para*-nitrophenolate] (µM/23 hr)	1/[*para*-nitrophenolate] (1/µM/23 Hr)	1/[*para*-nitrophenyl phosphate] (1/µM)	standard deviation [*para*-nitrophenol] (1/µM/23 Hr)
150	16.1	6.21E-02	6.67E-03	1.93E-03
200	19.7	5.08E-02	5.00E-03	8.30E-04
250	23.8	4.21E-02	4.00E-03	4.11E-04
300	26.8	3.73E-02	3.33E-03	4.90E-04
350	29.1	3.44E-02	2.86E-03	5.32E-04
400	32.4	3.08E-02	2.50E-03	1.58E-04
450	33.5	2.99E-02	2.22E-03	5.58E-04
500	50.7	1.97E-02	2.00E-03	2.83E-04
550	53.0	1.89E-02	1.82E-03	8.62E-05
1.00E+03	68.1	1.47E-02	1.00E-03	6.72E-05
2.00E+03	162	6.18E-03	5.00E-04	1.07E-04
4.00E+03	192	5.22E-03	2.50E-04	7.34E-05

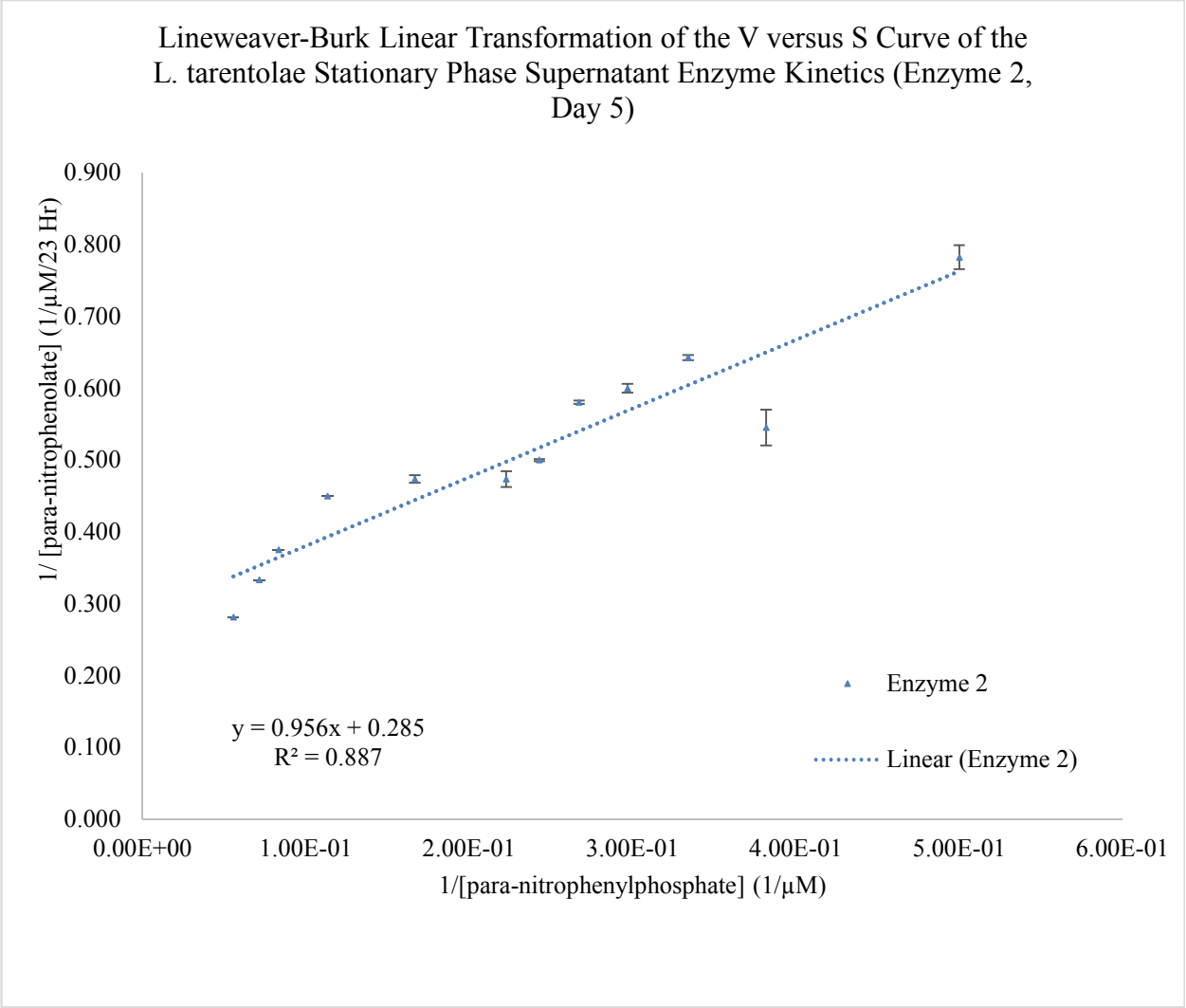
Lineweaver-Burk Linear Transformation of the V versus S Curve of the L. tarentolae Stationary Phase Supernatant Enzyme Kinetics (Enzyme 2, Day 5)
1/ [para-nitrophenolate] (1/µM/23 Hr)
0.900
0.800
0.700
0.600
0.500
0.400
0.300
0.200
0.100
0.000
0.00E+00
1.00E-01
2.00E-01
3.00E-01
4.00E-01
5.00E-01
6.00E-01
1/[para-nitrophenylphosphate] (1/µM)
y = 0.956x + 0.285
R² = 0.887
Enzyme 2
Linear (Enzyme 2)

Day 5
Enzyme 2
K_M (µM):
3.35±7.7E-02
V_{MAX} (µM/23 Hr):
3.51±2.9E-01

[para-nitrophenylphosphate] (µM)	Average [*para*-nitrophenolate] (µM/23 hr)	1/[*para*-nitrophenolate] (1/µM/23 Hr)	1/[*para*-nitrophenyl phosphate] (1/µM)	standard deviation [*para*-nitrophenol] (1/µM/23 Hr)
2.00	1.28	0.783	5.00E-01	1.66E-02
2.62	1.83	0.545	3.82E-01	2.49E-02
2.99	1.56	0.643	3.34E-01	3.56E-03
3.37	1.67	0.600	2.97E-01	6.18E-03
3.74	1.72	0.581	2.67E-01	2.25E-03
4.12	2.00	0.500	2.43E-01	1.59E-03
4.49	2.11	0.474	2.23E-01	1.10E-02
6.00	2.11	0.474	1.67E-01	5.40E-03
8.83	2.22	0.450	1.13E-01	0.00E+00
1.20E+01	2.67	0.375	8.33E-02	0.00E+00
1.40E+01	3.00	0.333	7.14E-02	0.00E+00
1.80E+01	3.56	0.281	5.56E-02	0.00E+00

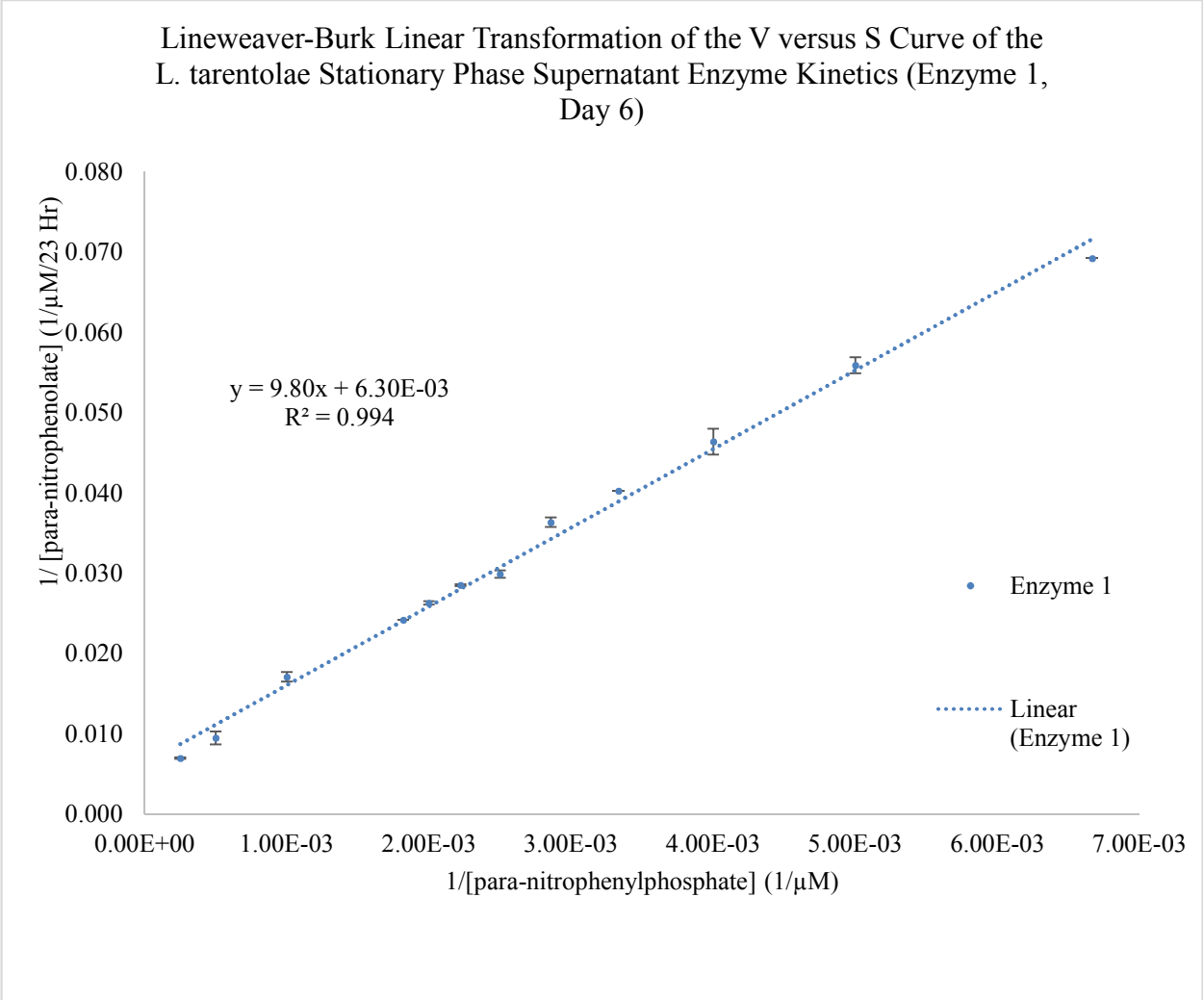
Lineweaver-Burk Linear Transformation of the V versus S Curve of the L. tarentolae Stationary Phase Supernatant Enzyme Kinetics (Enzyme 1, Day 6)
1/ [para-nitrophenolate] (1/µM/23 Hr)
0.080
0.070
0.060
0.050
0.040
0.030
0.020
0.010
0.000
y = 9.80x + 6.30E-03
R² = 0.994
Enzyme 1
Linear (Enzyme 1)
0.00E+00
1.00E-03
2.00E-03
3.00E-03
4.00E-03
5.00E-03
6.00E-03
7.00E-03
1/[para-nitrophenylphosphate] (1/µM)

Day 6
Enzyme 1
K_M (µM):
1.56E03±6.0E01
V_{MAX} (µM/23 Hr):
159±7.0

[para-nitrophenylphosphate] (µM)	Average [*para*-nitrophenolate] (µM/23 Hr)	1/[*para*-nitrophenolate] (1/µM/23 Hr)	1/[*para*-nitrophenyl phosphate] (1/µM)	standard deviation [*para*-nitrophenol] (1/µM/23 Hr)
150	14.4	6.92E-02	6.67E-03	1.93E-03
200	17.9	5.59E-02	5.00E-03	8.30E-04
250	21.6	4.64E-02	4.00E-03	4.11E-04
300	24.8	4.03E-02	3.33E-03	4.90E-04
350	27.5	3.64E-02	2.86E-03	5.32E-04
400	33.4	2.99E-02	2.50E-03	1.58E-04
450	35.1	2.85E-02	2.22E-03	5.58E-04
500	38.0	2.63E-02	2.00E-03	2.83E-04
550	41.3	2.42E-02	1.82E-03	8.62E-05
1.00E+03	58.4	1.71E-02	1.00E-03	6.72E-05
2.00E+03	105	9.51E-03	5.00E-04	1.07E-04
4.00E+03	143	6.98E-03	2.50E-04	7.34E-05

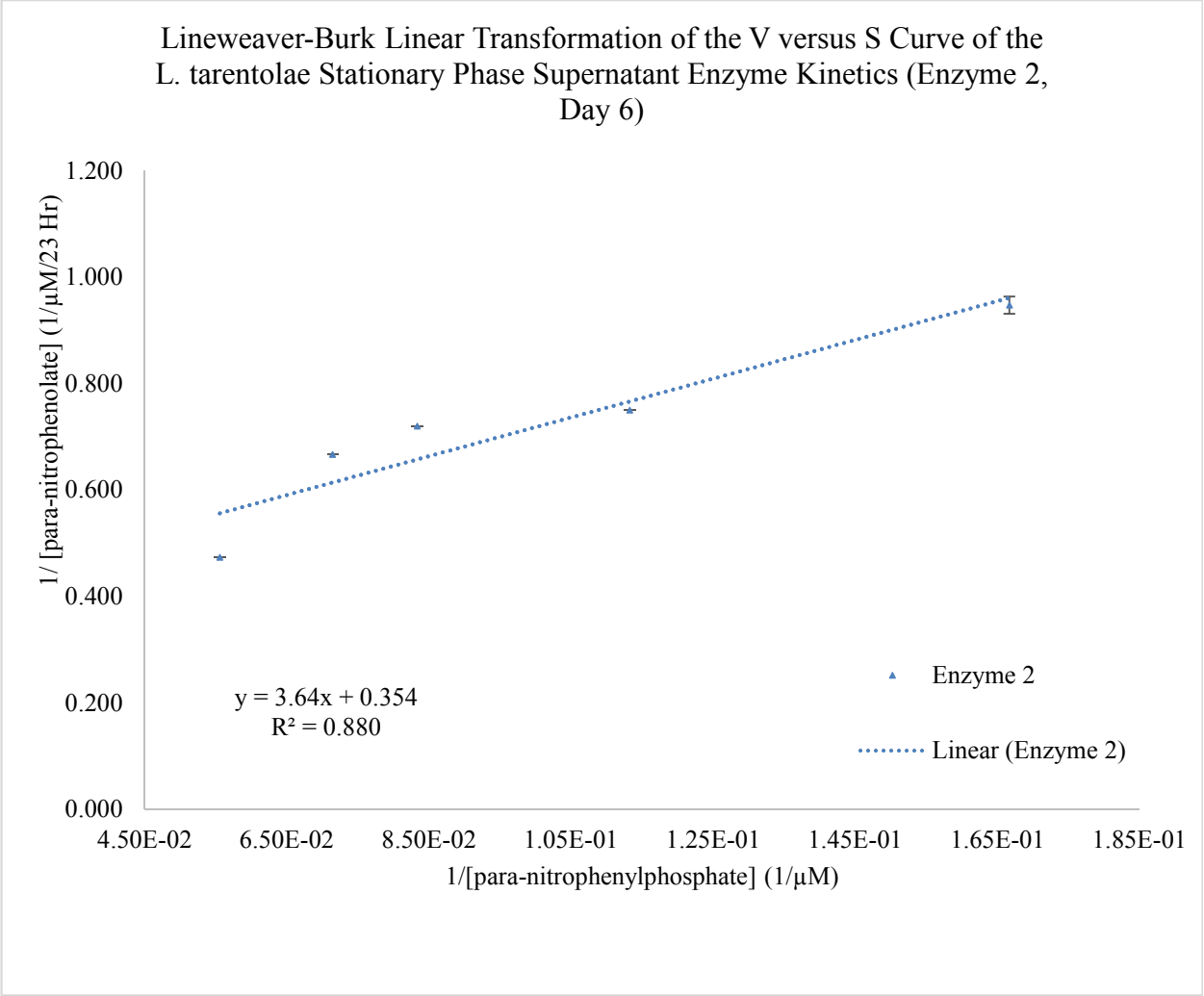
Lineweaver-Burk Linear Transformation of the V versus S Curve of the L. tarentolae Stationary Phase Supernatant Enzyme Kinetics (Enzyme 2, Day 6)
1/ [para-nitrophenolate] (1/µM/23 Hr)
1.200
1.000
0.800
0.600
0.400
0.200
0.000
4.50E-02
6.50E-02
8.50E-02
1.05E-01
1.25E-01
1.45E-01
1.65E-01
1.85E-01
1/[para-nitrophenylphosphate] (1/µM)
y = 3.64x + 0.354
R² = 0.880
Enzyme 2
Linear (Enzyme 2)

Day 6
Enzyme 2
K_M (µM): 10.3±8.1E01
V_{MAX} (µM/23 Hr): 2.82±1.9E-01

[para-nitrophenylphosphate] (µM)	Average [*para*-nitrophenolate] (µM)/23 Hr	1/[*para*-nitrophenolate] 1/(µM/23 Hr)	1/[*para*-nitrophenyl phosphate] (1/µM)	standard deviation [*para*-nitrophenol] 1/(µM/23 Hr)
6.00	1.06	0.947	1.67E-01	1.61E-02
8.83	1.33	0.750	1.13E-01	0.00E+00
12.0	1.39	0.720	8.33E-02	0.00E+00
14.0	1.50	0.667	7.14E-02	0.00E+00
18.0	2.11	0.474	5.56E-02	0.00E+00

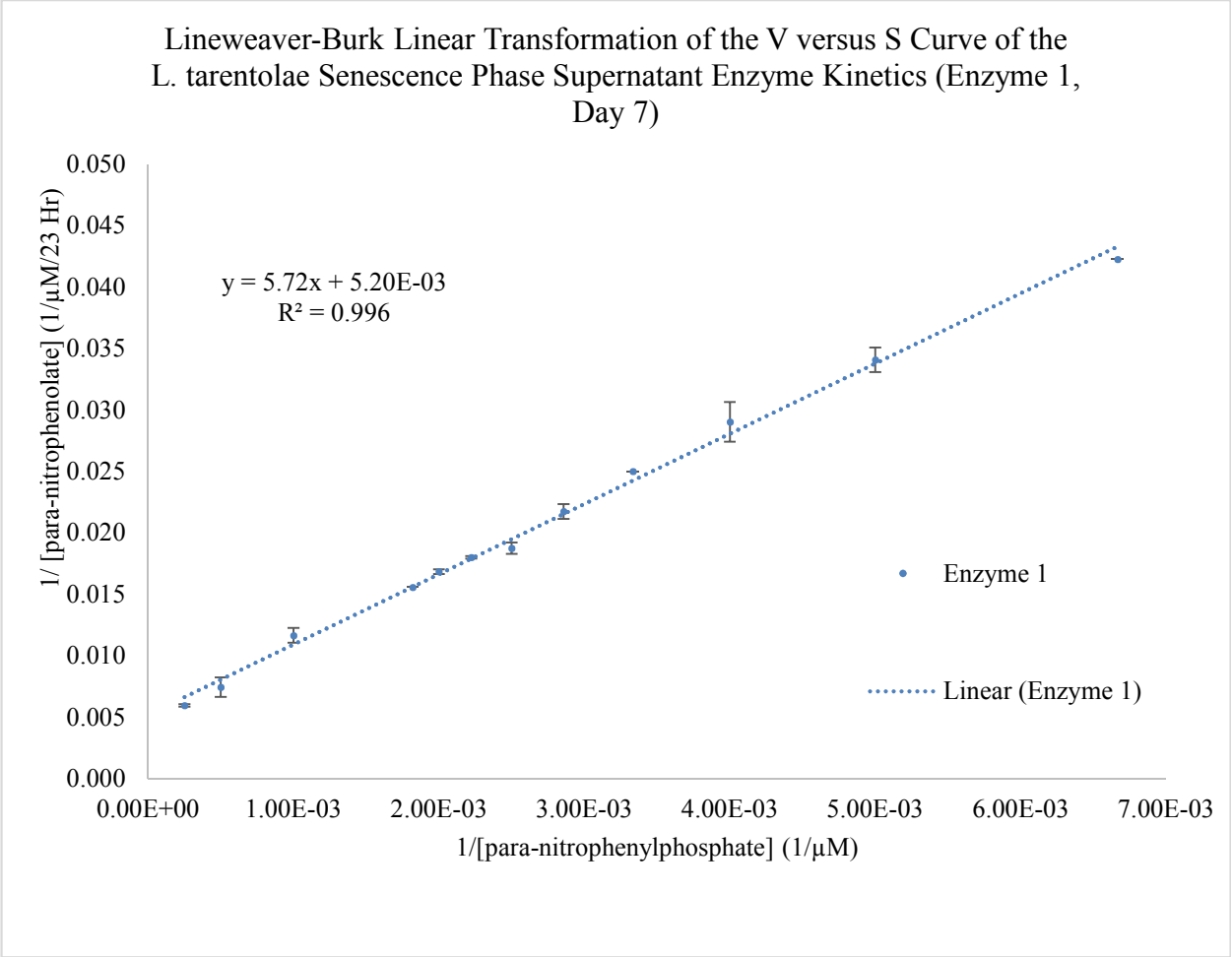
Lineweaver-Burk Linear Transformation of the V versus S Curve of the L. tarentolae Senescence Phase Supernatant Enzyme Kinetics (Enzyme 1, Day 7)
y = 5.72x + 5.20E-03
R² = 0.996
1/ [para-nitrophenolate] (1/µM/23 Hr)
1/[para-nitrophenylphosphate] (1/µM)
Enzyme 1
Linear (Enzyme 1)
0.050
0.045
0.040
0.035
0.030
0.025
0.020
0.015
0.010
0.005
0.000
0.00E+00
1.00E-03
2.00E-03
3.00E-03
4.00E-03
5.00E-03
6.00E-03
7.00E-03

Day 7
Enzyme 1
K_M (µM):
1.10E03±3.0E01
V_{MAX} (µM/23 Hr):
192±9.0

[para-nitrophenylphosphate] (µM)	Average [*para*-nitrophenolate] (µM/23 Hr)	1/[*para*-nitrophenolate] (1/µM/23 Hr)	1/[*para*-nitrophenyl phosphate] (1/µM)	standard deviation [*para*-nitrophenol] (1/µM/23 Hr)
150	23.7	4.23E-02	6.67E-03	4.36E-04
200	29.3	3.41E-02	5.00E-03	1.79E-04
250	34.4	2.90E-02	4.00E-03	2.45E-04
300	40.0	2.50E-02	3.33E-03	4.89E-05
350	46.0	2.17E-02	2.86E-03	2.50E-04
400	53.3	1.88E-02	2.50E-03	2.70E-04
450	55.6	1.80E-02	2.22E-03	2.53E-04
500	59.4	1.68E-02	2.00E-03	1.13E-04
550	64.3	1.56E-02	1.82E-03	1.07E-04
1.00E+03	85.8	1.17E-02	1.00E-03	1.65E-04
2.00E+03	134	7.44E-03	5.00E-04	2.90E-04
4.00E+03	168	5.95E-03	2.50E-04	4.50E-05

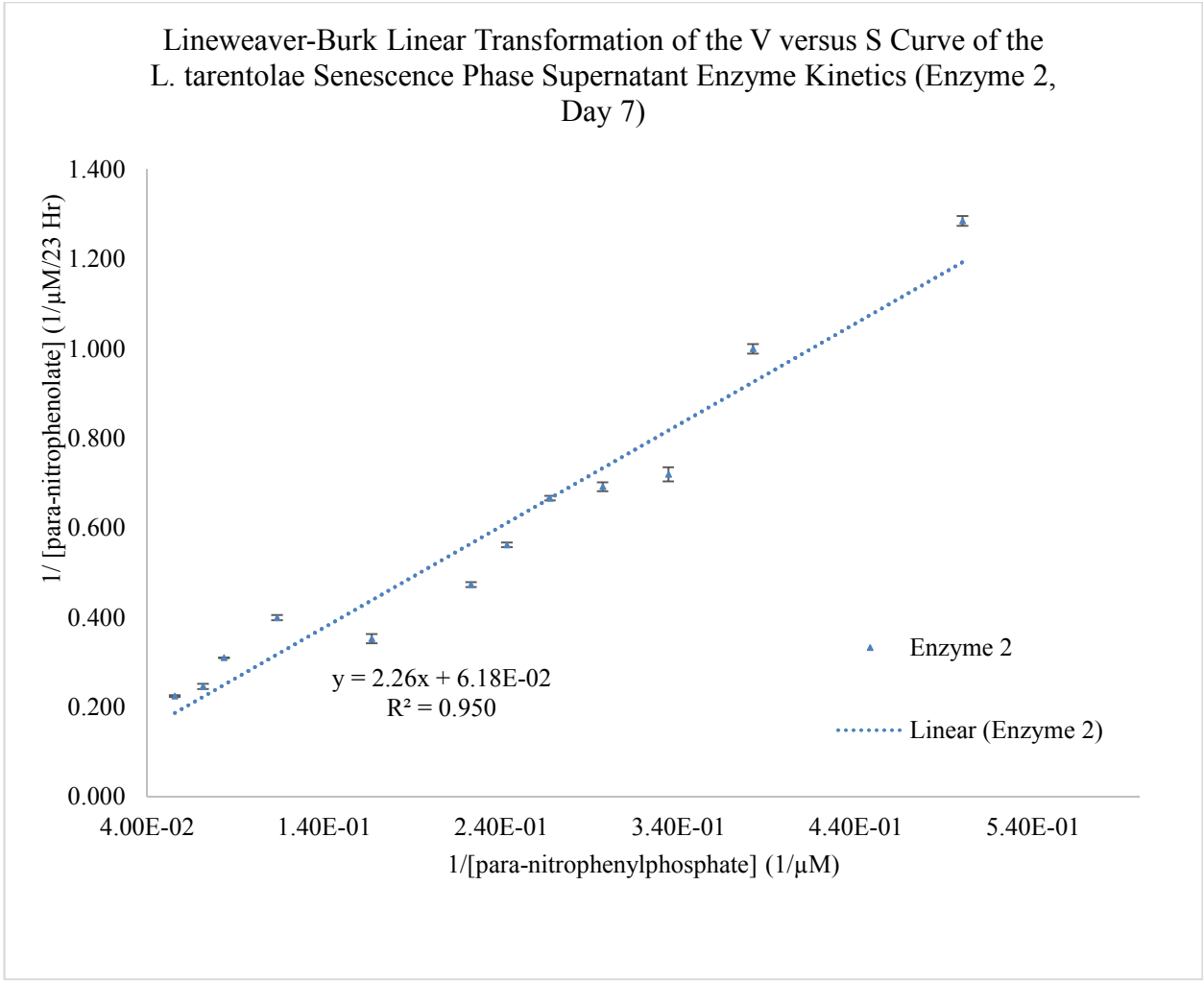
Lineweaver-Burk Linear Transformation of the V versus S Curve of the L. tarentolae Senescence Phase Supernatant Enzyme Kinetics (Enzyme 2, Day 7)
1/ [para-nitrophenolate] (1/µM/23 Hr)
1.400
1.200
1.000
0.800
0.600
0.400
0.200
0.000
4.00E-02
1.40E-01
2.40E-01
3.40E-01
4.40E-01
5.40E-01
1/[para-nitrophenylphosphate] (1/µM)
y = 2.26x + 6.18E-02
R² = 0.950
Enzyme 2
Linear (Enzyme 2)

Day 7
Enzyme 2
K_M (µM): 36.6±1.8
V_{MAX} (µM/23 Hr): 16.2±7.0E-01

[para-nitrophenylphosphate] (µM)	Average [*para*-nitrophenolate] (µM/23 Hr)	1/[*para*-nitrophenolate] (1/µM/23 Hr)	1/[*para*-nitrophenyl phosphate] (1/µM)	standard deviation [*para*-nitrophenol] (1/µM/23 Hr)
2.00	0.778	1.29	5.00E-01	1.08E-02
2.62	1.00	1.00	3.82E-01	1.09E-02
2.99	1.39	0.720	3.34E-01	1.59E-02
3.37	1.44	0.692	2.97E-01	9.98E-03
3.74	1.50	0.667	2.67E-01	5.38E-03
4.12	1.78	0.563	2.43E-01	5.16E-03
4.49	2.11	0.474	2.23E-01	5.64E-03
6.00	2.83	0.353	1.67E-01	1.01E-02
8.83	2.50	0.400	1.13E-01	5.92E-03
1.20E+01	3.22	0.310	8.33E-02	4.99E-04
1.40E+01	4.06	0.247	7.14E-02	5.94E-03
1.80E+01	4.44	0.225	5.56E-02	1.90E-03

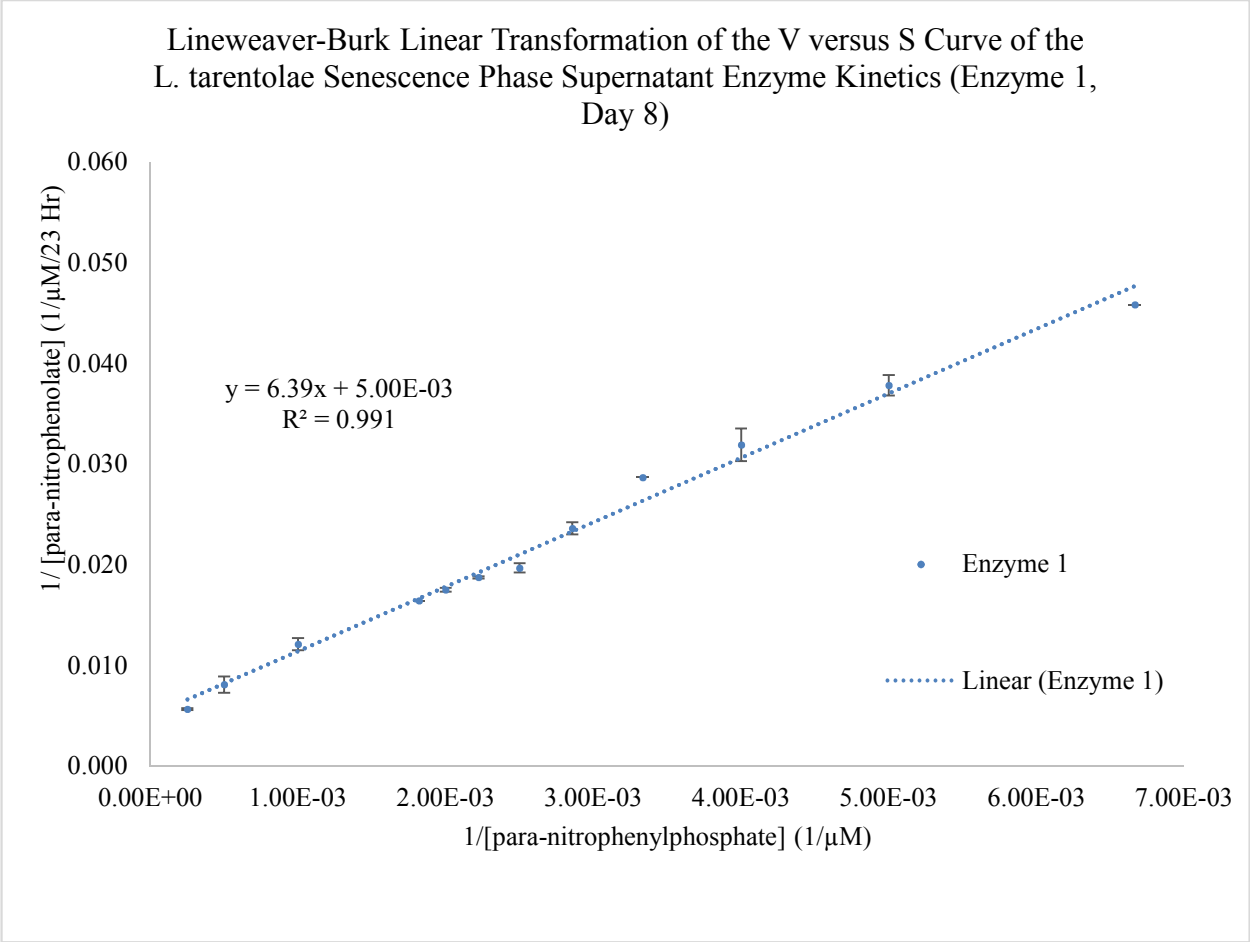
Lineweaver-Burk Linear Transformation of the V versus S Curve of the L. tarentolae Senescence Phase Supernatant Enzyme Kinetics (Enzyme 1, Day 8)
1/ [para-nitrophenolate] (1/µM/23 Hr)
0.060
0.050
0.040
0.030
0.020
0.010
0.000
y = 6.39x + 5.00E-03
R² = 0.991
Enzyme 1
Linear (Enzyme 1)
0.00E+00
1.00E-03
2.00E-03
3.00E-03
4.00E-03
5.00E-03
6.00E-03
7.00E-03
1/[para-nitrophenylphosphate] (1/µM)

Day 8 **Enzyme 1** **K_M (µM):** **1.28E03±5.0E01** **V_{MAX} (µM/23 Hr):** **200±8.0**				
[para-nitrophenylphosphate] (µM)	**Average [*para*-nitrophenolate] (µM/23 Hr)**	**1/[*para*-nitrophenolate] (1/µM/23 Hr)**	**1/[*para*-nitrophenyl phosphate] (1/µM)**	**standard deviation [*para*-nitrophenol] (1/µM/23 Hr)**
150	21.8	4.58E-02	6.67E-03	2.61E-02
200	26.4	3.78E-02	5.00E-03	1.02E-02
250	31.3	3.19E-02	4.00E-03	1.04E-02
300	34.9	2.87E-02	3.33E-03	8.04E-03
350	42.3	2.36E-02	2.86E-03	2.89E-03
400	50.8	1.97E-02	2.50E-03	1.69E-03
450	53.3	1.88E-02	2.22E-03	1.09E-03
500	57.1	1.75E-02	2.00E-03	2.89E-03
550	60.8	1.64E-02	1.82E-03	3.39E-04
1.00E+03	82.4	1.21E-02	1.00E-03	2.10E-03
2.00E+03	123	8.11E-03	5.00E-04	6.53E-04
4.00E+03	176	5.68E-03	2.50E-04	0.00E+00

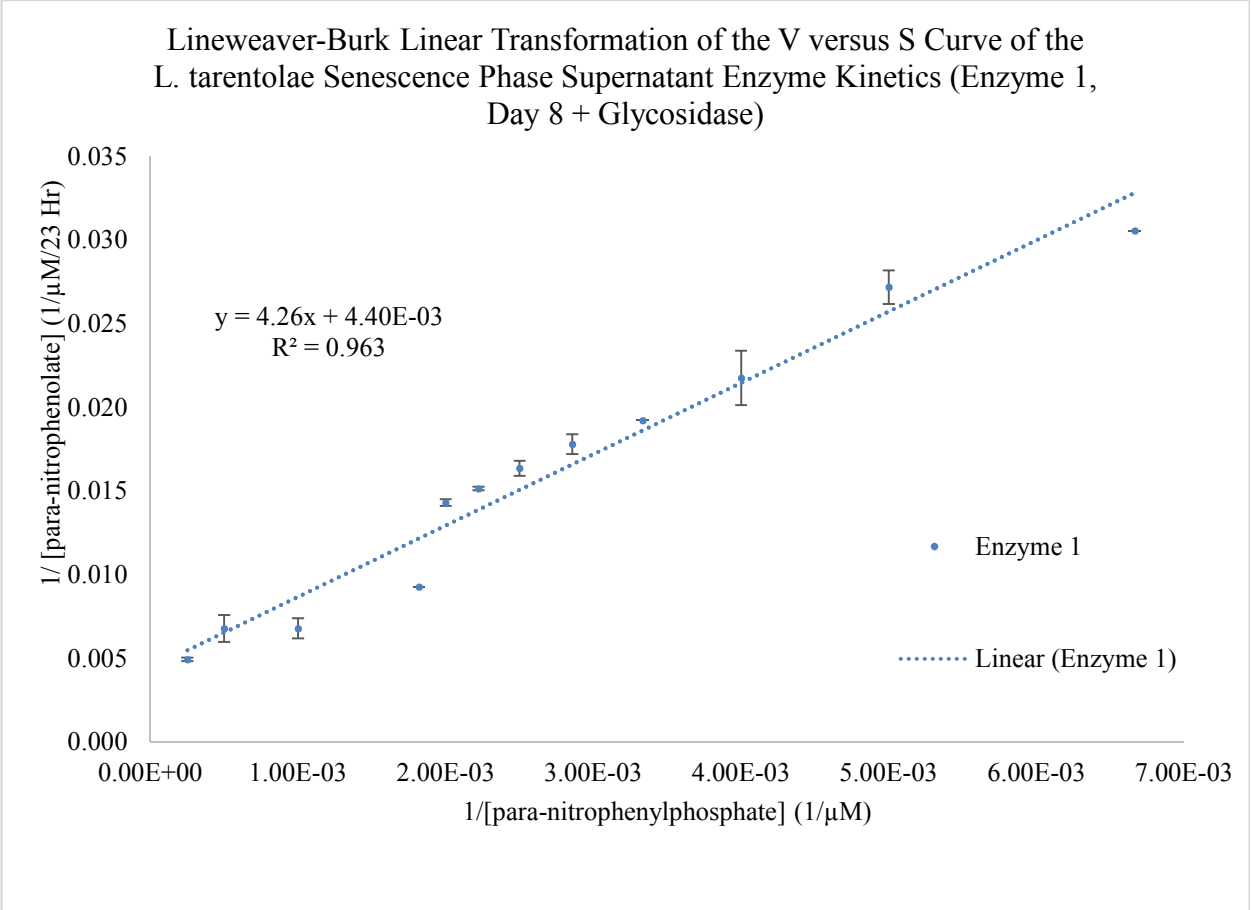
Lineweaver-Burk Linear Transformation of the V versus S Curve of the L. tarentolae Senescence Phase Supernatant Enzyme Kinetics (Enzyme 1, Day 8 + Glycosidase)
1/ [para-nitrophenolate] (1/µM/23 Hr)
0.035
0.030
0.025
0.020
0.015
0.010
0.005
0.000
y = 4.26x + 4.40E-03
R² = 0.963
Enzyme 1
Linear (Enzyme 1)
0.00E+00
1.00E-03
2.00E-03
3.00E-03
4.00E-03
5.00E-03
6.00E-03
7.00E-03
1/[para-nitrophenylphosphate] (1/µM)

Day 8 + Glycosidase Enzyme 1

K_M (µM): 968±1.3E02

V_{MAX} (µM/23 Hr): 227±50

[para-nitrophenylphosphate] (µM)	Average [*para*-nitrophenolate] (µM/23 Hr)	1/[*para*-nitrophenolate] (1/µM/23 Hr)	1/[*para*-nitrophenyl phosphate] (1/µM)	standard deviation [*para*-nitrophenol] (1/µM/23 Hr)
150	32.7	3.06E-02	6.67E-03	9.53E-03
200	36.8	2.72E-02	5.00E-03	1.26E-02
250	45.9	2.18E-02	4.00E-03	6.42E-03
300	52.1	1.92E-02	3.33E-03	1.33E-03
350	56.2	1.78E-02	2.86E-03	1.39E-03
400	61.1	1.64E-02	2.50E-03	5.06E-03
450	66.0	1.52E-02	2.22E-03	3.00E-03
500	69.9	1.43E-02	2.00E-03	2.69E-03
550	108	9.28E-03	1.82E-03	1.32E-03
1.00E+03	147	6.78E-03	1.00E-03	0.00E+00
2.00E+03	147	6.78E-03	5.00E-04	0.00E+00
4.00E+03	203	4.93E-03	2.50E-04	0.00E+00

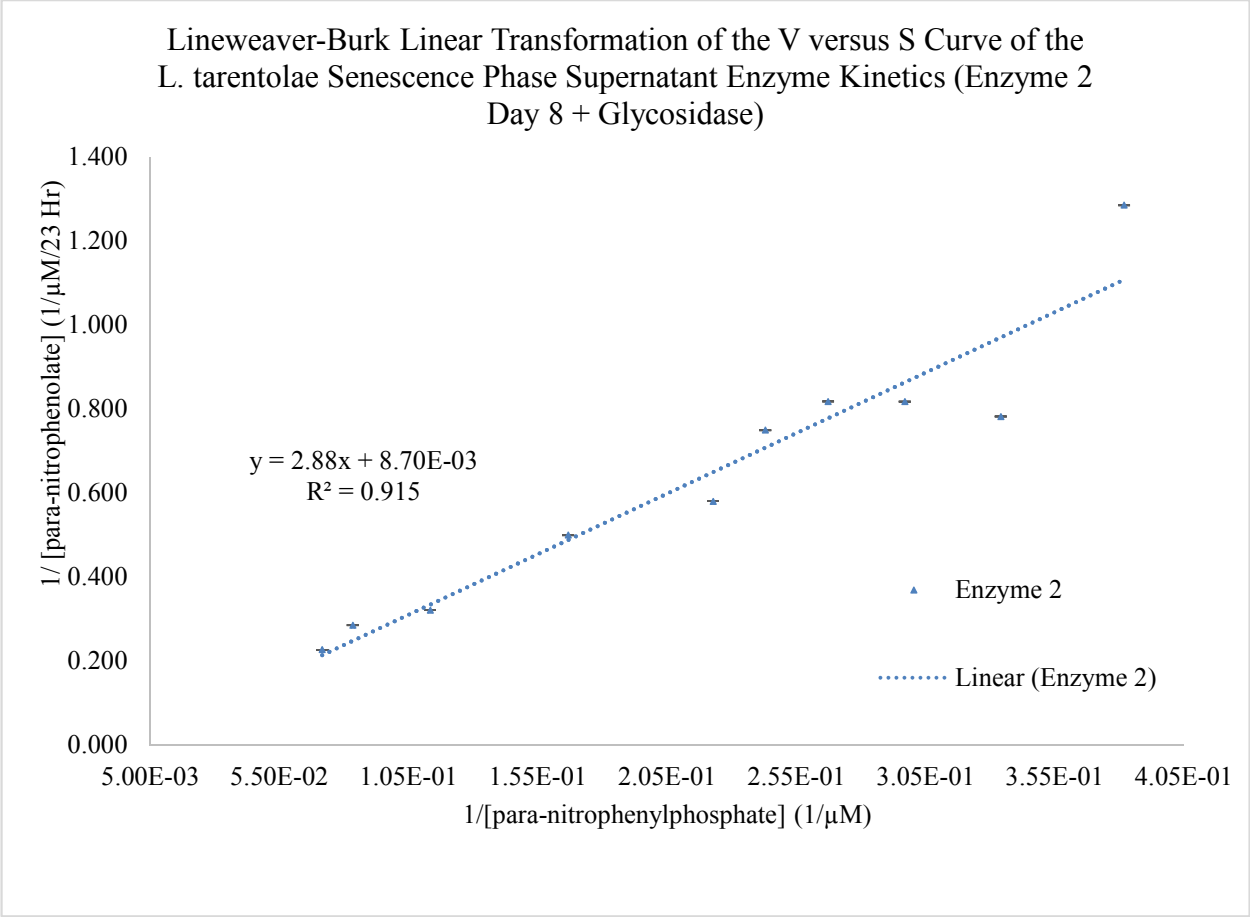
Lineweaver-Burk Linear Transformation of the V versus S Curve of the L. tarentolae Senescence Phase Supernatant Enzyme Kinetics (Enzyme 2 Day 8 + Glycosidase)
1/ [para-nitrophenolate] (1/µM/23 Hr)
1.400
1.200
1.000
0.800
0.600
0.400
0.200
0.000
y = 2.88x + 8.70E-03
R² = 0.915
Enzyme 2
Linear (Enzyme 2)
5.00E-03
5.50E-02
1.05E-01
1.55E-01
2.05E-01
2.55E-01
3.05E-01
3.55E-01
4.05E-01
1/[para-nitrophenylphosphate] (1/µM)

Day 8 + Glycosidase Enzyme 2

K_M (µM): 331±14

V_{MAX} (µM/23 Hr): 115±17

[para-nitrophenylphosphate] (µM)	Average [*para*-nitrophenolate] (µM/23 Hr)	1/[*para*-nitrophenolate] (1/µM/23 Hr)	1/[*para*-nitrophenyl phosphate] (1/µM)	standard deviation [*para*-nitrophenol] (1/µM/23 Hr)
2.00	0.278	3.600	5.00E-01	4.99E-04
2.62	0.778	1.286	3.82E-01	5.44E-04
2.99	1.28	0.783	3.34E-01	6.06E-04
3.37	1.22	0.818	2.97E-01	4.42E-04
3.74	1.22	0.818	2.67E-01	4.25E-04
4.12	1.33	0.750	2.43E-01	2.90E-05
4.49	1.72	0.581	2.23E-01	1.75E-04
6.00	2.00	0.500	1.67E-01	1.37E-04
8.83	3.11	0.321	1.13E-01	3.07E-04
12.0	3.50	0.286	8.33E-02	5.76E-05
14.0	4.39	0.228	7.14E-02	6.42E-05
18.0	26.5	3.77E-02	5.56E-02	8.58E-05